



University of Kerbala

College of Science

Department of chemistry

Synthesis, biological activity and structural study of D- galactose- based 1,2,3- Triazole Derivatives

A thesis

submitted to Council of the College of Science

University of Kerbala

As part of completing the requirements for a master's degree

Chemistry Science

By

Halah Husam AbdulKadhim

Supervisor

by

Prof. Dr. Adnan Ibrahim Mohammed

Prof. Dr. Baker Abdel-Zahra Joda

1443 A.H

2022 A.D

بِسْمِ اللَّهِ الرَّحْمَنِ الرَّحِيمِ

{يَرْفَعِ اللَّهُ الَّذِينَ آمَنُوا مِنْكُمْ وَالَّذِينَ أُوتُوا الْعِلْمَ دَرَجَاتٍ وَاللَّهُ
بِمَا تَعْمَلُونَ خَبِيرٌ}

صَدَقَ اللَّهُ الْعَلِيِّ الْعَظِيمِ

سُورَةُ الْمُجَادَلَةِ الْآيَةَ (١١)

Supervisors Certification

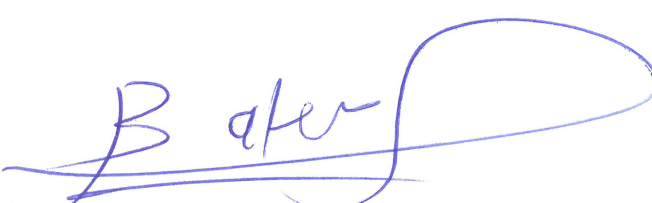
we certify this thesis conducted under our supervision at the department of chemistry, College of science, University of Kerbala, as a partial fulfillment of the requirements for the degree of M.Sc. in Chemistry.

Signature: P.P. Dr. Thawar Mahdi Madlool

Name: Prof. Dr. Adnan Ibrahim Mohammed

Address: University of Kerbala – College of Science

Date: 31 / 10 / 2022

Signature: 

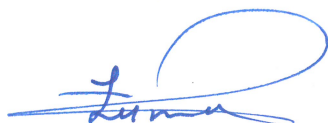
Name: Prof. Baker Abdel-zahra Joda

Address: University of Kerbala – College of Science

Date: 26 / 10 / 2022

Report of the Head of the Chemistry Department

According to the recommendation presented by the Chairman of the Postgraduate Studies Committee, I forward this thesis “ **Synthesis, biological activity and structural study of D- galactose- based 1,2,3- Triazole Derivatives** ” for examination.



Signature:

Prof.Dr. Luma M. Ahmed

Head of Chemistry Department

Address: University of Kerbala, College of Science, Department of Chemistry

Date: 30 / 10 / 2022

Examination Committee Certification

We certify that we have read this thesis entitled " **Synthesis, biological activity and structural study of D- galactose- based 1,2,3- Triazole Derivatives**

" as the examining committee, examined the student "

Halah Husam AbdulKadhim"

on its contents, and that in our opinion, it is adequate for the partial fulfillment of the requirements for the Degree of Master in Science of chemistry.



Signature:

Name: **Dr. Zeid Hassan Abood**

Title: Professor

Address: University of Kerbala – College of Science, Department of Chemistry

Date: 3/7/2022

(Chairman)

Signature



Name: **Faiq Fathallah Karam**

Title: Professor

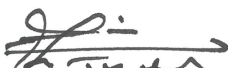
Address: University of Al-Qadisiyah

College of Science, Department of

Chemistry.

Date: 6/7/2022

(Member)



P.P. Dr. Thamer Mahdi Mahdi

Signature:

Name: **Dr. Adnan Ibrahim Mohammed**

Title: Professor

Address: University of Kerbala, College of Science, Department of Chemistry

Date: 31/10/2022

(Member & Supervisor)

Signature



Name: **Karem Jaber Sabah**

Title: Professor

Address: University of Kufa

College of Science, Department of Chemistry.

Date: 6/7/2022

(Member)

Signature:

Name: **Baker Abdel-Zahra Joda**

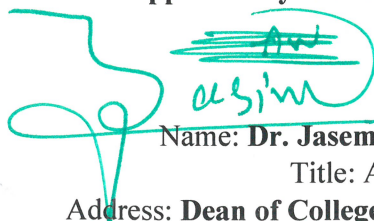
Title: Professor

Address: University of Kerbala – College of Science Department of Chemistry

Date: 6/7/2022

(Member & Supervisor)

Approved by the council of the College of Science



Signature:

Name: **Dr. Jasem Hanoon Hashim Al-Awadi**

Title: Assistant Professor

Address: **Dean of College of Science, University of Kerbala.**

Date: 31/10/2022

Dedication

To the biggest lover and supporter. **my mother**

To The Kind Spirited and smile carrier... my **father**

To my inspiration... **my brothers and Russel**

To the source of my power, my support, and my love... my husband, **Ali.**

To the apple of my eye, my daughter **Mia.**

And to all **my friends.**

Acknowledgement

I would like to thank God for granting me this work.

I extend my sincere thanks to my first supervisor, Professor **Dr. Adnan Ibrahim Mohammad**, for his support and for providing me with abundant scientific and practical advice. Also, my second supervisor, Assistant Professor **Dr. Baker Abdel-Zahra Joda**, for his assistance in conducting the analytics. I also thank my husband, the **pharmacist, Ali Saad Mahmoud**, for his support throughout the research days. I thank my friend **Zainab Muhammad Kadhem** for providing useful information and helping me in the laboratory. Also, thanks are due to **Mr. Hussein Mubarak Al-Asadi** and **M.Sc. Pharmacist hashim hasan Hashim** for the assistance. I would like to thank the **Faculty of Science, University of Karbala, Department of Chemistry** for providing the right environment for work, as well as a lot of supplies.

Abstract

This study included synthesis of new galactose based 1,2,3-triazoles containing fluorobenzyl moiety and monitor the toxicity profile against the MSC. At the beginning, 2-fluor-, 3-fluoro and 4-fluorobenzyl azides **68a–c** were prepared by the reaction of corresponding benzyl bromides **68a–c** with sodium azide in DMSO at fifty degrees for 24h to obtain the mentioned azido compounds in very good to excellent yield 81–92%. In a parallel step, zinc chloride and sulfuric acid were used to catalyze the reaction of D-galactose (**69**) with excess of acetone at ambient temperature for 6h to obtain the α -D-galactose diacetone (**70**) in very good yield 81%. This derivative was reacted with propargyl bromide in DMF at 0 °C–r.t. to produce Alkynyl- α -D-galactosyl derivative **71** in 88% yield. Moreover, the conformation of derivative **71** was determined using computational study and 2D NMR technique. In addition, 1,2,3-triazole derivatives **72a–c** were synthesized through the copper(I)-catalyzed alkyne-azide cycloaddition (CuAAC). Alkyne **71** was reacted with azides **68a–c** **in the aid of Na ascorbate and CuSO₄.5H₂O in DMSO at 50 °C for 36h to get** the targeted 1,2,3-triazole derivatives **72a–c** in 83–90% yield. The synthesized compounds have been characterized through NMR(nuclear magnetic resonance), FTIR(Fourier-transform infrared), HSQC(heteronuclear single quantum coherence), COSY(correlated spectroscopy), HMBC(heteronuclear multiple bond correlation), and HRMS(high-resolution mass spectrometry). Compounds **72a–c** **had been studied towards** human being mesenchymal stem cells and **it discovered that these derivatives hold fair** cytotoxicity.

Abbreviations

2D	Two dimensional
COSY	Correlated spectroscopy
¹³C NMR	Carbon nuclear magnetic resonance
¹⁹F NMR	Fluorine nuclear magnetic resonance
¹H NMR	Proton nuclear magnetic resonance
COVID	Corona virous disease
IUPAC	International Union of Pure and Applied Chemistry
CuAAC	Copper(I)-catalyzed azide-alkyne cycloaddition
DMF	Dimethylformamide
DMSO	Dimethyl sulfoxide
EtOAc	Ethyl acetate
FT-IR	Fourier-transform infrared
US	Ultrasound
TZVP	Triple Zeta Valence Plus Polarization
EDTA	Ethylenediamine tetraacetic acid
DEME	Dulbecco's modified
HMBC	Heteronuclear multiple bond correlation
HRMS	High-resolution mass spectrometry
HSQC	Heteronuclear single quantum coherence
<i>J</i>	Coupling constant
M	Molar
m.p.	Melting point
ppm	Part per million

r.t.	Room temperature
<i>R_f</i>	Retention factor
TLC	Thin layer chromatography

Table of Contents

Abstract	VII
Abbreviations	VIII
1. Introduction	1
1.1. Heterocyclic compounds as Five-membered ring	2
1.2. Triazole derivatives	3
1.3 .1,2,3-Triazole compounds	4
1.3.1. 1,2,3-Triazole synthesis	4
1.3.1.1. Alkyne-azide cycloaddition reaction	6
1.3.1.2. Copper-mediate cycloaddition reaction (Click reaction)	8
1.3.1.3 Novel strategies for synthesis of 1,2,3-triazoles	11
1.4. Application of 1,2,3, -triazole derivatives	14
1.4.1.Medicinal and biological purposes	14
1.5. The objectives of this thesis	22
2.Experimental Part	23
2.1. Typical methods	23
2.2. Preparation methods and Identification	23
2.2.1. Method 1: Preparation of azido fluorobenzyl derivatives 68a– c (Improved method)	23
2-Fluorobenzene azide (68a)	24

3-Fluorobenzene azide (68b)	24
4-Fluorobenzene azide (68c)	25
2.2.2. Synthesis of α -D-galactose diacetonide (70) (improved procedure)	25
2.2.3. Synthesis of 6-O-propargyl- α -D-galactose diacetonide (71)	26
2.2.4. General procedure 2: preparation of 1,2,3-triazoles	27
Compound 72a	27
Compound 72b	28
Compound 72c	29
2.3. Computational method	30
2.4. Triazole' cytotoxicity (improved Procedure)	30
2.4.1. Sample' preparation	30
2.4.2. Cell' maintenance	30
2.4.3. Cell' culture	31
3. Results and discussion	32
3.1. Preparation of fluorine-containing azido benzyl compounds 68a–c	33
3.3. Synthesis of 6-O-prop-2-ynyl-1,2:3,4-diacetonide- α -D-galactose (72)	41
Table 1. Effect of the initial reaction temperature on the alkyne yield	44
3.4. Synthesis of triazole derivatives 72a–c	49

Table 3. Comparison of $^{13}\text{C}\{^1\text{H}\}$ NMR data of triazoles 72a–c	59
3.5. Cytotoxicity of triazole derivatives 72a–72c	78
Table 4. Cytotoxicity of triazoles 72a–72c against human MSC	79
3.6 Conclusion	80
3.7 Prospective work	81

List of figures

Figure 13. Fourier-transform infrared spectrum of the azide 68a	35
Figure 14. Fourier-transform infrared spectrum of the azide 68b	35
Figure 15. Fourier-transform infrared spectrum of the azide 68c	35
Figure 16. Proton NMR chart (CDCl ₃ , 600 MHz) of azide 68a	36
Figure 17. Proton NMR chart (CDCl ₃ , 600 MHz) of azide 68b	37
Figure 18. Proton NMR chart (CDCl ₃ , 600 MHz) of azide 68c	37
Figure 19. Carbon-13 NMR chart (CDCl ₃ , 150 MHz) of azide 68a	38
Figure 20. Carbon-13 NMR chart (CDCl ₃ , 150 MHz) of azide 68b	39
Figure 21. Carbon-13 NMR chart (CDCl ₃ , 150 MHz) of azide 68c	39
Figure 22. Fluorine-19 NMR chart (CDCl ₃ , 564 Mhz) of azide 68a	40
Figure 23. Fluorine-19 NMR chart (CDCl ₃ , 564 Mhz) of azide 68b	40
Figure 24. Fluorine-19 NMR chart (CDCl ₃ , 564 Mhz) of azide 68c	41
Figure 25. Fourier-transform infrared spectrum of derivative 70	42
Figure 26. Proton NMR chart (CDCl ₃ , 300 MHz) of compound 70	43
Figure 27. Carbon-13 NMR chart (CDCl ₃ , 75 MHz) of compound 70	44
Figure 28. Fourier-transform infrared spectrum of derivative 71	45
Figure 29. Proton NMR (CDCl ₃ , 300 MHz) of compound 71	46
Figure 30. Magnified ¹ H– ¹ H COSY spectrum (Chloroform, 300 MHz) of derivative 71	47
Figure 31. Carbon NMR (CDCl ₃ , 75 MHz) of compound 71	47
Figure 32. Chair conformations of pyranoses	48
Figure 33. The suggested conformation of compound 71 based on computational study and NMR spectra	48

Figure 34. Fourier-transform infrared spectrum of derivative 72a	51
Figure 35. Fourier-transform infrared spectrum of derivative 72b	51
Figure 36. Fourier-transform infrared spectrum of derivative 72c	52
Table 2. Comparison of ¹ H NMR data of triazoles 72a–c	53
Figure 37. NMR (CDCL ₃ , 600 MHz) of compound 72a	54
Figure 38. Proton NMR (CDCL ₃ , 600 MHz) of compound 72b	54
Figure 39. Proton NMR (CDCL ₃ , 600 MHz) of compound 72c	55
Figure 40. Magnified aromatic region proton nuclear magnetic resonance spectrum (CDCL ₃ , 600 MHz) of triazole 72a	55
Figure 41. Magnified aromatic region proton nuclear magnetic resonance spectrum (CDCL ₃ , 600 MHz) of triazole 72b	56
Figure 42. Magnified aromatic region proton nuclear magnetic resonance spectrum (CDCL ₃ , 600 MHz) of triazole 72c	56
Figure 43. Magnified aliphatic region proton nuclear magnetic resonance spectrum (CDCL ₃ , 600 MHz) of triazole 72a	57
Figure 44. Magnified aliphatic region proton nuclear magnetic resonance spectrum (CDCL ₃ , 600 MHz) of triazole 72b	57
Figure 45. Magnified aliphatic region proton nuclear magnetic resonance spectrum (CDCL ₃ , 600 MHz) of triazole 72c	58
Figure 46. Carbon NMR (CDCL ₃ , 150 MHz) of triazole 72a	60
Figure 47. Carbon NMR (CDCL ₃ , 150 MHz) of triazole 72b	60
Figure 48. Carbon NMR (CDCL ₃ , 150 MHz) of triazole 72c	61
Figure 49. Magnified aromatic region carbon-13 nuclear magnetic resonance spectrum (CDCL ₃ , 150 MHz) of triazole 72a	61
Figure 50. Magnified aromatic region carbon-13 nuclear magnetic resonance spectrum (CDCL ₃ , 150 MHz) of triazole 72b	62
Figure 51. Magnified aromatic region carbon-13 nuclear magnetic resonance spectrum (CDCL ₃ , 150 MHz) of triazole 72c	62

Figure 52. Fluorine-19 NMR chart (CDCl ₃ , 564 MHz) of compound 72a	63
Figure 53. Fluorine-19 NMR chart (CDCl ₃ , 564 MHz) of compound 72b	64
Figure 54. Fluorine-19 NMR chart (CDCl ₃ , 564 MHz) of triazole 72c	64
Figure 55. Magnified Fluorine-19-NMR chart (CDCl ₃ , 564 MHz) of compound 72a	65
Figure 56. Magnified Fluorine-19-NMR chart (CDCl ₃ , 564 MHz) of compound 72b	65
Figure 57. Magnified Fluorine-19-NMR chart (CDCl ₃ , 564 MHz) of compound 72c	66
Figure 58. Zoomed in ¹ H- ¹ H COSY (600 MHz, CDCl ₃) of compound 72a	67
Figure 59. Zoomed in ¹ H- ¹ H COSY (600 MHz, CDCl ₃) of compound 72b	67
Figure 60. Zoomed in ¹ H- ¹ H COSY (600 MHz, CDCl ₃) of compound 72c	68
Figure 61. Magnified ¹ H- ¹ H COSY (CDCl ₃ , 600 MHz) of triazole 72a	68
Figure 62. Magnified ¹ H- ¹ H COSY (CDCl ₃ , 600 MHz) of triazole 72b	69
Figure 63. Magnified ¹ H- ¹ H COSY (CDCl ₃ , 600 MHz) of triazole 72c	69
Figure 64. Magnified aromatic region ¹ H- ¹³ C HSQC (CDCl ₃ , 600 MHz) of triazole 72a	70
Figure 65. Magnified aromatic region ¹ H- ¹³ C HSQC (CDCl ₃ , 600 MHz) of triazole 72b	71
Figure 66. Magnified aromatic region ¹ H- ¹³ C HSQC (CDCl ₃ , 600 MHz) of triazole 72c	71
Figure 67. Magnified aliphatic region ¹ H- ¹³ C HSQC (CDCl ₃ , 600 MHz) of triazole 72a	72

Figure 68. Magnified aliphatic region ^1H - ^{13}C HSQC (CDCl_3 , 600 MHz) of triazole 72b	72
Figure 69. Magnified aliphatic region ^1H - ^{13}C HSQC (CDCl_3 , 600 MHz) of triazole 72c	73
Figure 70. Magnified aliphatic region ^1H - ^{13}C HMBC (CDCl_3 , 600 MHz) of triazole 72a	73
Figure 71. Magnified aliphatic region ^1H - ^{13}C HMBC (CDCl_3 , 600 MHz) of triazole 72b	74
Figure 72. Magnified aliphatic region ^1H - ^{13}C HMBC (CDCl_3 , 600 MHz) of triazole 72c	74
Figure 73. High-resolution mass spectrum of triazole 72a	75
Figure 74. High-resolution mass spectrum of triazole 72b	76
Figure 75. High-resolution mass spectrum of triazole 72c	77
Figure 76. MSCs Cytotoxicity analyses using almarBlue method that planted 24h on top of triazoles 72a–72c	79

CHAPTER ONE
INTRODUCTION

1. Introduction

Carbocyclic compounds are molecules, in which their rings are made up only of carbon atoms.¹ Whereas, in heterocycles compounds, at least there is one carbon on the ring that has been replaced by a heteroatom such as N, O or S. A heterocyclic system need not be restricted to a single ring. An aromatic heterocycle is called a heteroaromatic.² Over half of all-natural products are heterocycles.³⁻⁵ Moreover, heterocyclic rings are contained in an extremely large number of pharmacologically active molecules. e.g, coenzymes, nucleic acid bases, amino acids (histidine, proline, tryptophan), porphyrins, flavones and the ring-formed sugar.^{6,7} The nomenclature of heterocycles is not that simple, according to IUPAC three nomenclature rules are allowed: the Hantzsch-Widman Nomenclature, the replacement nomenclature and the common names. The type of heteroatom is often indicated by a prefix; Aza- for N, oxa- for O, thia- for S.⁸ In general, heterocycles can be classified according to the type and number of heteroatoms; ring size and nature of the ring, whether it is saturated or unsaturated (i.e, electronic structure).^{9,10} They are usefully divided into three main groups according to their degree of saturation:

- Saturated heterocycles (like the acyclic derivatives)
- partially unsaturated heterocycles (alkenes)
- Heteroaromatics (containing aromatic rings).

The heterocyclic compounds can contain three, four, five, six or seven membered rings. (Figure 1):

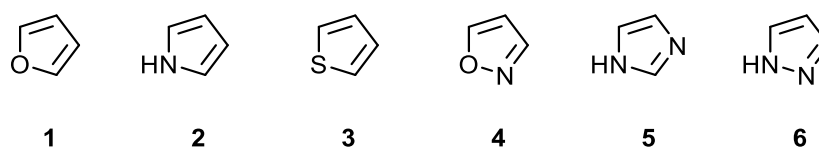


Figure (1-1) Five-membered rings heterocyclic compounds

1.1. Heterocyclic compounds as five-membered ring

The mother compounds of this family are; furan (**1**), pyrrole (**2**) and thiophene (**3**), which possess the constructions shown in (Figure 1).¹¹ The saturated derivatives of these structures are called tetrahydrofuran (**7**), pyrrolidine (**8**) and tetrahydrothiophene (**9**), respectively. The bicyclic compounds made of furan, pyrrole or thiophene ring fused to a benzene ring are referred to as indole (**10**), benzofuran (**11**) and benzothiophene (**12**), respectively (Figure 2).

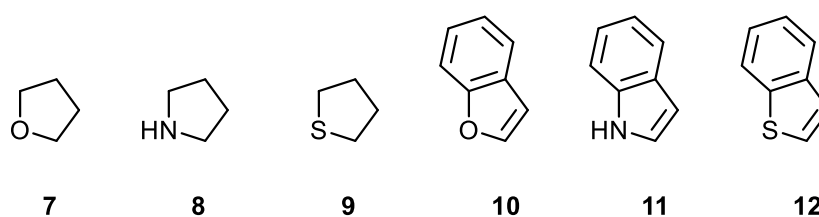


Figure (1-2) Derivatives of Furan, Pyrrole and Thiophene

Nitrogen heterocycle pyrrole occurs in bone oil (also called animal oil), in which it is formed by the decomposition of proteins when heated. Pyrrolidine ring is found in the amino acids such as proline (**13**) and hydroxyproline (**14**), which are components of many proteins, and are found in particularly high concentrations in collagen, the structural protein of bones, tendons, ligaments and skin.^{12,13} Pyrrole derivatives are widespread in alkaloids, a large class of alkaline organic nitrogen compounds that are primarily produced by plants,¹⁴ such as nicotine (**15**) (Figure 3). The heme group of the oxygen-carrying protein haemoglobin and related compounds such as myoglobin; the chlorophylls, which are the light harvesting pigments of green plants and other photosynthetic organisms; and vitamin B12 are all formed from four pyrrole units linked in a larger ring system known as porphyrin, like that of Chlorophyll b.¹⁵

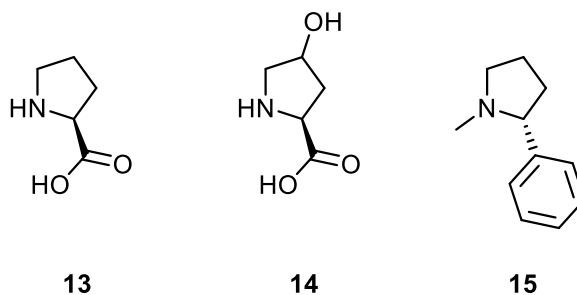


Figure (1-3) Pyrrolidine-containing natural products

1.2. Triazoles derivatives

In heterocyclic compounds, the presence of three nitrogen atoms represents an interesting subclass of materials. Triazole is a five-membered, unsaturated, planar, π -excessive heteroaromatic containing three nitrogen atoms in the cyclic ring system.¹⁶ Triazoles are crystals soluble in water / alcohol with a melting point of 120 °C and white to yellow in color.¹⁷ The name triazole was first given to the carbon- nitrogen ring system C₂N₃H₃ by Bladin,¹⁸ who described these derivatives in the nineteenth century. The most important types of triazole are 1,2,3-triazole (**16**) and the 1,2,4-triazole (**17**) (Figure 4):

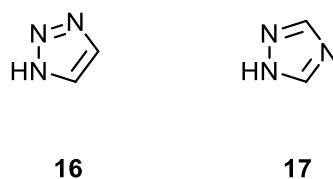


Figure (1-4). Structures of 1,2,3-triazole and 1,2,4-triazole

Numerous natural products are possessing triazole ring have broad pharmacological activities. The biological applications contain, and not limited to, biological anticonvulsant antioxidant, anti-urease¹⁹, anti-inflammatory^{20,21}, antimicrobial^{22,23}, and antimalarial activities²⁴.

1,2,4-Triazole is usually solid, easily soluble in polar solvents. During the last few years, 1,2,4-Triazole has been intensively studied due to its importance to various applications, especially anticancer, antifungal and antitubercular applications (Figure 5).

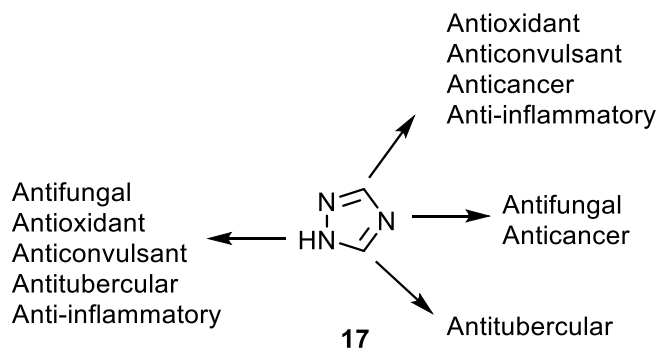
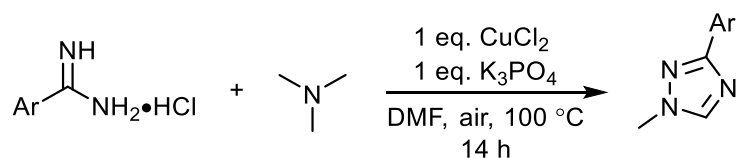


Figure (1-5) . The different pharmacological activities explored by different sites of 1,2,4-triazole

This paves the way to develop several methods for the synthesis of the 1,2,4-triazole using different conditions. 1,2,4-Triazoles can be synthesized via Cu-mediated reaction of amidines and trialkylamines using O_2 .²⁵



Scheme (1-1). Synthesis of 1,2,4-triazoles from amidines and trialkylamines in the presence of air

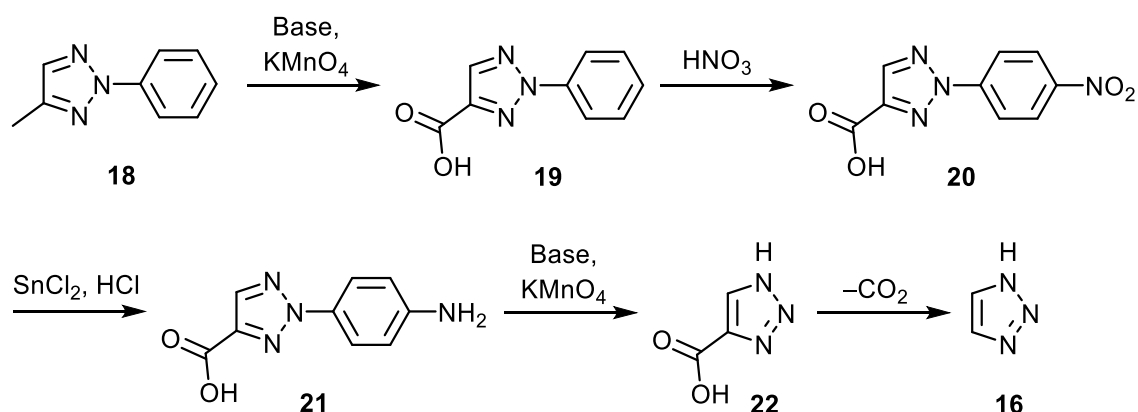
1.3. Compound of 1,2,3-Triazoles

1.3.1. Synthesis of 1,2,3-Triazoles

1,2,3-Triazole structure does not occur naturally, but its many synthetic derivatives were obtained. The most copacetic method of preparation of the trisubstituted triazoles

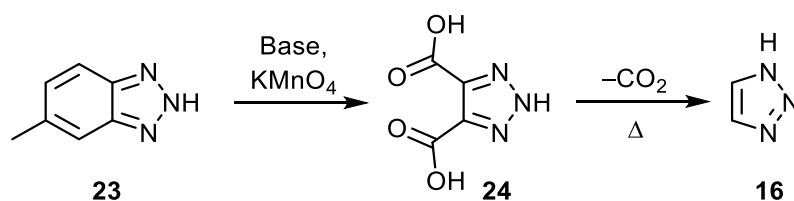
is from a diacylamine and a substituted hydrazine, this has been called the Einhorn-Brunner reaction.²⁶

Monocyclic 1,2,3-triazole synthetic was successful introduce in 1888.²⁷ Osotriazole is the name that has been used to describe certain 2-substituted 1,2,3-triazole derivatives.²⁸ 1*H*-1,2,3-Triazole (**16**) was successfully obtained from 2-phenyl-4-methyl-1,2,3-triazole (**18**) (Scheme 2)²⁹:



Scheme (1-2). Synthesis of 1*H*-1,2,3-triazole (**16**) from 1,2,3-triazole derivative **18**

The basic structure can be presented in benzotriazoles, by removing the fused benzene ring from methylbenzotriazole (**23**) oxidation, and thus also obtained the 1*H*-1,2,3-triazole (**16**) (Scheme 3)³⁰:



Scheme (1-3). Synthesis of 1*H*-1,2,3-triazole (**16**) from methylbenzotriazole (**23**)

1.3.1.1. Alkyne-azide cycloaddition reaction

In the [3 + 2] cycloaddition, a dipolarophile reacts with a 1,3-dipolar compound in a concerted, pericyclic reaction to form a 5-membered heterocycle.³¹ which includes a number of reactions that known as Huisgen cycloaddition.³² As dipolarophiles, alkynes, alkenes, but also multivalent groups, containing heteroatoms, such as nitriles or carbonyls, are also used. 1,3-dipolar compounds are substances that contain at least one heteroatom, and which can be described with at least one mesomeric boundary structure that contains two charges, that is called a dipole; such as: diazoalkanes, nitrile oxides, azides (Figure 6):

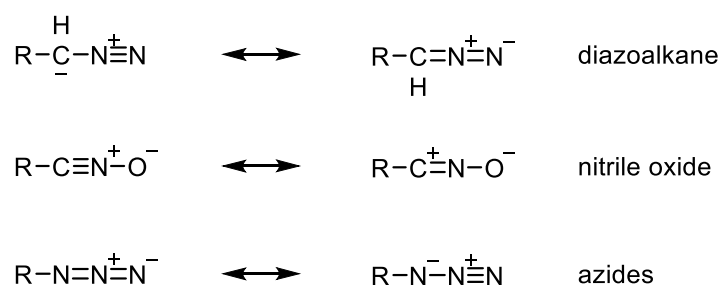
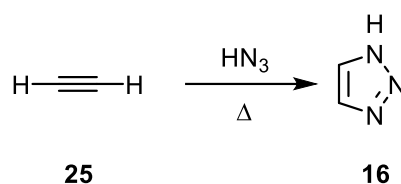


Figure (1-6). 1,3-dipolar compounds with mesomeric boundary structures

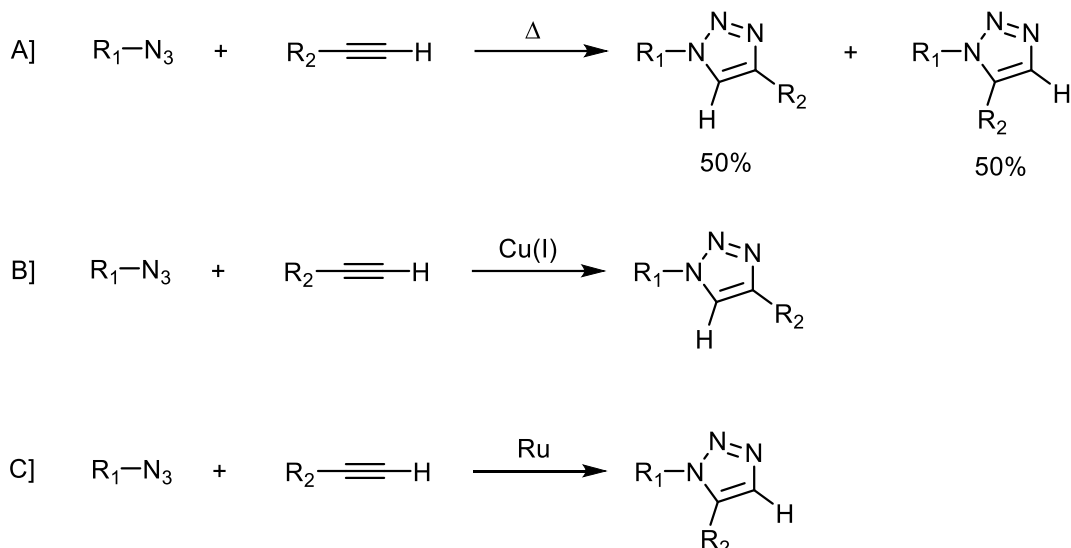
An important pathway to synthesize 1*H*-1,2,3-triazole (**16**) was made by the reaction of acetylene (**25**) with hydrazoic acid or organic azides (Scheme 4):



Scheme (1-4). Synthesis of compound **16** from acetylene

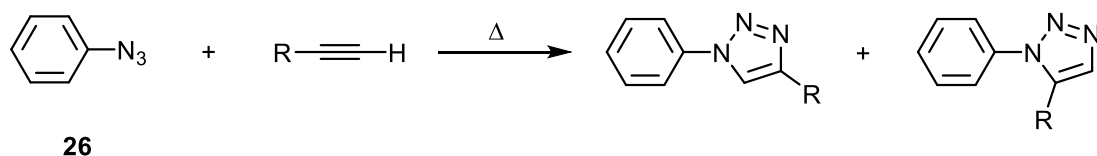
The remarkable thing about this reaction is that, unlike the other syntheses to 1,2,3-triazole derivatives, the heterocycle is rebuilt.³³ A rising problem start when the synthesis of 1,2,3-triazoles become more popular, it solved by the metal-catalyzed variants of this reaction. Usually, in the classic uncatalyzed [3 + 2] cycloaddition,

50:50 mixture of 1,4- and 1,5-substituted triazole is obtained, only the 1,4-substituted one is produced when using copper (I) as a catalyst, and only the 1,5-substituted one when using ruthenium as a catalyst derivative is obtained (Scheme 5):



Scheme (1-5). Comparison of the Huisgen cycloaddition (A) with the metal-catalyzed azide-alkyne cycloaddition (B and C)

The reaction of organoazides with alkynes lead to the investigation of synthesis of 1-phenyl-1,2,3-triazoles from phenyl azide (**26**) and acetylene derivatives. The reaction did not get much attention due to problem with final products (a mixture of regioisomers). Another problem is that, sometimes quite high reaction temperatures is required to overcome the activation energy. (Scheme 6)³⁴:



Scheme (1-6). The cycloaddition reaction of phenyl azide and acetylene derivatives

That is why the metal-catalyzed variant of the reaction, the Cu (I)-mediated alkyne-azide cycloaddition (CuAAC), in which only the 1,4-disubstituted 1,2,3-triazole is formed, paid more attention.

1.3.1.2. Copper-mediated cycloaddition reaction (Click reaction)

In the early 2002, two independently and simultaneously works were reported,^{35,36} demonstrated that the azide-alkyne cycloaddition can be catalyzed by copper (I) and thus proceeds faster and region selectively to the 1,4-substituted triazole.

Click chemistry can happen through small molecular building blocks, reliably on a small or large scale, can be connected to each other to synthesis larger molecules. This can be applied, among other things, to develop and synthesis of molecules with biological activity.^{37,38}

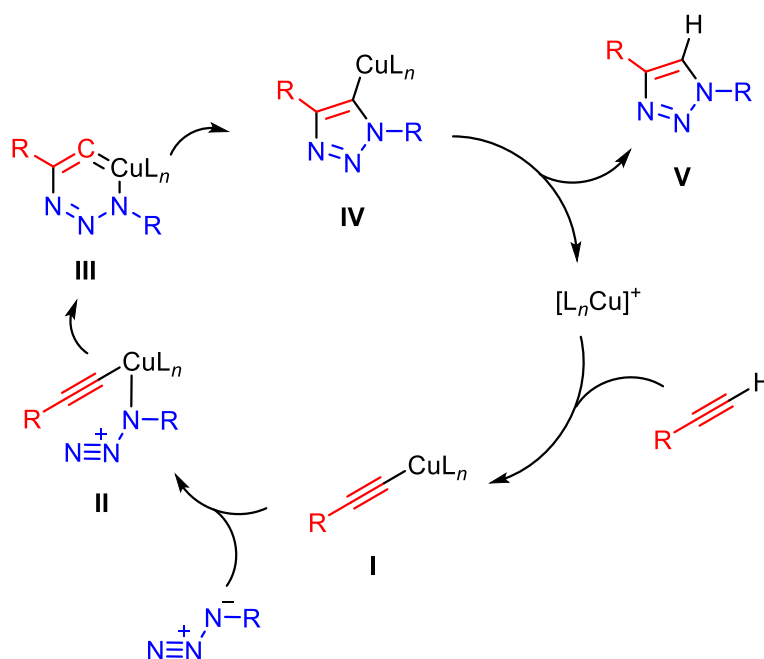
In order to be able to call a reaction a click reaction, it has certain rules such as the modular, extensively and applicable should run at the same time with very high yield. Moreover, the incidental by-products should be easily separable by non-chromatographic methods. Ideally, these reactions should not be sensitive to water or oxygen etc. Reactions that meet these requirements are, for example, cycloadditions of unsaturated compounds, in particular, 1,3-dipolar cycloadditions or also Diels-Alder-like reactions,^{39,40} since then it has been extensively investigated.⁴¹

These include the cycloaddition of azide and alkyne which proceeds to form a triazole ring.

The copper-catalyzed azide-alkyne cycloaddition (CuAAC) was a real breakthrough. The thermodynamically controlled CuAAC is characterized by its excellent compatibility with various functional groups and different solvents including water, simplicity, mild reaction conditions, as well as high pH tolerance.⁴² This makes the

CuAAC one of the most valuable tools for the synthesis and modification of complex organic frameworks and biologically relevant molecules.⁴³ The alkyne and azide functionalities can simply be introduced into one molecule and hardly go into side reactions with other functional groups or common reagents. Therefore, these functional groups can be unscathed by many synthesis stages. This further increases the significance of the CuAAC and has a large one share in success and broad applicability.⁴⁴

In CuAAC, a copper (I) specie is catalytically active. The proposed mechanism for this reaction suggests two copper atoms are involved in a catalytic cycle (Scheme 7)⁴⁵:



Scheme (1-7). Proposed mechanism of Cu-mediated click reaction

One of the simplest and most reliable sources of copper in CuAAC is copper(II) salts. For example, copper(II) sulfate can be reduced by sodium ascorbate, which is added in excess. The reaction can be carried out in aqueous solutions or in mixtures of water with different alcohols or with dimethyl sulfoxide (DMSO). The great advantage of the reduction of copper(II) salts is that this method tolerates oxygen in addition to

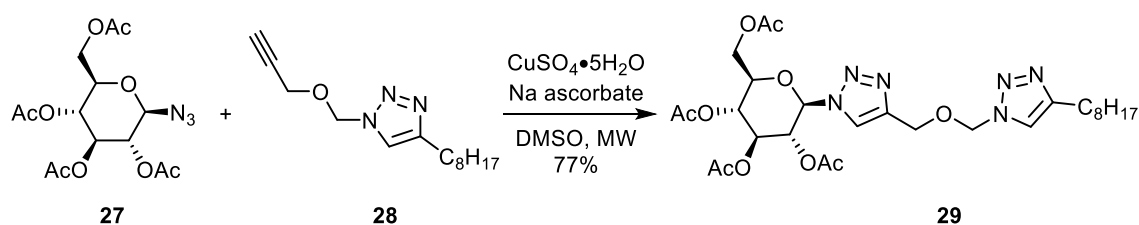
water. At the same time, however, this also represents a limiting factor for this method, as water- and oxygen-sensitive substrates cannot be implemented with this protocol.⁴⁶

In addition to the reduction of a copper (II) salt to copper (I), there is also the option of a direct use of copper (I) salt. This method requires anhydrous solvents because copper (I) in the Aqueous disproportionate to copper (0) and copper (II), as well as an inert atmosphere to the prevention of oxidation of the catalyst to copper (II). There is also the addition of a nitrogen base such as pyridine, *N,N*-diisopropylethylamine (DIPEA) or triethylamine (TEA), which also act as a ligand for the copper (I) species. The addition of an amine base to deprotonate the alkyne is only necessary in aprotic solvents, as the corresponding copper (I) acetylide is in aqueous forms media even under acidic conditions. DIPEA seems to be an excellent base, since this amine also has the CuAAC on surfaces such as that of microtiter plates or resins. Good results could also be achieved in toluene Copper (I) iodide, chloride or bromide as a catalyst, phosphorus ligands such as, for example Triphenylphosphine, and a base such as potassium acetate. Copper (I) salts are also suitable as a catalyst for CuAAC polymerization in organic media for the formation of polytriazoles, which would agglomerate in aqueous media. Good results were achieved in this application with (triethyl phosphite) copper (I) iodide. Catalysts such as tris (triphenylphosphine) copper (I) bromide are less suitable because the Staudinger reaction between triphenylphosphine and azide groups has a negative influence on the obtained molecular weight.⁴⁷⁻⁴⁹

1.3.1.3. Novel strategies for synthesis of 1,2,3-triazoles

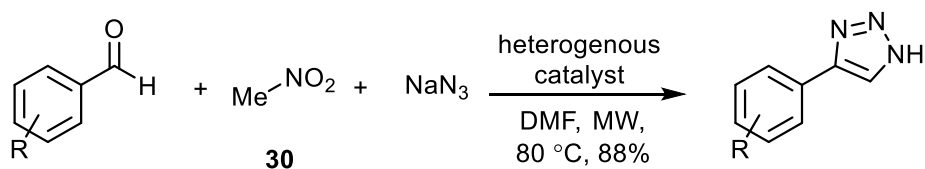
Although that the copper-catalyzed azide-alkyne cycloaddition (CuAAC) is fast reaction and has high regioselectivity, there are several pathways to accelerate the reaction, reduce the consumed energy or make it greener.

Mohammed *et al.*,⁵⁰ employed microwave to reduce the click reaction time from 48 h to 2 h by reacting of glucosyl azide (**27**) with alkynyl triazole **28** in the presence of $\text{CuSO}_4 \cdot 5\text{H}_2\text{O}$ and sodium ascorbate in DMSO to produce 4-(((1-*n*-Octyl-1*H*-1,2,3-triazol-4-yl)methoxy)methyl)-1-(2,3,4,6-tetra-*O*-acetyl- β -D-glucopyranosyl)1*H*-1,2,3-triazole (**29**) in 77% yield (Scheme 8):



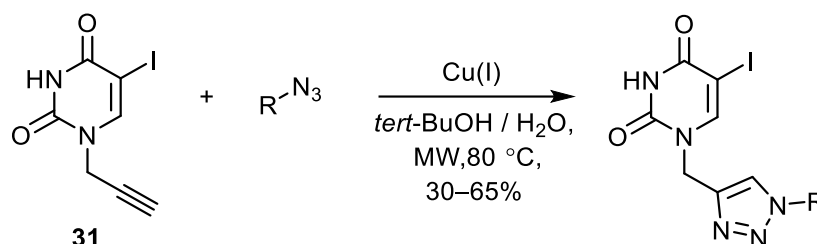
Scheme (1-8). Microwave-assisted synthesis of sugar-based bis-1,2,3-triazole **29**

Vergara-Arenas *et al.*,⁵¹ synthesized aryl 1,2,3-triazoles from the multi-component reaction of aryl aldehydes, nitromethane and sodium azide in the presence of heterogenous catalyst in DMF. The reaction is accelerated by microwaves irradiation at 80 °C for 30 minutes to give the desired products in 88% yield (Scheme 9):



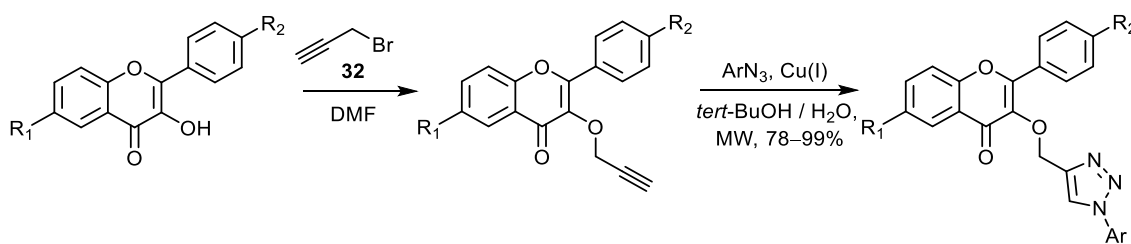
Scheme (1-9). Multi-Component Preparation of Aryl Triazoles in the Presence of Heterogenous Catalyst and Microwaves

Gregorić and co-workers⁵² utilized microwaves energy to prepare 1,4-disubstituted 1,2,3-triazole-linked pyrimidine-2,4-dione derivatives in fair yield from the reaction of alkynyl pyrimidines with organic azide derivatives in the presence of Cu(I) in *tert*-butanol / H₂O at 80 °C for 45 minutes. The prepared compounds found to possess potential anti-cancer activity (Scheme 10):



Scheme (1-10). Synthesis of pyrimidine-based 1,4-disubstituted 1,2,3-triazole

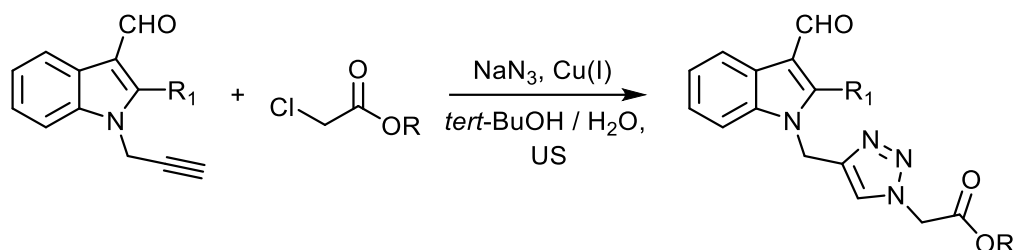
Znati et al.,⁵³ synthesized flavonoid-tethered 1,2,3 triazoles through the propargylation of the flavonoid core followed by microwave-assisted click reaction with aromatic azides (Scheme 11). The structures of the synthesized molecules were experimentally and theoretically determined, and compounds found to possess anticancer activity.



Scheme (1-11). Microwave-assisted synthesis of flavonoid-linked 1,2,3 triazoles

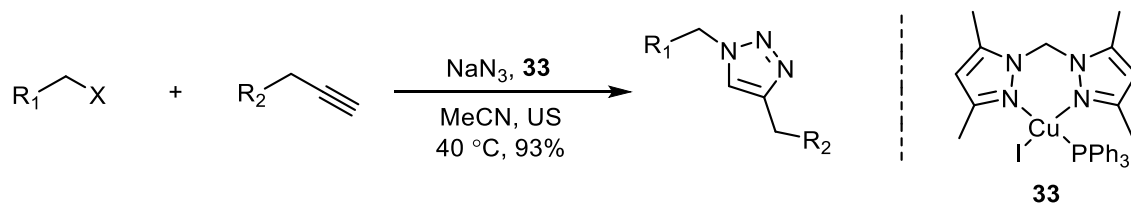
On the other hand, ultrasonic irradiation is recently employed in the synthesis of 1,4-disubstituted 1,2,3-triazoles as an environment friendly energy.⁵⁴ A multicomponent ultrasound-aided synthesis of 3-formylindole-containing 1,2,3-triazoles is recently

reported (Scheme 12).⁵⁵ The prepared compounds were examined against different kinds of pathogenic bacteria, and they exhibited potent antimicrobial activity.



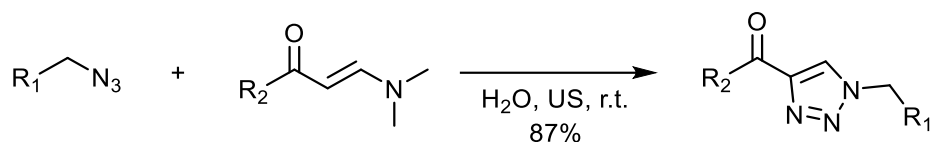
Scheme (1-12). Ultrasound-aided synthesis of 3-formylindole-containing 1,2,3-triazoles

Similarly, Castillo and co-workers⁵⁶ utilized ultrasonic radiation and bis(pyrazolyl)methan-bearing Cu(I) complex (**33**) to assist the formation of 1,4-disubstituted-1,2,3-triazoles in acetonitrile at 40 °C in excellent yields starting from three reactants (Scheme 13):



Scheme (1-13). Ultrasound-mediated synthesis 1,2,3-triazoles from three-components

Ultrasonic radiations have been used to synthesize 1,4-disubstituted-1,2,3-triazoles in 87% yield from the reaction of organic azides with amine-containing α,β -unsaturated carbonyl compounds in water at room temperature and in the absence of catalyst (Scheme 14)⁵⁷:



Scheme (1-14). Catalyst-free synthesis of 1,4-disubstituted-1,2,3-triazoles

1.4.Applications of 1,2,3-triazole derivatives

Because of their simple preparation and high product outcome, 1,2,3-triazoles have attracted the attention of the researchers globally. They are involved in many fields from pharmaceutical to the material applications.⁵⁸⁻⁶⁰

1.4.1. Medicinal and biological purposes

Owing to their exceptional skeleton features and extraordinary constancy towards numerous surroundings, 1,2,3-triazole derivatives were included in wide range of applications such as the design of drug and other utilities.⁶¹ Single important property of triazole derivatives is their performance as a hydrogen-bond (HB) contributor due to the hydrogen-5 which is bounded to an *sp*² C-5 atom and as a HB acceptor because of the existence of pyridine (*sp*²)- and pyrrole(*sp*³)-similar N atoms in their construction (Figure 7). What enhances their performance in the therapeutic applications.^{62,63}

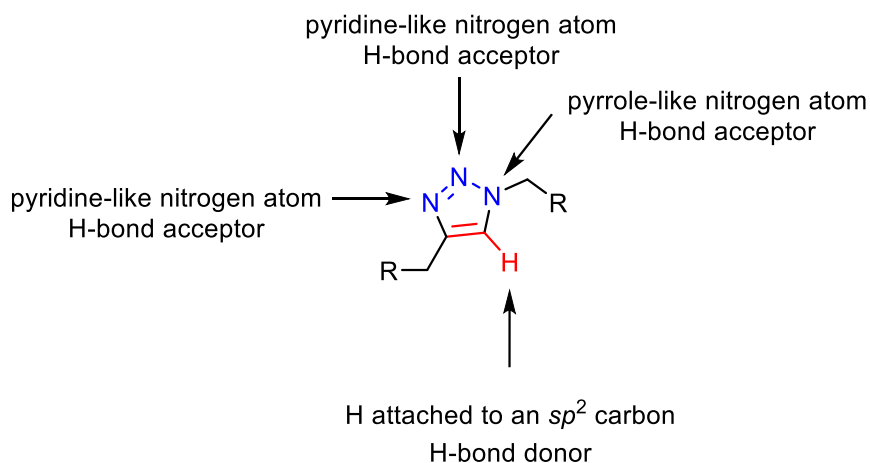


Figure (1-7) . Donor location and acceptor location in 1,2,3-triazoles

In the medicinal applications, 1,2,3-triazoles are included in many drugs that have been consumed as antiepileptic (Rufinamide (**34**))⁶⁴, antibiotic (Tazobactam (**35**))⁶⁵, anticancer (carboxyamiotriazole **36**)⁶⁶ (Figure 8), and even some pesticides used to control insects and weeds.⁶⁷

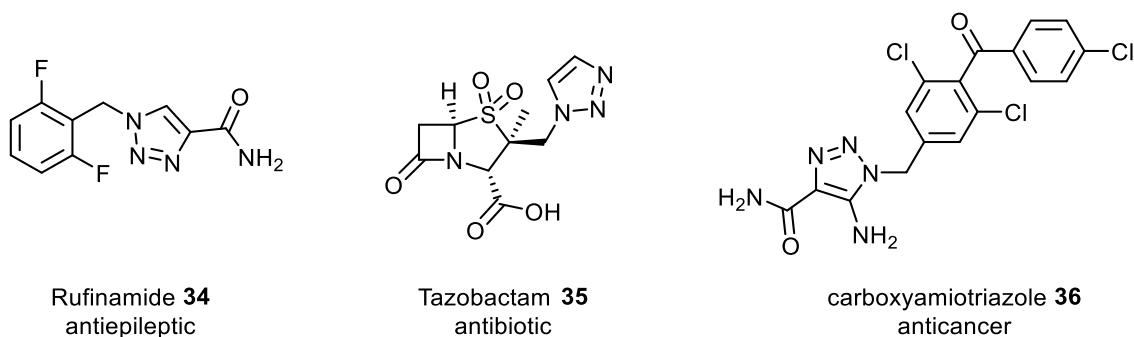


Figure (1-8). 1,2,3-Triazole-containing drugs

1,2,3-Triazole core can be considered as an amide bioisostere (Figure 9). Therefore, this heterocycle is extensively employed in the construction of linear and cyclic peptides.⁶⁸

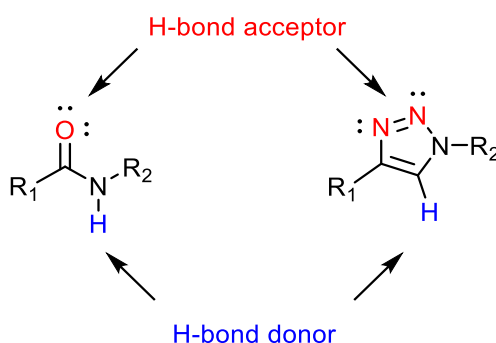


Figure 9. 1,2,3-Triazole as an amide bioisostere

The replacement of amide linkage by 1,2,3-triazole heterocycle play great role in the adjustment of the 3D shape of peptides.⁶⁹ Gabba et al.,⁷⁰ replaced the amide bond of the natural product migrastatin **37**, which is produced by *Streptomyces platensis* bacteria to inhibit fascin, by 1,2,3-triazole moiety to give compound **38** that have promising activity against breast cancer cells line MDA-MB-361 (Figure 10).

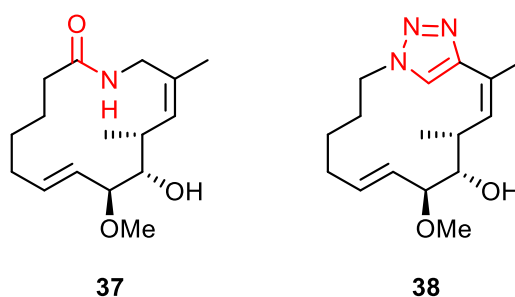
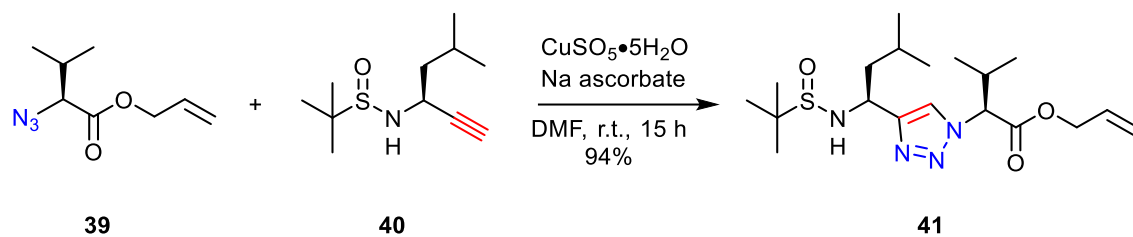


Figure (1-10) . Structure of migrastatin **37** and its triazole-containing analogous **38**

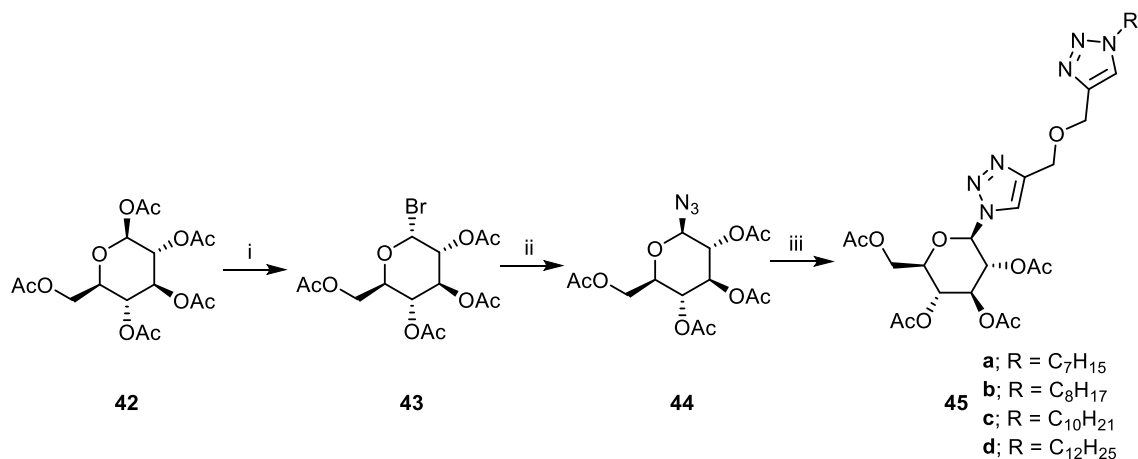
Schröder *et al.*⁷¹, synthesized the dipeptide **41** in 94% yield by the dimerization of α -azidoacid **39** with the alkyne **40** in the presence of copper sulfate and sodium ascorbate in a mixture of DMF / water at room temperature for 15 hours (Scheme 15). The conformation of the synthesized peptide has been studied in DMSO and water employing NMR and molecular dynamics. It was shown that the conformation of peptide in DMSO is different from that in water.



Scheme (1-15). Synthesis of dipeptide **41**

1,2,3-Triazoles are widely utilized in the field of carbohydrate chemistry through the tethering of these heterocycle to mono-, di or oligosaccharides. They are a powerful linkage as they are very stable and have hydrogen donor and acceptor events that can enhance the properties of sugar molecule.⁷²

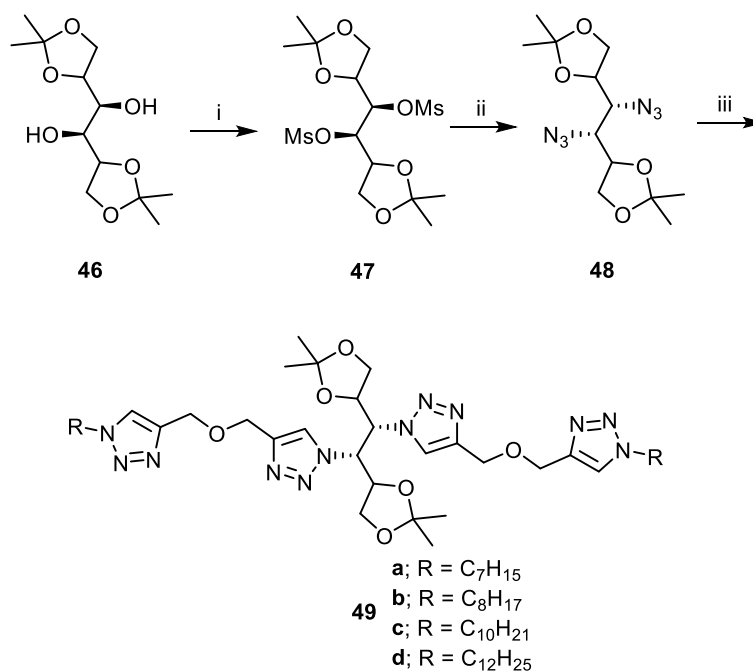
Sugar-based bis-1,2,3-triazoles derivatives **45a–d** have been synthesized by Mohammed and co-workers⁷³ starting from 1,2,3,4,6-penta-*O*-acetyl- β -D-glucopyranose (**42**) that was initially converted to glycosyl bromide **43** then to glycosyl azide **44** (Scheme 16). The synthesized bistriazole derivatives were characterized by advanced spectroscopic techniques and their biological activity was studied against bacteria. They found to have promising antibacterial activity.



Reagents and conditions: i) HBr in HOAc 80%, 0 °C–r.t., 2 h, 90%; ii) NaN₃, DMF, 50 °C; 3 h, 95%; iii) alkynyl triazoles, CuSO₄•5H₂O, Na ascorbate, DMSO, 36 h, 71–78%.

Scheme (1-16) . Preparation of bis-triazoles **45a–d** starting from compound **42**

The same research group utilized D-mannitol diacetonide (**46**) to synthesize tetrakis-1,2,3-triazole derivatives **49a–d**. In the first step, the hydroxyl groups of compound **46** were converted to excellent leaving groups through the reaction with methanesulfonyl chloride MsCl and triethylamine TEA in DCM to afford the dimesylate derivative **47**. The latter was reacted with sodium azide to give the diazido derivative **48**. This was then clicked with the previously prepared alkynyl triazoles to produce compounds **49a–d** in good yield (Scheme 17).⁷⁴ These compounds also exhibited moderate *in-vitro* antibacterial activity against *E. coli* and *S. aureus*.



Reagents and conditions: i) MsCl, TEA, DCM, 87%, -0 °C–r.t., 24 h, 90%; ii) NaN₃, DMF, 50 °C; 20 h, 75%; iii) alkynyl triazoles, CuSO₄•5H₂O, Na ascorbate, DMSO, 70 °C, 48 h, 70–83%.

Scheme (1-17) . Preparation of mannitol-based triazole derivatives **49a–d**

El-Malah et al.,⁷⁵ synthesized a library of monosaccharide-base 1,2,3-triazoles **50–52** via copper-catalyzed 1,3-cycloaddition reaction between propargyl glycosides and aromatic azides (Figure 11). The prepared compound showed excellent antimicrobial activity against *S. aureus*, *P. aeruginosa*, *C. albicans*, and *A. niger*.

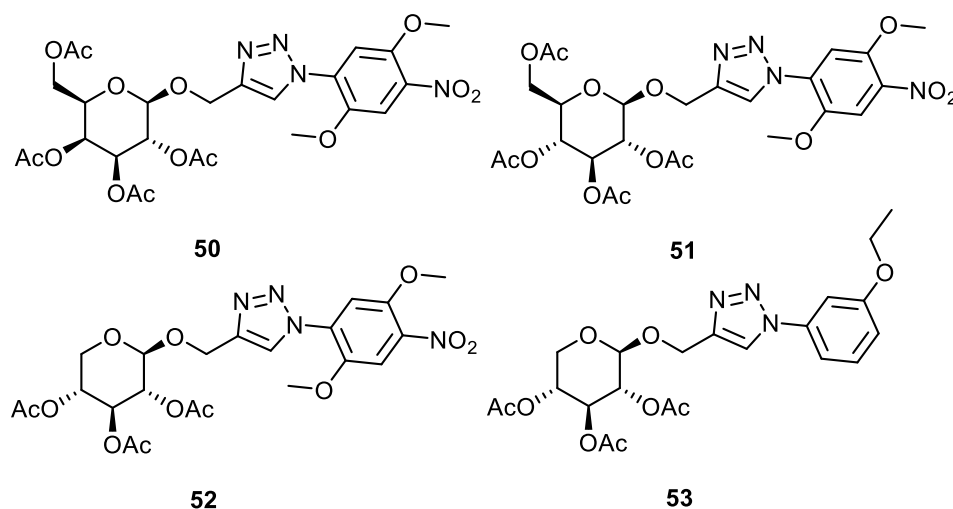
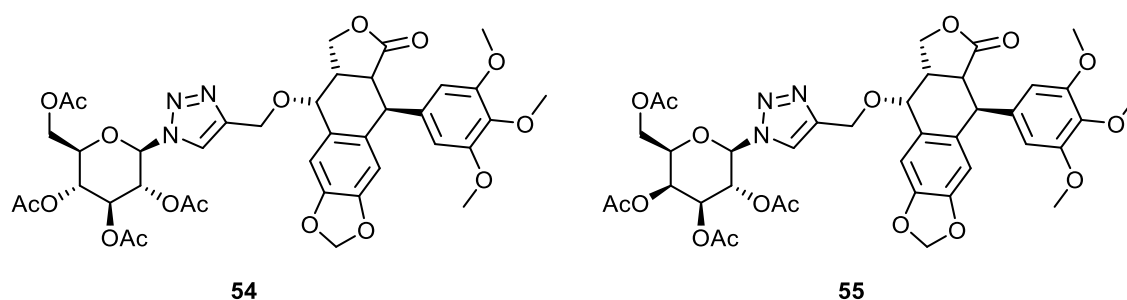
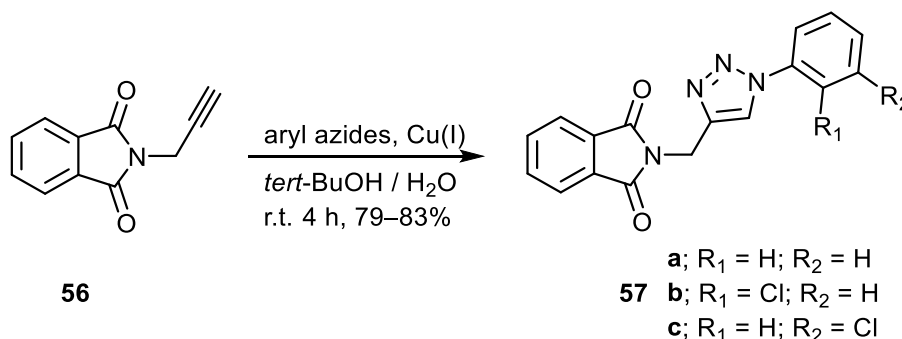


Figure (1-11). Antimicrobial monosaccharide-base 1,2,3-triazoles

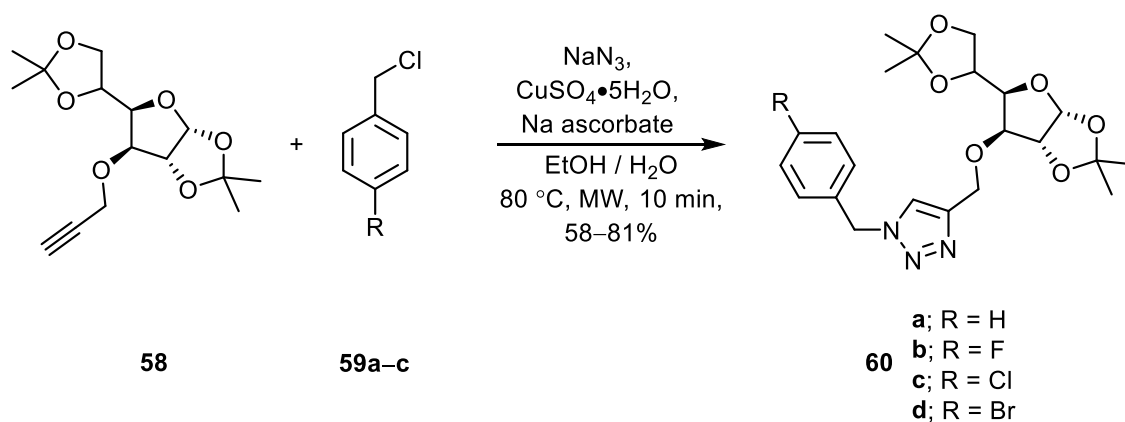
Glycosyl and galactosyl-based 1,2,3-triazole derivatives **54** and **55** (Figure 12) showed impressive *in-vitro* anticancer activity against breast cancer cells. These compounds have been prepared through the Ag(I)-catalyzed reaction of glycosyl or galactosyl azide with the 4- β -O-propargyl podophyllotoxin in ethanol at room temperature for 30 minutes.⁷⁶

**Figure (1-12)** . Sugar-podophyllotoxin-based 1,2,3-triazole derivatives **54** and **55**

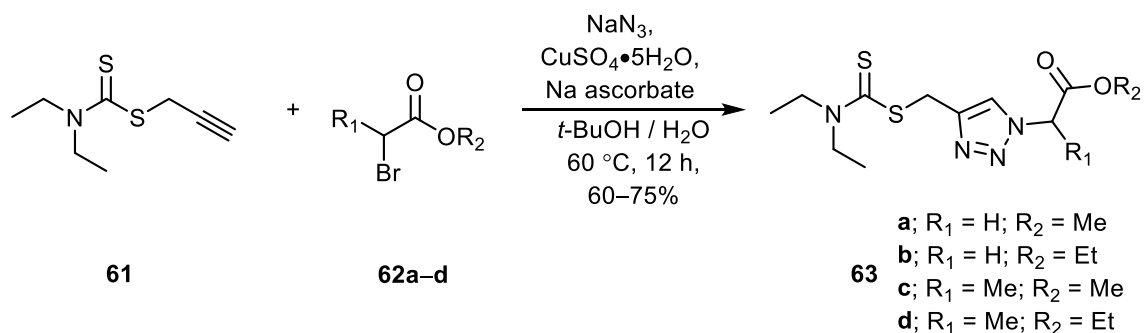
A recent study demonstrated that phthalimide-derived 1,2,3-triazole derivatives **57a–c** possess COVID-19 antiviral activity. The derivatives were prepared by the click reaction of N-propargylphthalimide (**56**) and various aromatic azides in *tert*-BuOH / water mixture (Scheme 18)⁷⁷:

**Scheme (1-18).** Synthesis of anti-COVID 19 triazole derivatives **57a–c**

A library of glucofuranose-tethered triazole compounds **60a–d** were prepared by one-pot reaction of 3-*O*-propargyl (1,2:5,6-di-*O*-isopropylidene- α -D-glucofuranose) (**58**) with the substituted benzyl chloride derivatives **59a–d** in the presence of sodium azide, copper sulfate and sodium ascorbate in a mixture of ethanol / water at 80 °C for 10 minutes. The reaction was accelerated by microwave irradiation and the produced compounds **60a–d** exhibited fair antimicrobial activity against *B. subtilis*, *S. aureus*, *E. coli*, *P. aeruginosa*, *C. utilis* and *A. niger* (Scheme 19)⁷⁸:

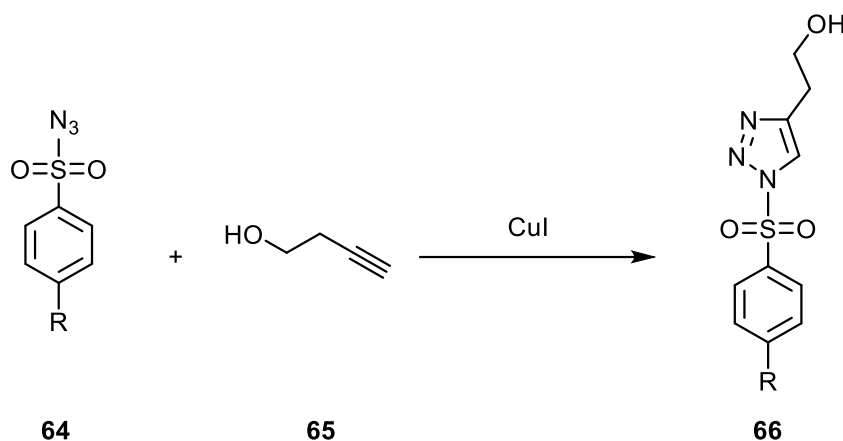


Scheme (1-19). Synthesis of glucofuranose-linked 1,2,3-triazole derivatives **60a–d** Karbasi *et al.*⁷⁹, synthesized of novel 1,2,3-triazole-dithiocarbamate hybrids **63a–d** in moderate to good yield starting from dithiocarbamate propargyl derivative **61** and studied the structural properties using density functional theory (DFT) approach. It is found that the electron density is located around the triazole ring (Scheme 20):



Scheme (1-20). Synthesis of 1,2,3-triazole-dithiocarbamate hybrids **63a-d**

1,2,3-Triazoles have been employed as anticorrosion agents.⁸⁰ Zhang et al.,⁸¹ recently synthesized the triazole derivative **66** through the copper-catalyzed 1,3-cycloaddition reaction of dodecylbenzenesulfonyl azide (**64**) to 3-butyn-1-ol (**65**). The anticorrosive activity of derivative **66** was investigated on pure copper and it showed high protection 96.9 % for copper films against alkaline solution (Scheme 21).



Scheme (1-21). Synthesis of anticorrosion agent **66**

1.5. The objectives of this thesis

There are three main objectives for this thesis: as shown below

- 1- Using Cu-mediated click reaction to prepare new triazole compounds beginning from D-galactose.
- 2- Besides the thin layer chromatography, all the synthesized derivatives are fully identified by FT-IR, proton NMR, carbon NMR, fluorine NMR, and 2D NMR.
- 3- The cytotoxicity of the target triazole compounds are tested versus mesenchymal stem cells MSCs.

CHAPTER TWO
EXPERIMENTAL
PART

2. Experimental Part

2.1. Typical methods

The chemicals were supplied from various chemicals' providers, and they were employed without further purifications. Oven-dried glassware were employed in all experiments. TLC plates used in the reactions monitoring are Al-supported silica 60 F₂₅₄ (0.2 mm) provided by Merck and KMnO₄ staining solution was utilized to visualise the spots. In the column chromatography, the stationary phase was silica gel 40–63 mesh and eluting solvents (ethyl acetate and hexane) were applied as mobile phase. Shimadzu FTIR spectrometer was used to measure the FTIR spectra of the prepared molecules. Bruker Advance III NMR instruments (300 or 600 MHz) were used to collect to record NMR spectra at 298 K (± 1 K), The NMR spectra were measured at Nuclear Magnetic Resonance Facility, Mark Wainwright Analytical Centre, The University of New South Wales, Sydney, Australia. Residual solvents peaks were utilised in the calibration of proton NMR and carbon NMR spectra. Chemical shifts were reported in part per million ppm. High resolution mass spectra HRMS were recorded at the Bioanalytical Mass Spectrometry Facility, Mark Wainwright Analytical Centre, The University of New South Wales UNSW, Sydney, Australia using Orbitrap LTQ XL ion trap MS in positive ion mode using electrospray ionisation (ESI) source.

2.2. Preparation methods and Identification

2.2.1. Method 1: Preparation of azido fluorobenzyl derivatives 68a–c

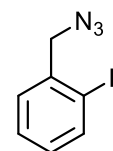
(Improved method)

To the stirred solution of the suitable fluorobenzyl bromide **67a–c** (10 mmol) in dimethyl sulfoxide (25 mL), sodium azide (1.95 g, 30 mmol) was added. The reaction

mixture was heated to 50 °C with stirring for one day. After which time, water (50 mL) was added to the suspension and mixture was extracted with EtOAc (3 × 50 mL). The collective ethyl acetate layers were washed with brine (2 × 50 mL), water (50 mL), dried with anhydrous sodium sulfate and evaporated to dryness under using rotary evaporator to give a yellowish liquid. The crude products were purified by column chromatography (silica gel, n-hexane / ethyl acetate; 10:0 → 9:1,) to give the proper azide derivative.⁸²

2-Fluorobenzene azide (68a)

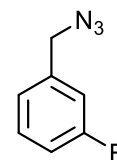
Pale liquid (1.36 g, 89%). $R_f = 0.75$ (EtOAc). FTIR (KBr) cm^{-1} : 3352, 3053, 2936, 2880, 2101, 1615, 1586, 1491, 1453, 1347, 1235, 1181, 1102, 1032, 942, 884, 838, 755, 668, 587, 550, 521, 423. $^1\text{H NMR}$ (CDCl_3 , 600 MHz) δ ppm:



7.35–7.31 (m, 2H, Ar-H), 7.16 (td, $J = 7.6, 1.0$ Hz, 1H, Ar-H), 7.11 (t, $J = 9.1$ Hz, 1H, Ar-H), 4.42 (s, 2H, Ar-CH₂). $^{13}\text{C NMR}$ (150 MHz, CDCl_3) δ ppm: 161.1 (d, $J = 247.4$ Hz, ArC), 130.6 (d, $J = 4.1$ Hz, ArC), 130.5 (d, $J = 8.6$ Hz, ArC), 124.4 (d, $J = 3.4$ Hz, ArC), 122.7 (d, $J = 15.3$ Hz, ArC), 115.7 (d, $J = 21.7$ Hz, Ar-C), 48.5 (d, $J = 3.1$ Hz, Ar-CH₂). $^{19}\text{F NMR}$ (CDCl_3 , 564 MHz) δ ppm: -117.8 (m, 1F, Ar-F).

3-Fluorobenzene azide (68c)

Pale liquid (1.23 g, 81%). $R_f = 0.75$ (EtOAc). FTIR (KBr) cm^{-1} : 3063, 2934, 2878, 2101, 1615, 1592, 1486, 1451, 1343, 1258, 1138, 1102, 1077, 942, 892, 861, 784, 751, 691, 556, 523, 442. $^1\text{H NMR}$ (CDCl_3 , 600 MHz) δ ppm: 7.35

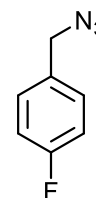


(m, 1H, Ar-H), 7.12 (m, 1H, Ar-H), 7.05–7.02 (m, 2H, Ar-H), 4.33 (s, 2H, Ar-CH₂). $^{13}\text{C NMR}$ (150 MHz, CDCl_3) δ ppm: 163.1 (d, $J = 246.5$ Hz, ArC), 138.1 (d, $J = 7.2$ Hz, ArC), 130.4 (d, $J = 8.5$ Hz, ArC), 123.6 (d, $J = 3.1$ Hz, ArC), 115.2 (d, $J = 21.0$

Hz, ArC), 115.2 (d, $J = 22.1$ Hz, Ar-C), 54.1 (Ar-CH₂). ¹⁹F NMR (CDCl₃, 564 MHz,) δ ppm: -112.4 (m, 1F, Ar-F).

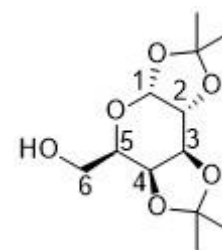
4-Fluorobenzene azide (68c)

Pale liquid (1.41 g, 92%). $R_f = 0.74$ (EtOAc). FTIR (KBr) cm^{-1} : 3044, 2932, 2878, 2101, 1601, 1511, 1451, 1343, 1225, 1156, 1096, 1015, 940, 880, 851, 822, 766, 664, 541, 481, 421. ¹H NMR (CDCl₃, 600 MHz,) δ ppm: 7.31–7.27 (m, 2H, Ar-H), 7.05–7.02 (m, 2H, Ar-H), 4.32 (s, 2H, Ar-CH₂). ¹³C NMR (150 MHz, CDCl₃) δ ppm: 162.6 (d, $J = 248.2$ Hz, ArC), 131.2 (d, $J = 3.1$ Hz, ArC), 130.0 (d, $J = 8.2$ Hz, ArC), 115.7 (d, $J = 21.8$ Hz, Ar-C), 54.2 (Ar-CH₂). ¹⁹F NMR (CDCl₃, 564 MHz) δ ppm: -113.7 (m, 1F, Ar-F).



2.2.2. Synthesis of α -D-galactose diacetonide (70) (improved procedure)⁸³

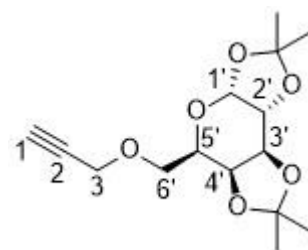
D-Galactose (**69**) (34.5 g, 0.19 mol) was added at r.t. in one batch to the mixture of zinc chloride (40 g, 0.29 mol), acetone (450 mL) and conc. H₂SO₄ (1.0 mL) to form a clear solution. The resulting white suspension was stirred for 6 h at r.t. The reaction mixture was quenched at 0 °C by the suspension of sodium carbonates (66.4 g, 0.61 mol) in distilled water (100 mL). The mixture was stirred for half an hour then filtered and the solid removed. Volatile solvent was reduced using rotary evaporator to give a yellow oil and aqueous layer were separated, and aqueous layer further extracted with diethyl ether (3 \times 125 mL). The combined organic layers were dried over anhydrous sodium sulfate, and the solvent removed in rotary evaporator to give α -D-galactopyranose diacetonide (**70**) as a pale-yellow oil (38.0 g, 81%) $R_f = 0.45$ (50:50 hexane/ether). FTIR (KBr) cm^{-1} : 3483, 2987, 2935, 1382, 1255, 1212, 1167, 1069, 1001, 899. ¹H NMR (300 MHz, CDCl₃) δ ppm: 5.56 (d, $J = 5.0$ Hz, 1H, H1), 4.60 (dd, $J = 8.0, 2.4$



Hz, 1H, H3), 4.32 (dd, $J = 5.0, 2.4$ Hz, 1H, H2), 4.26 (dd, $J = 7.9, 1.6$ Hz, 1H, H4), 3.86 (ddd, $J = 7.3, 4.7, 2.0$ Hz, H5), 3.83 (dd, $J = 10.7, 4.7$ Hz, 1H, H6a), 3.74 (dd, $J = 10.7, 7.3$ Hz, 1H, H6b), 2.37 (br s, 1H, OH), 1.52 (s, 3H, CH₃), 1.44 (s, 3H, CH₃), 1.32 (s, 6H, C(CH₃)₂). ¹³C {¹H} NMR (75 MHz, CDCl₃) δ ppm: 109.4 and 108.6 (2 \times C(CH₃)₂), 96.3 (C1), 71.5 (C4), 70.7 (C3), 70.5 (C2), 68.6 (C5), 62.3 (C6), 24.3 (CH₃), 24.9 (CH₃), 25.9 (CH₃), 26.0 (CH₃).

2.2.3. Synthesis of 6-*O*-propargyl- α -D-galactose diacetonide (71)⁸⁴

Propargyl bromide (2.1 mmol) was added dropwise to the mixture of α -D-galactose diacetonide (70) (0.51 g, 2 mmol) and sodium hydroxide (0.32 g, 8 mmol) in *N,N*-dimethylformamide (7 mL) at -15 °C. The reaction mixture



was then allowed warm to r.t. and was stirred for 24 h. After which time, the reaction quenched with cold water (25 mL) and extracted with ether (3 \times 50 mL). The combined extracts were dried over anhydrous sodium sulfate and evaporated to dryness by rotary evaporator. The residue was purified by column chromatography (silica gel, ether /*n*-Hexane 1:9) to give propargyl- α -D-galactosyl ether (71) as a white wax (1.11 g, 88%), $R_f = 0.42$ (50:50 Hexane/ ether). FTIR (KBr) cm^{-1} : 3253, 2922, 2853, 2109, 1459, 1377, 1258, 1213, 1101, 1066, 1004, 890. ¹H NMR (CDCl₃, 300 MHz) δ ppm: 5.54 (d, $J = 5.0$ Hz, 1H, H1'), 4.60 (dd, $J = 7.9, 2.4$ Hz, 1H, H3'), 4.31 (dd, $J = 5.0, 2.4$ Hz, 1H, H2'), 4.26 (dd, $J = 7.9, 2.0$ Hz, 1H, H4'), 4.24 (dd, $J = 15.9, 2.4$ Hz, 1H, H3a), 4.19 (dd, $J = 15.9, 2.4$ Hz, 1H, H3b), 3.99 (ddd, $J = 7.1, 6.2, 2.0$ Hz, 1H, H5'), 3.77 (dd, $J = 10.1, 6.2$ Hz, 1H, H6'a), 3.66 (dd, $J = 10.1, 7.1$ Hz, H, H6'b), 2.42 (t, $J = 2.4$ Hz, 1H, H1), 1.32 (s, 3H, CH₃), 1.34 (s, 3H, CH₃), 1.45 (s, 3H, CH₃), 1.54 (s, 3H, CH₃). ¹³C {¹H} NMR (CDCl₃, 75 MHz) δ ppm: 109.3 and 108.6 (2 \times

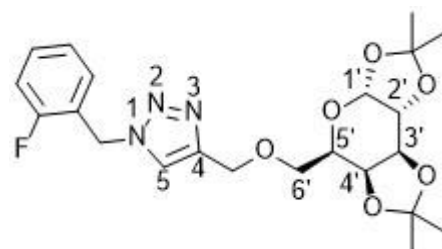
C(CH₃)₂), 96.3(C1'), 79.6 (C2), 74.6 (C1), 71.2 (C4'), 70.6 (C3'), 70.4 (C2'), 68.7 (C6'), 66.7 (C5'), 58.4 (C3), 24.4 (CH₃), 24.9 (CH₃), 25.9 (CH₃), 26.0 (CH₃).

2.2.4. General procedure 2: Preparation of 1,2,3-triazoles⁸⁵

A suitable fluorobenzyl azide (1.1 mmol, 0.17 g) was added to the mixture of propargyl ether **71** (1.1 mmol, 0.31 g) Na ascorbate (0.020 g, 0.1 mmol), and copper sulphate pentahydrate (0.013 g, 0.005 mmol) in dimethyl sulfoxide (3 mL). The mixture was heated to 50 °C with stirring for 36 h. Then, the mixture was quenched with distilled water (30 mL), extracted with ethyl acetate (3 × 30 mL), the merged ethyl acetate layers washed with brine (2 × 25 mL), dried over anhydrous sodium sulfate and evaporated by rotary evaporator. The residue was purified by column chromatography (silica gel, *n*-hexane / ethyl acetate; 2:1 → 1:2,) to give the corresponding triazole derivative.

Compound 72a

Pale-yellow syrup (0.38 g, 87%); *R_f* = 0.58 (ethyl acetate). FTIR (KBr) cm⁻¹: 3140, 3057, 2987, 2933, 1620, 1589, 1494, 1460, 1379, 1305, 1255, 1213, 1170, 1101, 1070, 1004, 920, 893, 860, 800, 763,



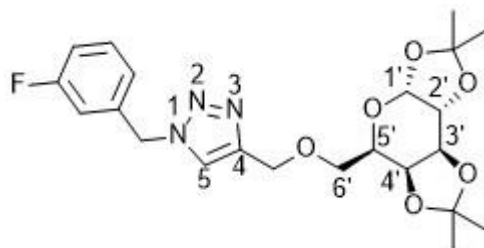
734, 700, 650, 513, 435. ¹H NMR (CDCl₃, 600 MHz) δ ppm: 7.58 (s, 1H, H5), 7.33 (dddd, *J* = 13.6, 7.3, 5.4, 1.7 Hz, 1H, Ar-H), 7.24 (td, *J* = 7.5, 1.7 Hz, 1H, Ar-H), 7.13 (td, *J* = 7.5, 1.0 Hz, 1H, Ar-H), 7.09 (m, 1H, Ar-H), 5.55 (s, 2H, Ar-CH₂-triazole), 5.50 (d, *J* = 5.0 Hz, 1H, H1'), 4.69 (d, *J* = 12.5 Hz, 1H, triazole-CH₂-CHO), 4.66 (d, *J* = 12.5 Hz, 1H, triazole-CH₂-CHO), 4.57 (dd, *J* = 8.0, 2.4 Hz, 1H, H3'), 4.28 (dd, *J* = 5.0, 2.4 Hz, 1H, H2'), 4.21 (dd, *J* = 7.9, 1.9 Hz, 1H, H4'), 3.97 (ddd, *J* = 7.1, 5.4, 1.8 Hz, 1H, H5'), 3.70 (dd, *J* = 10.3, 5.5 Hz, 1H,

H6'a), 3.64 (dd, $J = 10.2, 7.0$ Hz, H, H6'b), 1.49 (s, 3H, CH₃), 1.40 (s, 3H, CH₃), 1.30 (s, 6H, C(CH₃)₂). ¹³C NMR (150 MHz, CDCl₃) δ ppm: 160.6 (d, $J = 247.8$ Hz, ArC), 145.8 (C4), 131.0 (d, $J = 7.8$ Hz, ArC), 130.7 (d, $J = 3.0$ Hz, ArC), 124.9 (d, $J = 4.0$ Hz, ArC), 122.8 (C5), 122.0 (d, $J = 14.3$ Hz, ArC), 115.9 (d, $J = 21.2$ Hz, ArC), 109.3 (C(CH₃)₂), 108.6 (C(CH₃)₂), 96.4 (C1'), 71.2 (C4'), 70.7 (C3'), 70.6 (C2'), 69.4 (C6'), 66.8 (C5'), 65.0 (triazole-CH₂-CHO), 47.7 (d, $J = 4.3$ Hz, Ar-CH₂-triazole), 26.1 (CH₃), 26.0 (CH₃), 25.0 (CH₃), 24.0 (CH₃). ¹⁹F NMR (564 MHz, CDCl₃) δ ppm: -118.2 (m, 1F, Ar-F). HRMS-ESI [M + Na]⁺ calculated for C₂₂H₂₈FN₃O₆Na⁺: 472.1854; found: 472.1851.

Compound 72b

Pale-yellow syrup (0.36 g, 83%); $R_f = 0.58$

(ethyl acetate). FTIR (KBr) cm⁻¹: 3138, 3063, 2987, 2931, 1618, 1593, 1489, 1454, 1379, 1307, 1255, 1213, 1170, 1101, 1070, 1004, 920,

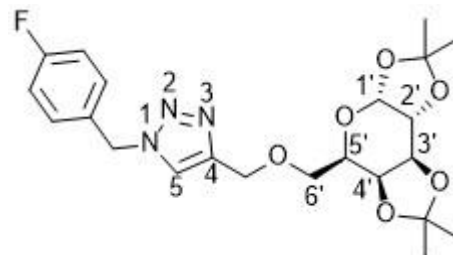


893, 862, 781, 754, 684, 650, 515, 439. ¹H NMR (600 MHz, CDCl₃) δ ppm: 7.52 (s, 1H, H5), 7.34 (ddd, $J = 13.7, 7.9, 5.8$ Hz, 1H, Ar-H), 7.05–7.02 (m, 2H, Ar-H), 6.95 (dt, $J = 9.2, 1.8$ Hz, 1H, Ar-H), 5.51 (d, $J = 5.0$ Hz, 1H, H1'), 5.50 (s, 2H, Ar-CH₂-triazole), 4.71 (dd, $J = 12.5, 0.5$ Hz, 1H, triazole-CH₂-CHO), 4.68 (dd, $J = 12.6, 0.5$ Hz, 1H, triazole-CH₂-CHO), 4.58 (dd, $J = 7.9, 2.4$ Hz, 1H, H3'), 4.29 (dd, $J = 5.0, 2.4$ Hz, 1H, H2'), 4.22 (dd, $J = 7.9, 1.9$ Hz, 1H, H4'), 3.98 (ddd, $J = 7.0, 5.6, 1.8$ Hz, 1H, H5'), 3.71 (dd, $J = 10.3, 5.4$ Hz, 1H, H6'a), 3.66 (dd, $J = 10.3, 7.1$ Hz, H, H6'b), 1.50 (s, 3H, CH₃), 1.40 (s, 3H, CH₃), 1.31 (s, 6H, C(CH₃)₂). ¹³C NMR (150 MHz, CDCl₃) δ ppm: 163.1 (d, $J = 247.9$ Hz, ArC), 146.1 (C4), 137.1 (d, $J = 7.1$ Hz, ArC), 130.9 (ArC), 123.7 (C5), 122.7 (d, $J = 26.1$ Hz, ArC), 115.9 (d, $J = 20.9$ Hz, ArC), 115.2 (d, $J = 22.1$ Hz, ArC), 109.4 (C(CH₃)₂), 108.7 (C(CH₃)₂), 96.5 (m, 1C,

C1'), 71.3 (C4'), 70.8 (d, $J = 17.5$ Hz, C3'), 70.6 (m, 1C, C2'), 69.5 (C6'), 66.8 (m, 1C, C5'), 65.0 (triazole $-\underline{\text{C}}\text{H}_2-\text{CHO}$), 53.6 (Ar- $\underline{\text{C}}\text{H}_2$ -triazole), 26.1 (CH₃), 26.0 (CH₃), 25.0 (m, CH₃), 24.6 (m, CH₃). ¹⁹F NMR (564 MHz, CDCl₃) δ ppm: -111.6 (dddd, $J = 15.1, 9.3, 5.9, 0.7$ Hz, 1F, Ar-F). HRMS-ESI [M + Na]⁺ calculated for C₂₂H₂₈FN₃O₆Na⁺: 472.1854; found: 472.1851.

Compound 72c

Pale-yellow syrup (0.40 g, 90%); $R_f = 0.58$ (ethyl acetate). FTIR (KBr) cm⁻¹: 3138, 3068, 2987, 2929, 1651, 1606, 1512, 1458, 1379, 1303, 1253, 1217, 1168, 1105, 1072, 1004, 893, 854, 785, 736,



700, 694, 644, 503, 418. ¹H NMR (600 MHz, CDCl₃) δ ppm: 7.48 (s, 1H, H5), 7.25 (app t, $J = 7.5$, 2H, Ar-H), 7.05 (app t, $J = 8.6$ Hz, 2H, Ar-H), 5.51 (d, $J = 5.1$ Hz, 1H, H1'), 5.48 (s, 2H, Ar- $\underline{\text{C}}\text{H}_2$ -triazole), 4.70 (d, $J = 12.5$ Hz, 1H, triazole- $\underline{\text{C}}\text{H}_2$ -CHO), 4.67 (d, $J = 12.6$ Hz, 1H, triazole- $\underline{\text{C}}\text{H}_2$ -CHO), 4.58 (dd, $J = 7.9, 2.4$ Hz, 1H, H3'), 4.29 (dd, $J = 5.0, 2.4$ Hz, 1H, H2'), 4.22 (dd, $J = 7.9, 1.9$ Hz, 1H, H4'), 3.97 (ddd, $J = 7.0, 5.4, 1.7$ Hz, 1H, H5'), 3.70 (dd, $J = 10.3, 5.5$ Hz, 1H, H6'a), 3.65 (dd, $J = 10.3, 7.0$ Hz, H, H6'b), 1.50 (s, 3H, CH₃), 1.41 (s, 3H, CH₃), 1.312 (s, 3H, CH₃), 1.31 (s, 3H, CH₃). ¹³C NMR (150 MHz, CDCl₃) δ ppm: 163.0 (d, $J = 247.8$ Hz, ArC), 146.0 (C4), 130.6 (d, $J = 3.3$ Hz, ArC), 130.1 (d, $J = 8.7$ Hz, ArC), 122.4 (C5), 116.2 (d, $J = 21.9$ Hz, Ar-C), 109.4 (C(CH₃)₂), 108.7 (C(CH₃)₂), 96.5 (C1'), 71.3 (C4'), 70.8 (C3'), 70.6 (C2'), 69.5 (C6'), 66.8 (C5'), 65.0 (triazole $-\underline{\text{C}}\text{H}_2-\text{CHO}$), 53.5 (Ar- $\underline{\text{C}}\text{H}_2$ -triazole), 26.18 (CH₃), 26.1 (CH₃), 25.0 (CH₃), 24.6 (CH₃). ¹⁹F NMR (564 MHz, CDCl₃) δ ppm: -112.8 (m, 1F, Ar-F). HRMS-ESI [M + Na]⁺ calculated for C₂₂H₂₈FN₃O₆Na⁺: 472.1854; found: 472.1853.

2.3. Computational method

The computational study was performed using the ORCA 4.2.1 software.^{86,87} The initial structures of compound **71** were drawn using the Avogadro program and were energy minimized at the B3LYP/def2-TZVP level of theory. The optimized geometries were verified by performing frequency calculation at B3LYP/def2-TZVP level (zero imaginary frequencies). Subsequently, single point energy calculations at the MO6-2X/def2-TZVP level were performed with solvation method using the conductor-like polarizable continuum model (CPCM) in chloroform (CHCl₃).

2.4. Triazoles' cytotoxicity (improved Procedure)⁸⁸

2.4.1. Samples' Preparation

A mixture of (water / DMSO; 9:1) (20 μ L) was briefly added to the prepare triazole derivatives **72a–c** until they were totally solubilized. The volume was the completed with MiliQ water to (200 μ L) to make up 1mM stock solution. The later was consequently diluted to prepare the diluted solution (0.5 mM).

2.4.2. Cells' Maintenance

Mesenchymal stem cells MSCs have been collected in section three when they achieved 80% confluency by adding pre-heated 0.25% Trypsin-ethylene diamine tetraacetate. Next, it was kept in the incubator at 37 °C provided with 5% carbon dioxide for five minutes. The trypsinization have being neutralized by the addition of media of cells' growth that consists of 10% FBS, 1% penicillin/streptomycin in Dulbecco's Modified Eagle Medium when cells have been entirely removed form the flask. The mixture in the cell has been transferred in 15 mL tube and centrifuged at 600 rpm for six minutes. The supernatant was removed, and cell pellet was then re-suspended in 1 mL cell growth media.

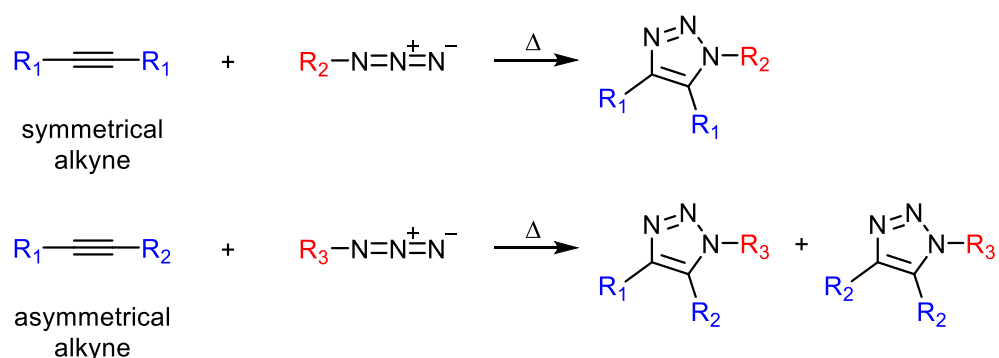
2.4.3. Cells' Culture

A Polystyrene 96 well plate was employed to triplicate deposit the solutions of compounds **72a–c** (1.0 mM) and (0.5 mM) and 5000 cells/well added atop of samples. The untreated cells in the same cell density were used as control. Then, the plate was left overnight at 37 °C incubator supplied with 5% carbon dioxide. AlamarBlue test (catalog # DAL1025, Thermo Fisher scientific) was employed to screen the viability rate. Temporarily, 10% alamarBlue in Dulbecco's Modified Eagle Medium solution was added on every well. Samples have been kept in the incubator for 4 h and the fluorescence with 560 Excitation /590 Emission was collected using CLARIOstar plate reader.⁸⁸

***CHAPTER THREE
RESULTS AND
DISCUSSION***

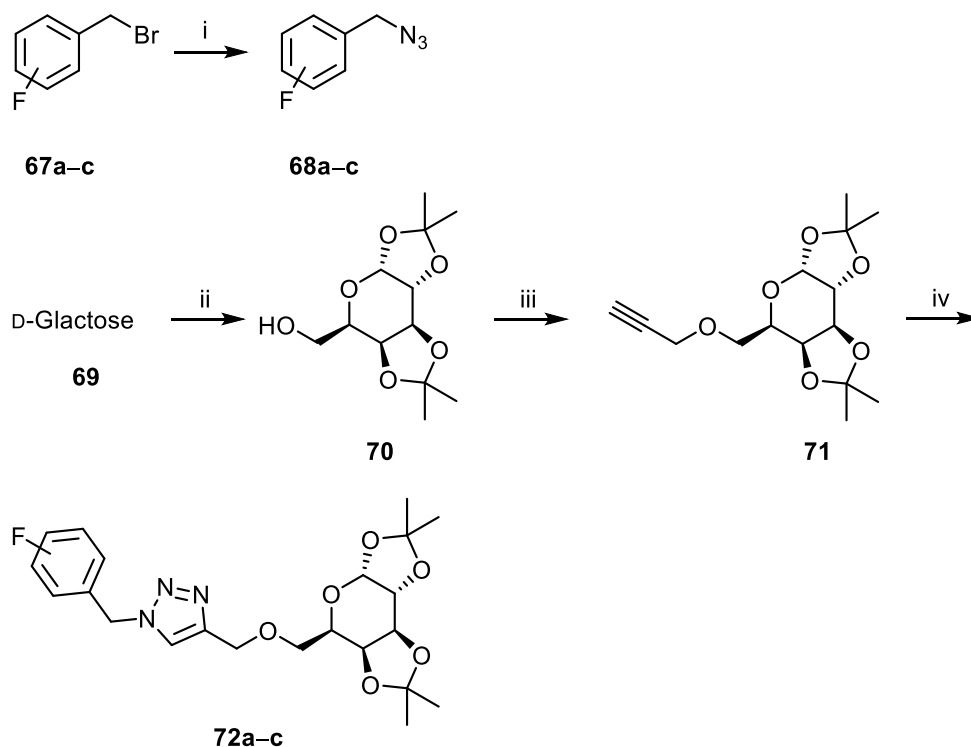
3. Results and Discussion

Heterocyclic compounds are one of the essential components of pharmaceuticals and medications. They can be oxygen, nitrogen or sulfur-containing heterocycles or comprising of two different heteroatoms.⁸⁹ The most common rings available in the biologically active compounds are furans, pyrroles, thiophens, piperidines, oxazoles, imidizoles and triazoles. The latter one is found in two possible isomers; 1,2,3-triazole and 1,2,4-triazoles, and both have significant potency in the drug design. 1,2,3-Triazole products were progressively prepared since the invention of Cu-mediated alkyne-azide 1,3-dipolar cycloaddition reaction in the commencing of the last 2000s. Initially, they were synthesized through the thermal 1,3-cycloaddition reaction of alkynes with organic azides to give one isomer when symmetrical alkyne is utilized and two isomers in the case of using asymmetrical alkyne (Scheme 22)⁹⁰:



Scheme (3-22). Thermal 1,3-dipolar cycloaddition reaction of alkynes and azides

In this work, three new D-galactose-based-triazole compounds **72a–c** have been synthesized starting from the commercially available D-galactose (**69**) using convenient synthetic route (Scheme 23):

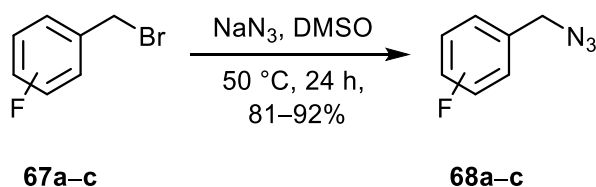


Reagents and conditions: i] NaN_3 , DMSO, 50 °C, 24 h, 81–92%; ii] acetone, ZnCl_2 , H_2SO_4 , r.t., 6 h, 81%; iii] propargyl bromide, 0 °C–r.t., 24 h, 88%; iv] **68a-c**, Na ascorbate, $\text{CuSO}_4 \cdot 5\text{H}_2\text{O}$, 50 °C, 36 h, 83–90%

Scheme (3-23). Preparation of D-galactose-based-triazole compounds **72a-c**

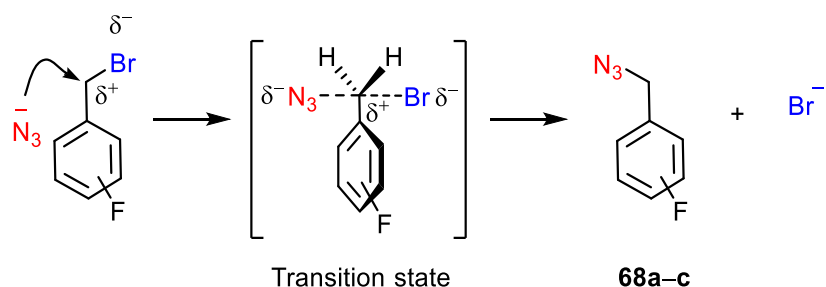
3.2. Preparation of fluorine-containing azido benzyl compounds **68a-c**

1-(Bromomethyl)-fluorobenzene derivatives **67a-c** were treated with sodium azide through $\text{S}_{\text{N}}2$ mechanism^{91,92} in dimethyl sulfoxide at fifty degree for one day to produce the corresponding 1-(azidomethyl)-fluorobenzene derivatives **68a-c** in 81–92% yields (Scheme 24).



Scheme (3-24). Synthesis of 1-(azidomethyl)-fluorobenzene derivatives **68a-c**

As expected, the yield of the *ortho* and *para* fluorine-substituted isomers compounds **68a** (89%) and **68c** (92%) was higher than that of the isomer **68b** (81%). This is due to the electron-withdrawing effect of fluorine at *ortho* and *para* positions is higher than that of *meta* and the substituted reaction followed S_N2 mechanism (Scheme 25)⁹³:



Scheme (3-25). Proposed mechanism of the synthesis of compounds **68a-c**

FT-IR spectra of compounds **68a-c** (Figures 13–15) demonstrated the presence of Carbon–Hydrogen Ar ν bands around 3050 cm⁻¹ besides the typical azide ν band localized at 2100 cm⁻¹. The carbon-carbon Ar double bond ν bands appeared at 1600 cm⁻¹ and 1580 cm⁻¹. Moreover, the Carbon–Fluorine Ar ν bands appeared higher than 1220 cm⁻¹.

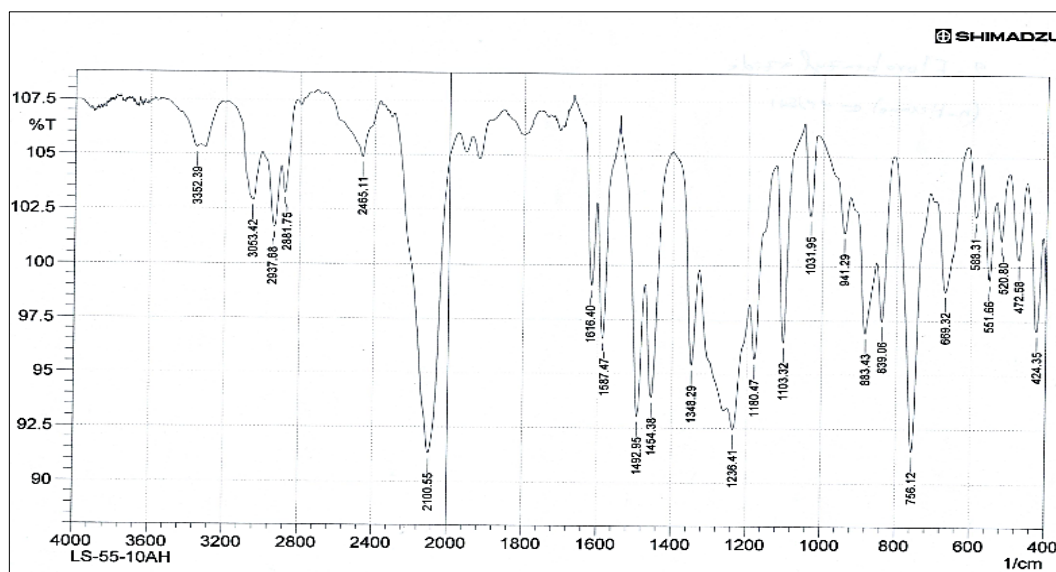


Figure (3-13). Fourier-transform infrared spectrum of the azide **68a**

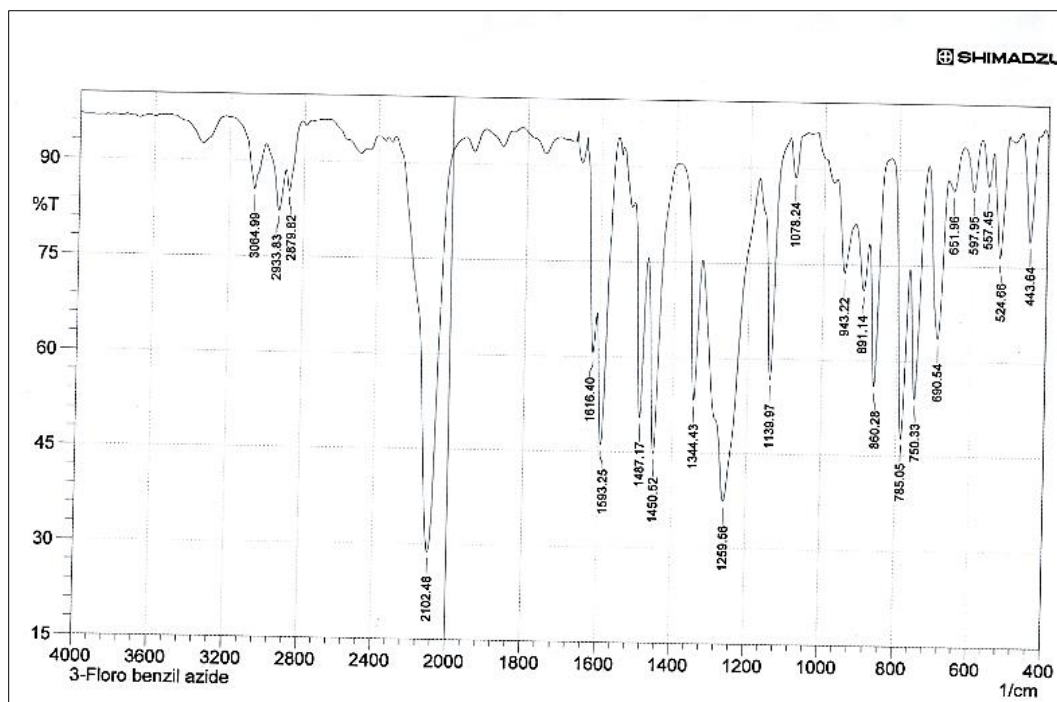


Figure (3-14). Fourier-transform infrared spectrum of the azide **68b**

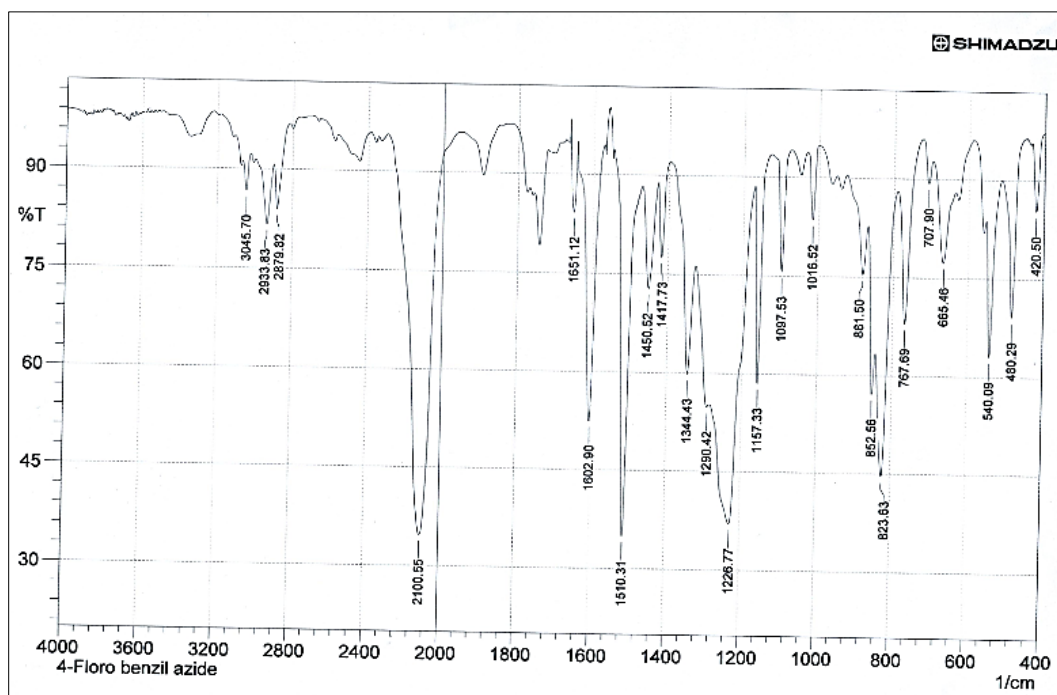


Figure (3-15). Fourier-transform infrared spectrum of the azide **68c**

The structures of azido benzyl compounds **68a–c** have also been confirmed by NMR technical. ^1H NMR charts (Figures 16–18) of those derivatives revealed four protons-

integrated multiplet from δ 7.51 ppm to 7.00 ppm belong to the aromatic protons and singlets around δ 4.35 ppm assigned to the methylene protons.

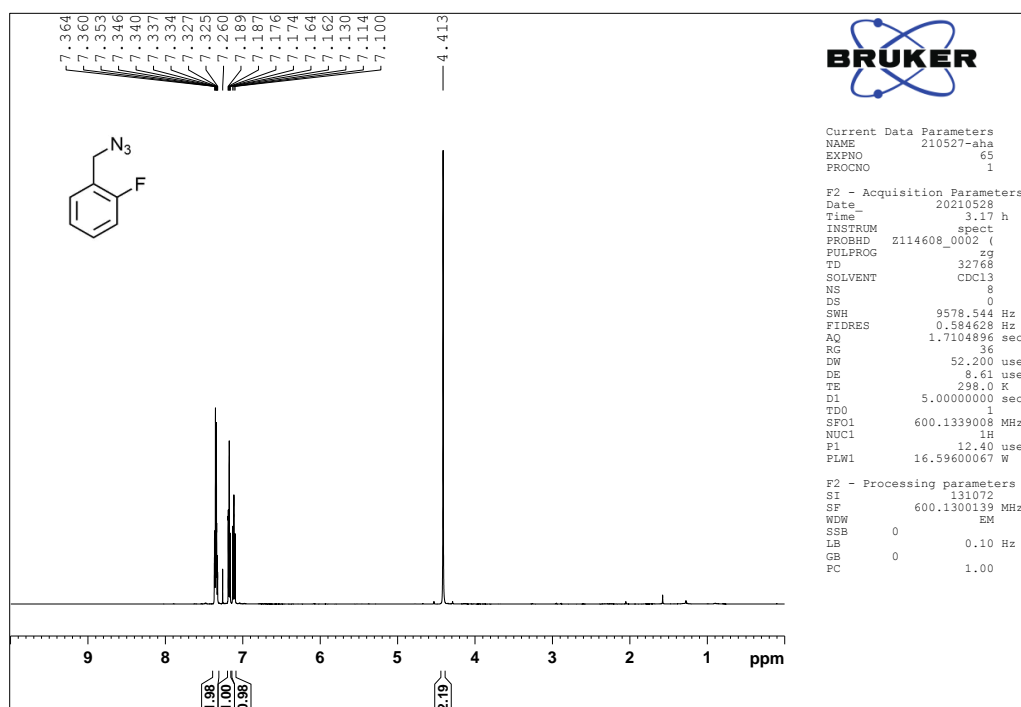


Figure (3-16). Proton NMR chart (CDCl₃, 600 MHz) of azide **68a**

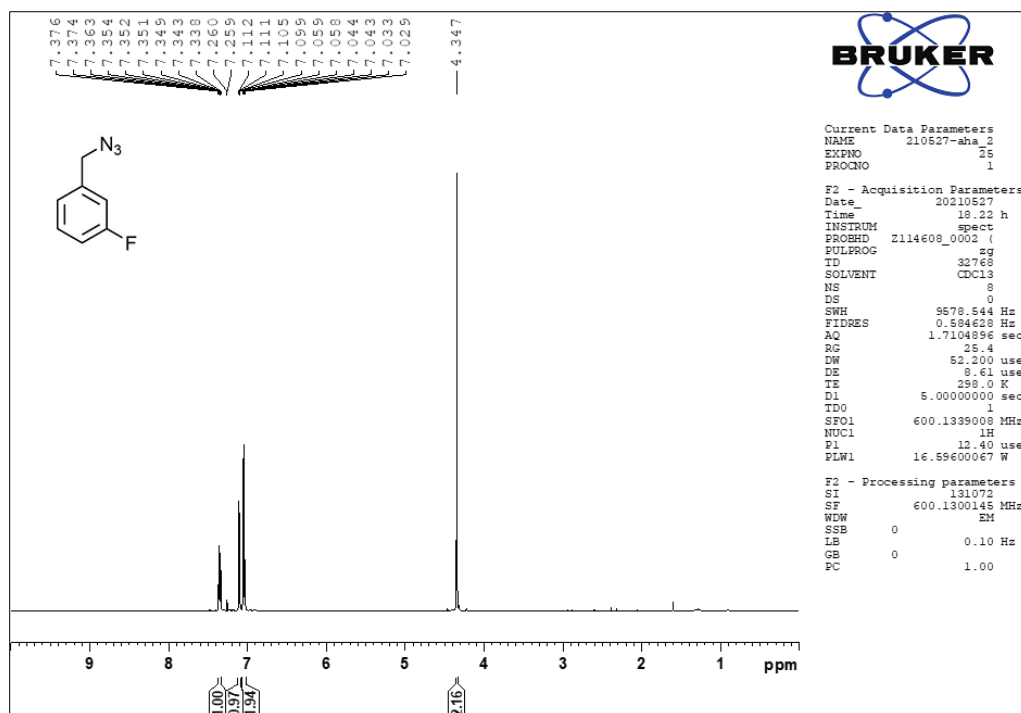


Figure (3-17). Proton NMR chart (CDCl₃, 600 MHz) of azide **68b**

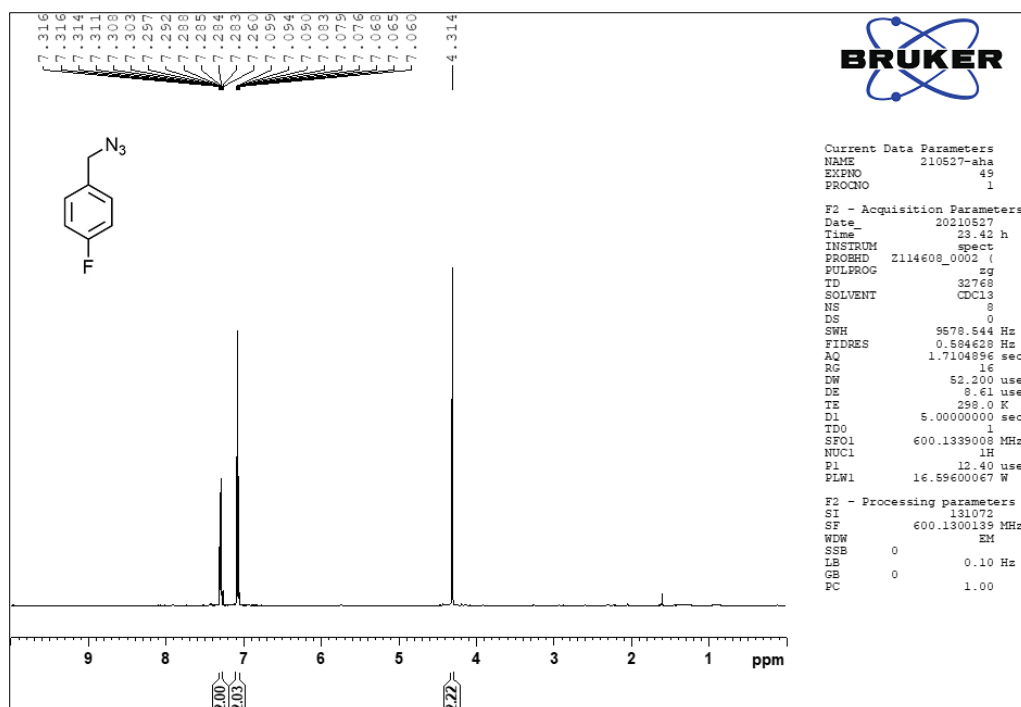
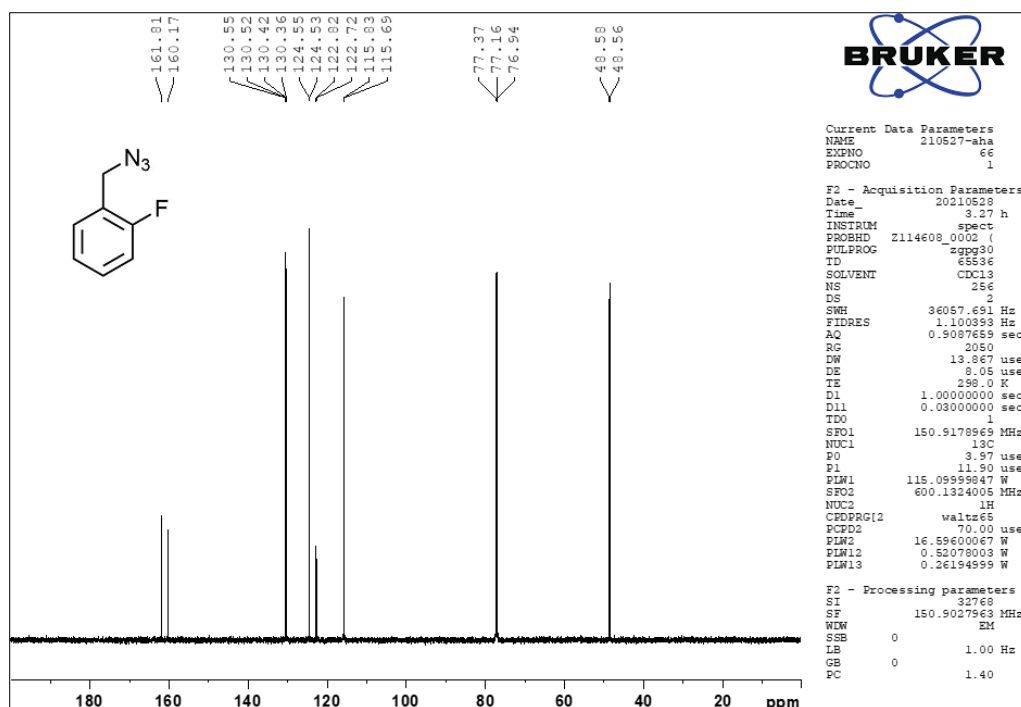
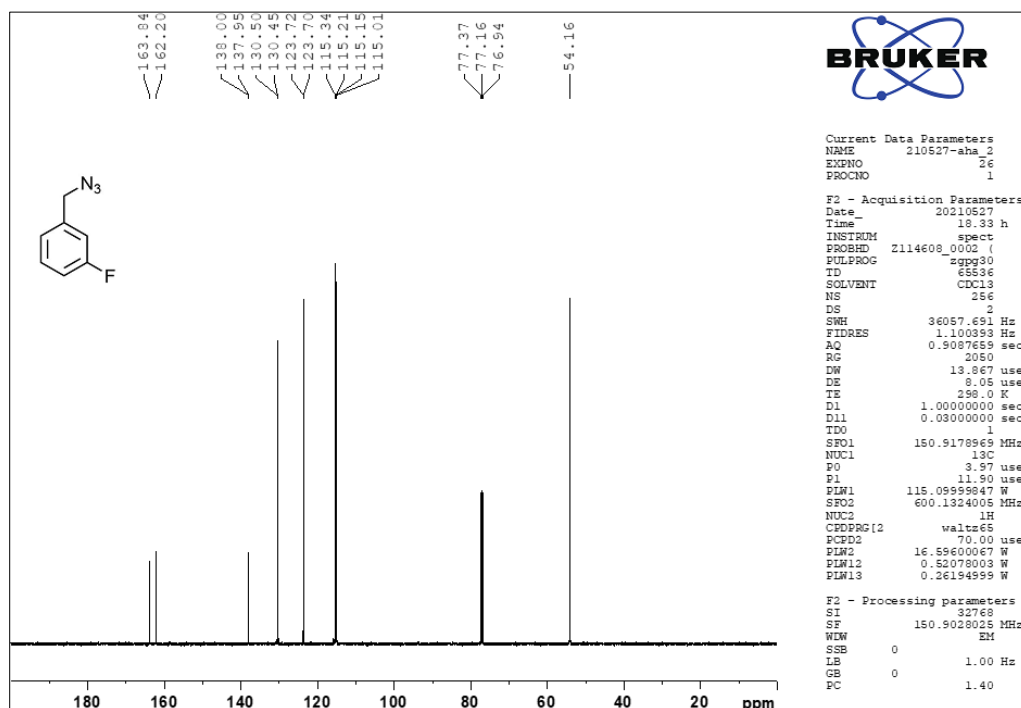
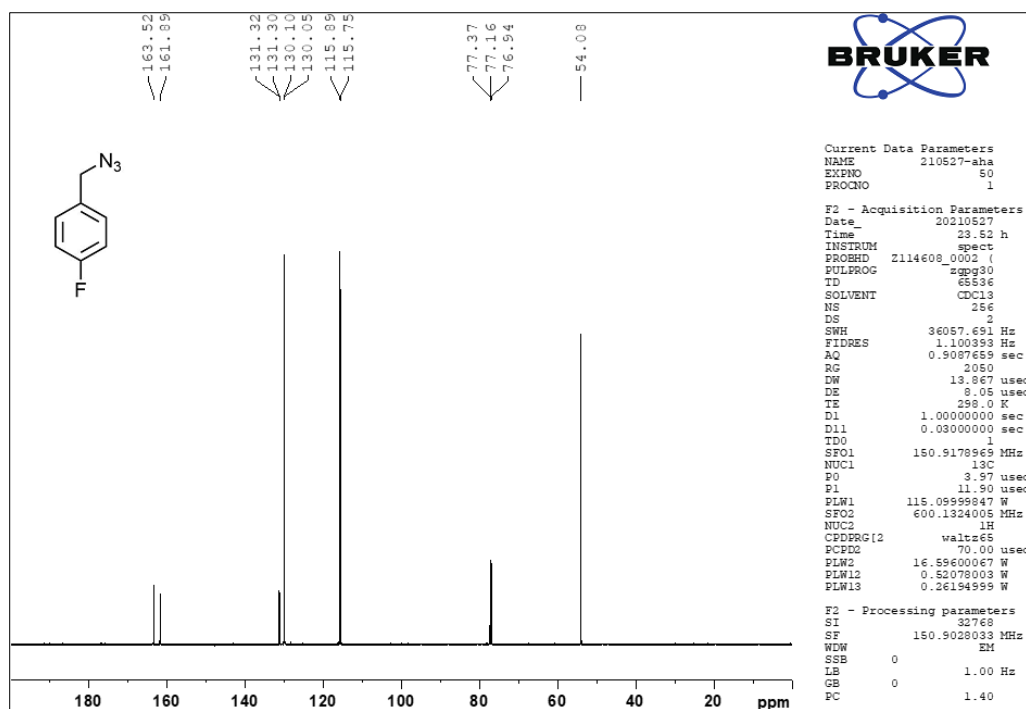
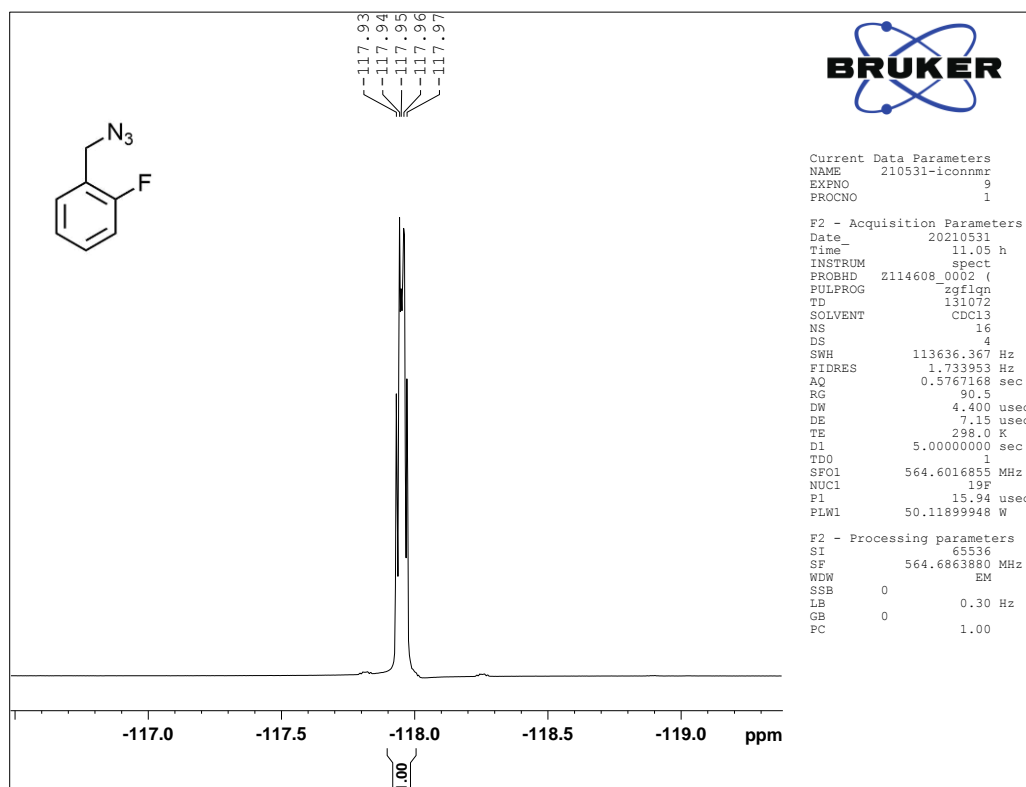
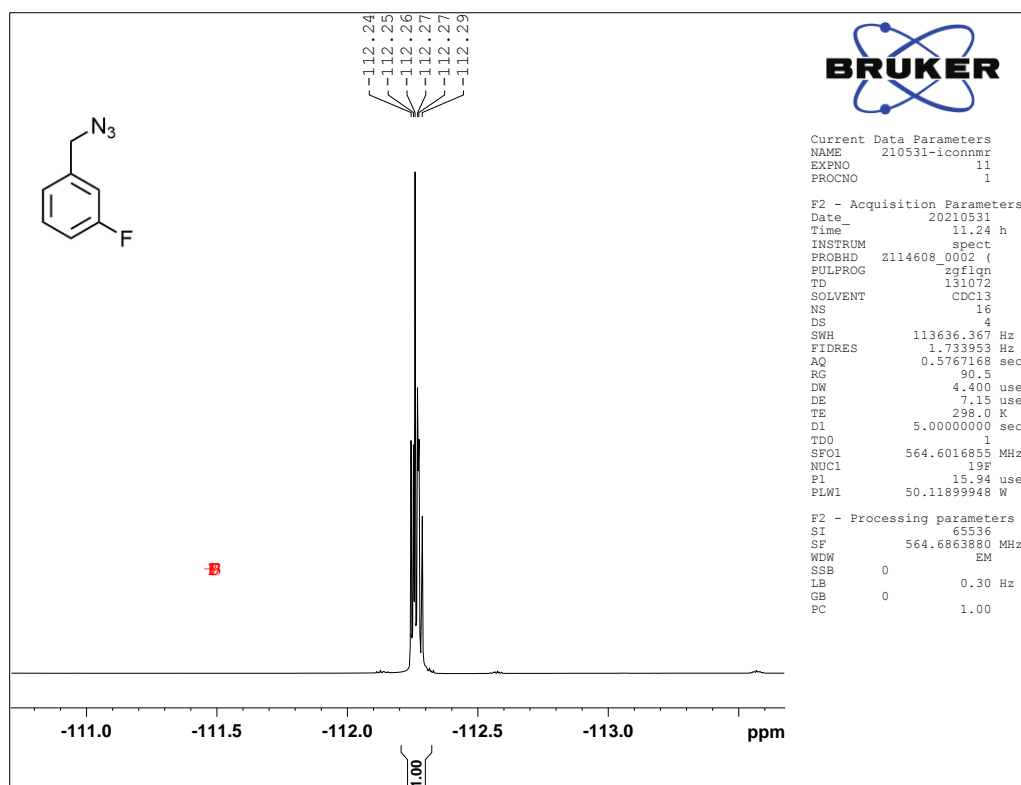
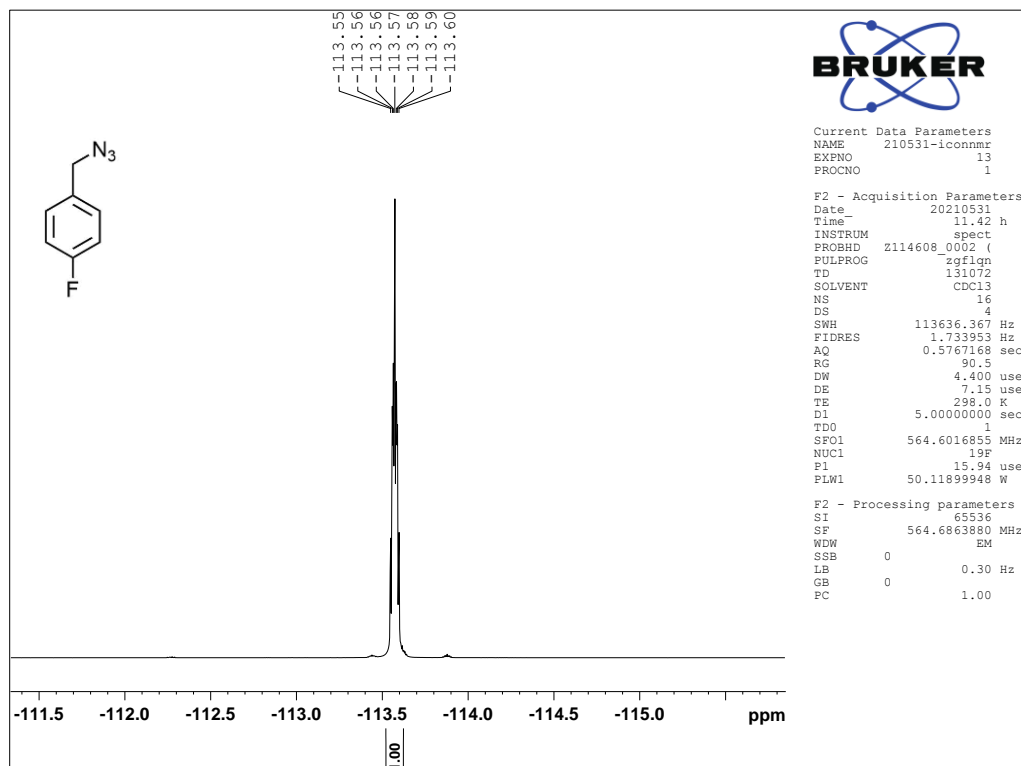


Figure (3-18). Proton NMR chart (CDCl_3 , 600 MHz) of azide **68c**

The fluorine effect results in splitting of the aromatic carbon signals.⁹⁴ This effect can be clearly shown in the ^{13}C NMR spectra of compounds **68a–c** (Figures 19–21). For example, the aromatic carbon that directly bound to the fluorine atom appears near 162 ppm with a very large $J \sim 245$ Hz. Furthermore, the signal of benzylic carbon of the ortho isomer appears at 48.7 ppm whereas other isomers meta and *para* have the same signal at 54.2 ppm and 54.1 ppm respectively. Moreover, all azido compounds demonstrated one fluorine signal as a multiplet at δ -117.9 ppm, -112.3 ppm and -113.6 ppm for *ortho*-, *meta*- and *para*-isomers respectively in their ^{19}F NMR spectra (Figures 22–24).

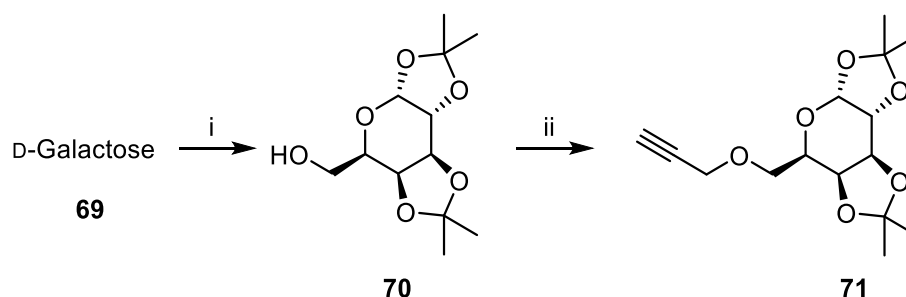
Figure (3-19). Carbon-13 NMR chart (CDCl₃, 150 MHz) of azide **68a**Figure (3-20). Carbon-13 NMR chart (CDCl₃, 150 MHz) of azide **68b**

Figure (3-21). Carbon-13 NMR chart (CDCl₃, 150 MHz) of azide **68c**Figure (3-22). Fluorine-19 NMR chart (CDCl₃, 564 MHz) of azide **68a**

Figure (3-23). Fluorine-19 NMR chart (CDCl₃, 564 MHz) of azide **68b**Figure (3-24). Fluorine-19 NMR chart (CDCl₃, 564 MHz) of azide **68c**

3.3.Synthesis of 6-*O*-prop-2-ynyl-1,2:3,4-diacetonide- α -D-galactose (**72**)

The target alkyne **5** has been synthesized from D-galactose (**69**) in two subsequent steps (Scheme 26):



Reagents and conditions: i] Acetone, ZnCl₂, H₂SO₄, 0 °C–r.t., 5 h, 81%;
ii] propargyl bromide, DMF, –20 °C–r.t., 24 h, 88%

Scheme (3-26). Synthesis of alkyne **71** from D-galactose (**69**)

Acetone is widely utilized in carbohydrate chemistry as a protecting group particularly for the *syn* vicinal diols.⁹⁵ The reaction of the hexose **69** with excess of acetone in the assistance of zinc chloride and sulfuric acid at room temperature for five hours afforded α -D-galactose diacetonide (**70**) in a very good yield 81%. FTIR spectrum (Figure 25) of compound **70** shows; a broad band at 3483 cm⁻¹ belongs to the (Oxygen–Hydrogen) ν , medium bands at 2987 and 2935 cm⁻¹ attributed to the (C–H) stretching, a sharp band at 1382 cm⁻¹ corresponding to the (Carbon–Hydrogen) bending, and the sharp bands between 1225 cm⁻¹ and 1069 cm⁻¹ due to the (Carbon–Oxygen) and (Carbon–Oxygen–Carbon) ν .

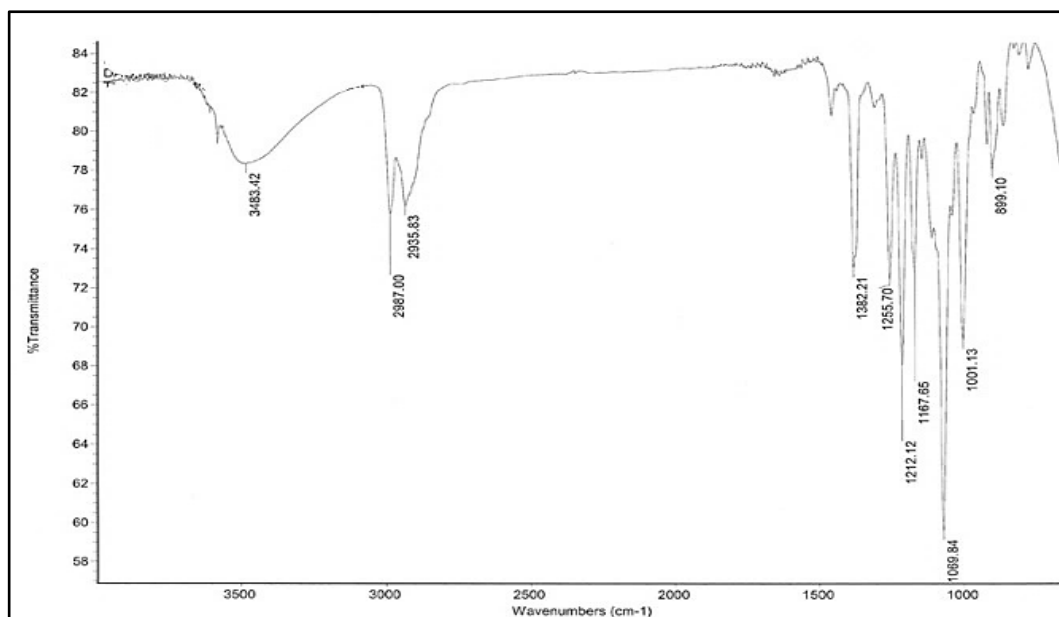


Figure (3-25). Fourier-transform infrared spectrum of derivative **70**

The formation of compounds **70** has also been evidenced by ^1H NMR (300 MHz, CDCl_3) spectrum (Figure 26) that displays a doublet at 5.56 ppm with the coupling constant ($J = 5.0$ Hz) attributed to the anomeric proton; a doublet of doublet centred at 4.60 ppm ($J = 8.0, 2.4$ Hz) due to H-3 of the pyran ring, another doublet of doublet centred at 4.32 ($J = 5.0, 2.4$ Hz) belongs to the H-2, a doublet of doublet of H-4 localized at 4.26 ($J = 7.9, 1.6$ Hz), a doublet of doublet of doublet localized at 3.86 ($J = 7.3, 4.7$ Hz) attributed to H-5, and two doublets of doublets at 3.83 ppm ($J = 10.7, 4.7$ Hz) and 3.74 ppm ($J = 10.7, 7.3$ Hz) due to methylene protons H-6 in addition to the singlets at 2.37 ppm, 1.52 ppm, 1.44 ppm, and 1.32 ppm that attributed to the hydroxyl proton and the isopropylidene protons respectively.

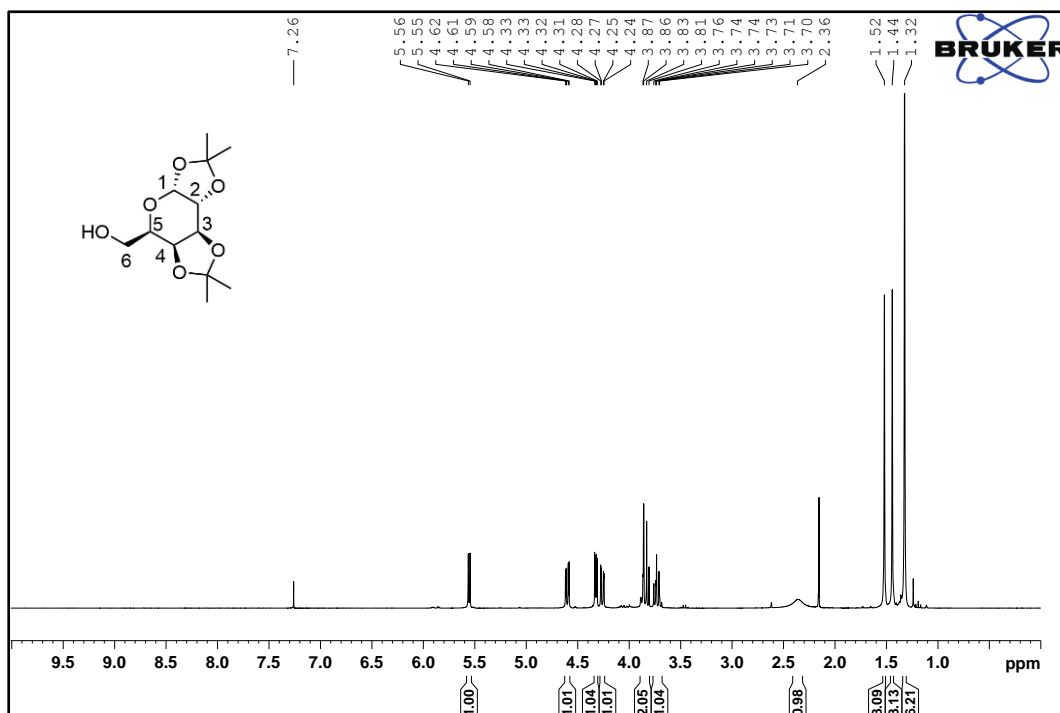


Figure (3-26). Proton NMR chart (CDCl₃, 300 MHz) of compound **70**

Moreover, the structure of alcohol **70** is assigned by ¹³C {¹H} NMR (75 MHz, CDCl₃) spectrum (Figure 27) that exhibits two signals at 109.4 ppm and 108.6 ppm attributed to the quaternary carbons of the isopropylidene protecting groups. The carbon signals at 96.3 ppm, 71.5 ppm, 70.7 ppm, 70.5 ppm, 68.6 ppm, and 62.3 ppm are confirmed to C1, C4, C3, C2, C5, and C6 respectively. Finally, the signals belong to methyl group appear at 24.3, 24.9, 25.9, and 26.0 ppm.

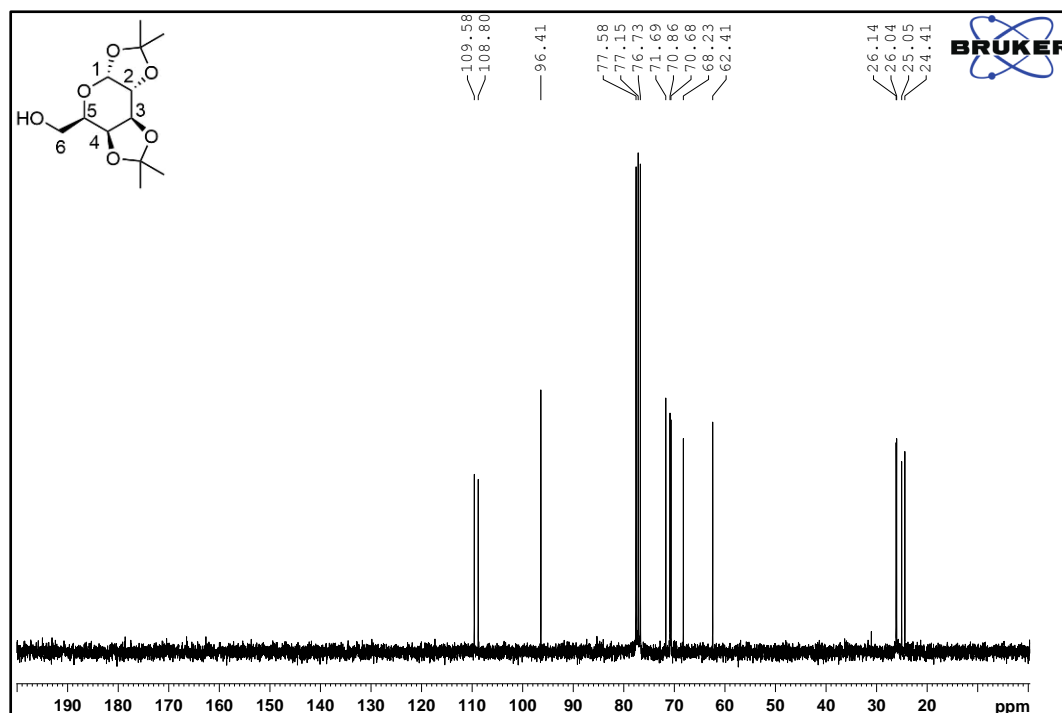


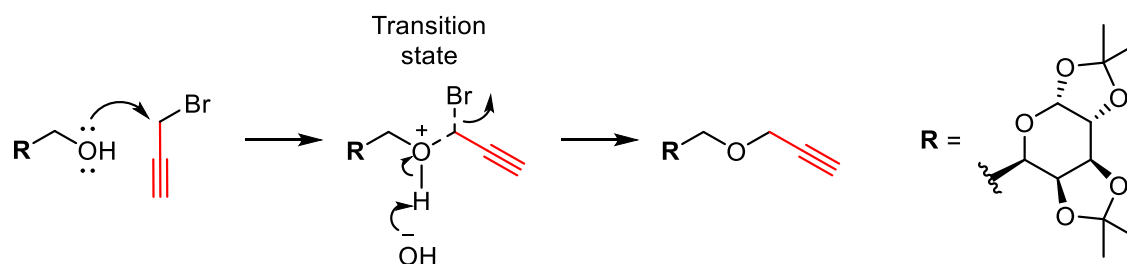
Figure (3-27). Carbon-13 NMR chart (CDCl₃, 75 MHz) of compound **70**

Treatment of galactose diacetone **70** with 3-bromoprop-1-yne in the presence of sodium hydroxide in *N,N*-dimethylformamide at $-20\text{ }^{\circ}\text{C}$ to room temperature for 24 h gave 6-*O*-prop-2-ynyl- α -D-galactose diacetone (**71**) in 88% yield. First, the addition of 3-bromoprop-1-yne to the reaction mixture is crucial in the determination of the yield of reaction. The effect of temperature, in the addition of the propargyl bromide, on the reaction outcome is illustrated in Table 1.

Table (3-1). Effect of the Initial Reaction Temperature on The Alkyne yield

Entry	Temperature $^{\circ}\text{C}$	Yield
1	r.t.	57%
2	0	62%
3	-5	70%
4	-10	82%
5	-20	88%

The lower the temperature at the addition of propargyl bromide to an alcohol, the higher the reaction yield. This could be attributed to the formation of allenes during the reaction⁹⁶ It is suggested that the formation of compound **71** follows the S_N2 mechanism in its initial step. Then, proton is subtracted due the base effect (Scheme 27):



Scheme (3-27). Suggested mechanism of the formation of compound **71**

The disappearance of the (O–H) stretching band at 3483 cm⁻¹ and the appearance of the bands at 3253 cm⁻¹ and 2109 cm⁻¹ due to the stretching of (≡C–H) and (C≡C) respectively in the FTIR spectrum (Figure 5) are excellent evidence of the formation of alkyne **71**.

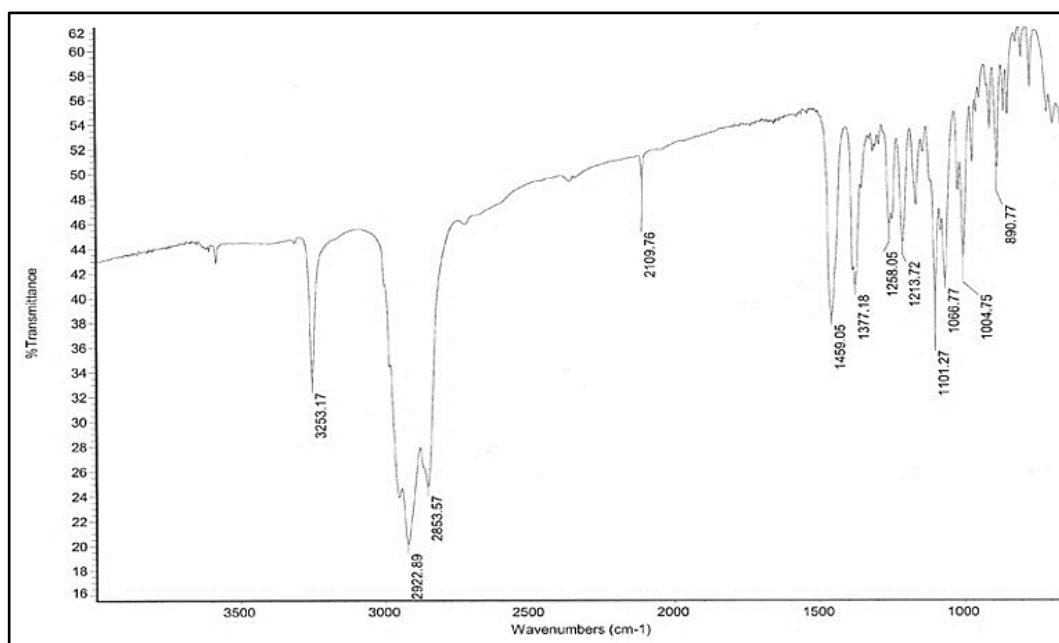


Figure (3-28). Fourier-transform infrared spectrum of derivative **71**

Further proof of the formation of compound **71** is introduced by ^1H NMR spectrum (Figure 29) that displays two doublets of doublets centred at 4.23 ppm and 4.20 ppm corresponding to the methylene H-3 having coupling constants 15.9 Hz and 2.4 Hz. Moreover, the appearance of triplet at 2.42 ppm ($J = 2.4$ Hz) belongs to the acetylenic proton H-1 is another evidence of formation of the alkyne **5**.

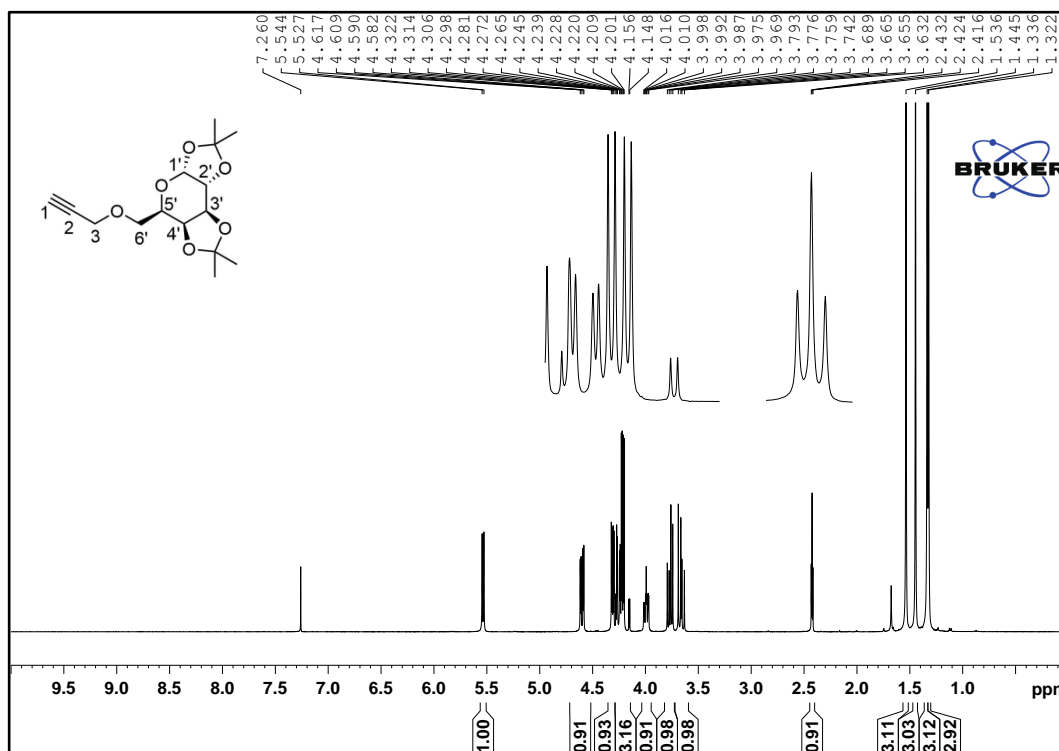


Figure (3-29). Proton NMR chart (CDCl_3 , 300 MHz) of compound **71**

A cross peak is shown in the COSY spectrum (Figure 30) between the two doublets of doublets centred at 4.23 ppm and 4.20 ppm and the triplet at 2.42 ppm which means the presence of the long-range coupling.⁹⁷

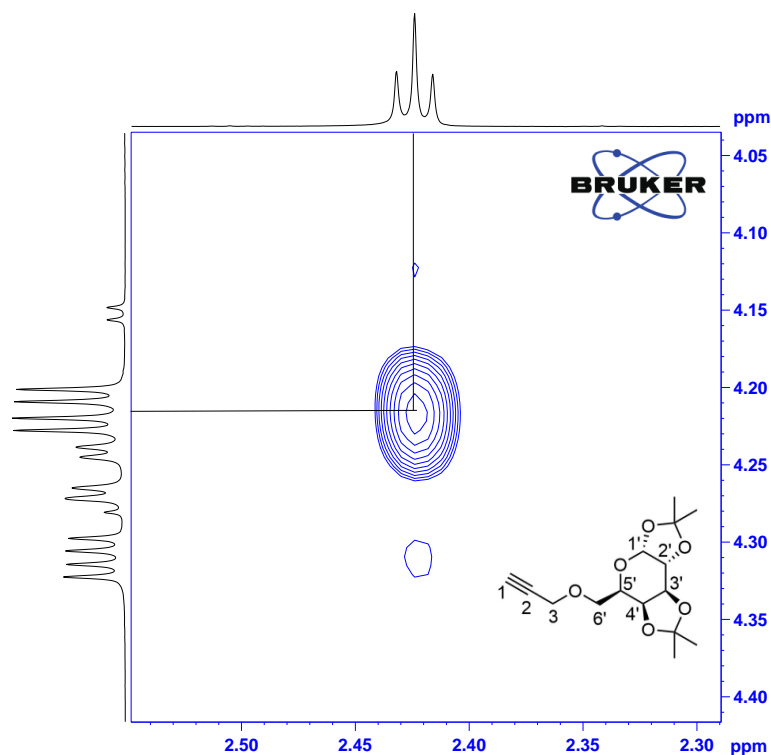


Figure 3-30 . Magnified ^1H - ^1H COSY (CDCl_3 , 300 MHz) spectrum of derivative **71**

The ^{13}C NMR spectrum of compound **71** (Figure 31) shows three new signals at 79.8, 74.7 ppm and 58.7 ppm belonging to C2, C1 and C3 respectively.

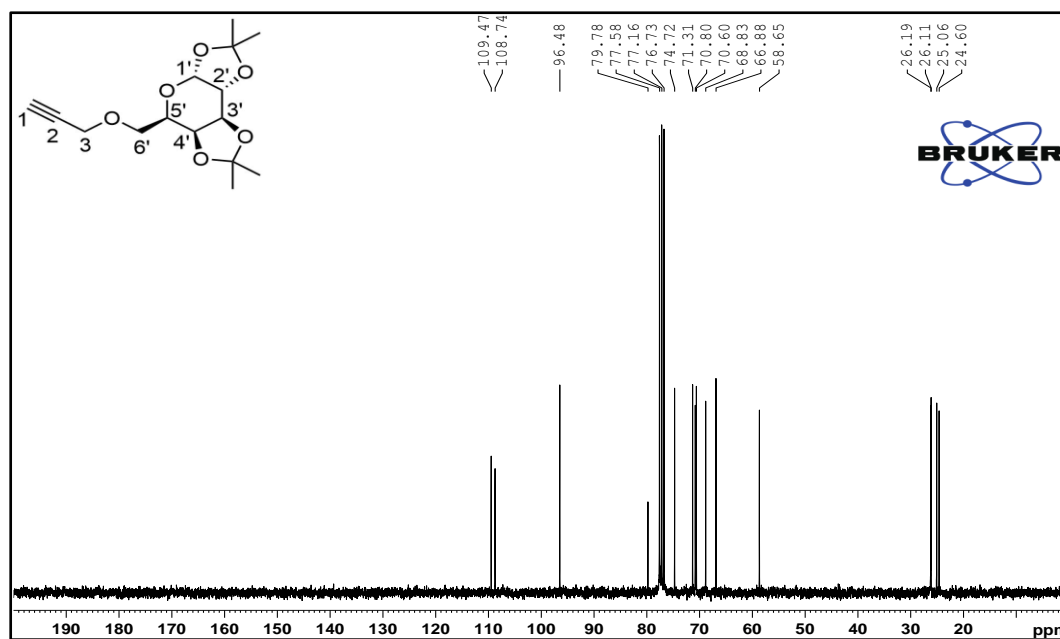


Figure (3-31). Carbon-13 NMR chart (CDCl_3 , 75 MHz) of compound **71**

It is important to affirm the conformation of the derivative **71** before progressing to the synthesis of triazole derivatives. It is widely known that the preferred 3D shape of the pyranose six-membered ring in the saccharides is chair conformations 4C_1 and ${}^4C^1$ (Figure 32).^{98,99}

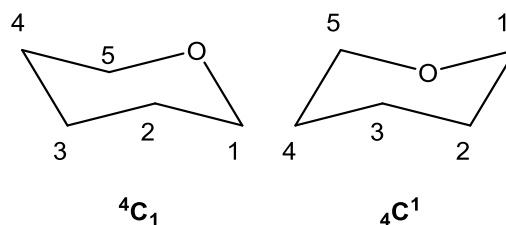


Figure (3-32). Chair conformations of pyranoses

The computational study of compound **71** demonstrated that the lowest energy galactopyranose ring adopted chair 3C_0 conformation (Figure 33). According to Karplus equation, the magnitude of coupling constant decreases as the dihedral angle between the vicinal hydrogen atoms raises from 0° to 90° and then starts to increase with the raise of the angle.¹⁰⁰ In the suggested 3D shape of the six-membered ring, the dihedral angle between H2' and H3' is approximately 90° and this is confirmed by 1H NMR as the coupling constant ${}^3J_{H,H}$ between H2' and H3' is 2.4 Hz.

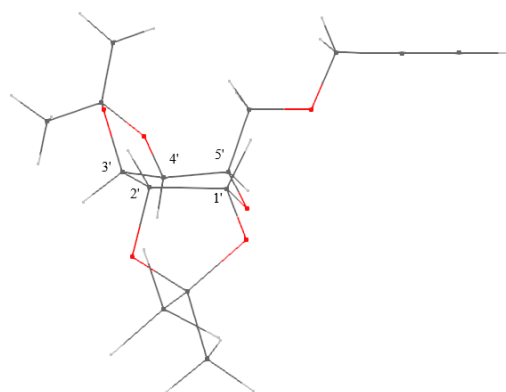
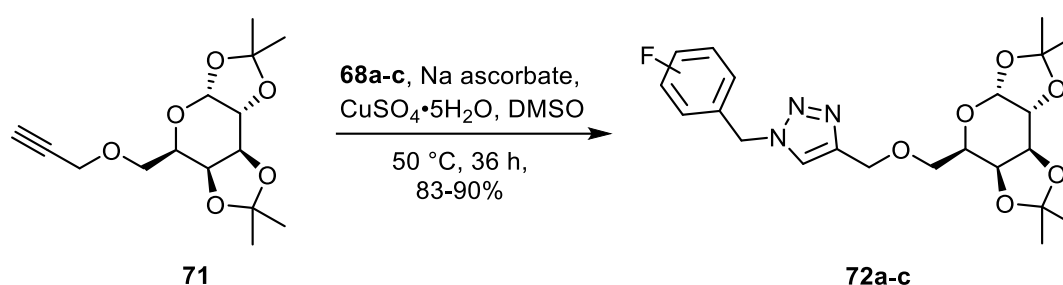


Figure (3-33). The suggested conformation of compound **71** based on computational study and NMR spectra

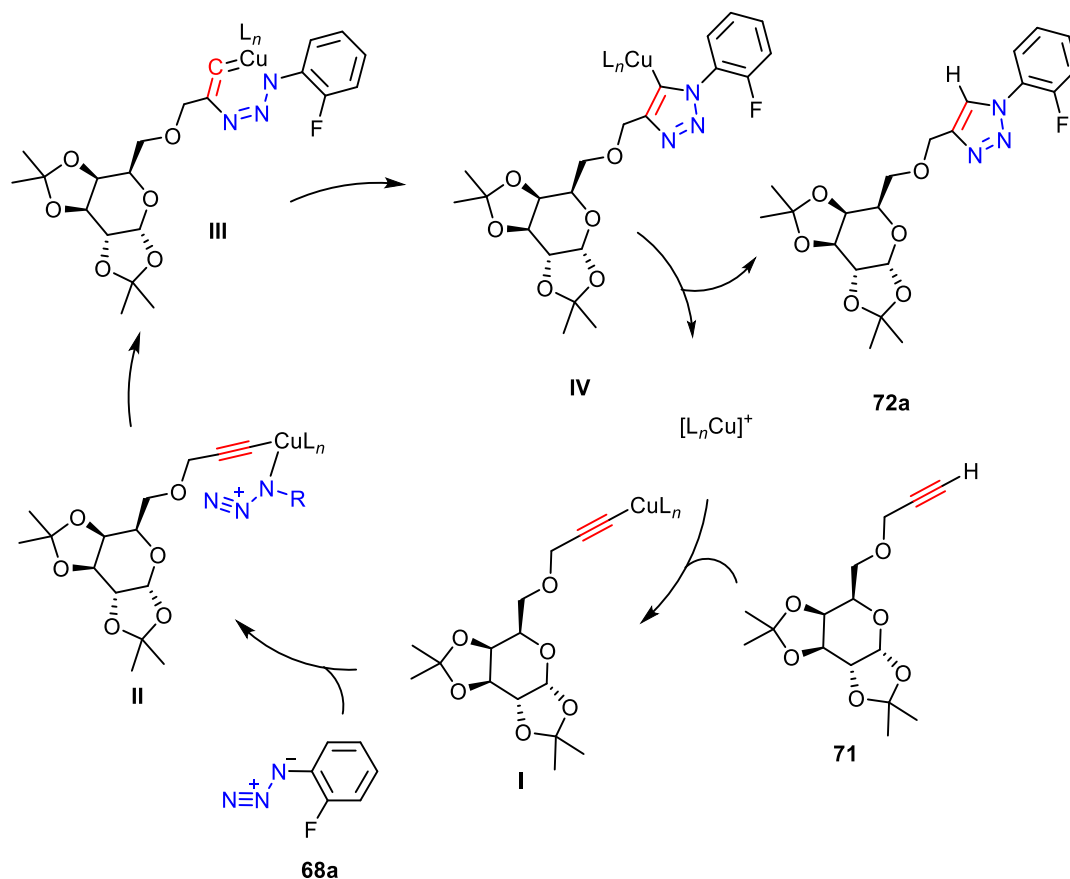
3.4.Synthesis of triazole derivatives 72a–c

After the synthesis and determination of the conformation of the alkyne precursor **71**, the work moved to the final step in the preparation scheme which was the click reaction. The reaction of benzyl azides **68a–c** separately with the propargyl-sugar ether **71** in DMSO as a solvent and in the aid of the mixture of Na ascorbic acid salt and copper sulphate pentahydrate at fifty degrees for 36 h afforded triazole derivatives **72a–c** in a very good to an excellent yield (Scheme 28):



Scheme (3-28). Preparation of triazole compounds **72a–c**

The proposed mechanism of Cu(I)-mediated alkyne-azide reaction (CuAAC) is shown in (Scheme 29).⁴⁵ First, Cu(I) is generated *in situ* through the reduction of copper sulphate pentahydrate which is the Cu(II) source Na ascorbate. Then, alkyne **71** binds with copper (I) to form copper (I)-acetylide **I** followed by the formation of copper complex with the electron-dense nitrogen. Next, the N atom of the organic azide is confronted by the high electronegative *sp*-carbon to produce the six-membered ring intermediate **III**. Ring reduction of the latter gives the intermediate **IV** that finally releases the Cu-complex to the cycle and gives the regio-selective product **72a**. The structure of the other triazole compounds **72b–c** follow similar mechanistic pathway.



Scheme (3-28). Proposed mechanism of the synthesis of compound **72a**⁴⁵

The creation of compounds **72a–c** is assigned by FT-IR spectra (Figures 34–36) that exhibited stretching bands referred to C–H triazole at approximately 3140 cm^{-1} , the aromatic stretching bands C–H located at 3064 cm^{-1} , the ν C=C bands appeared near 1600 cm^{-1} and 1500 cm^{-1} and the distinguishing ν C–F stretching band that appeared from 1240 to 1220 cm^{-1} .

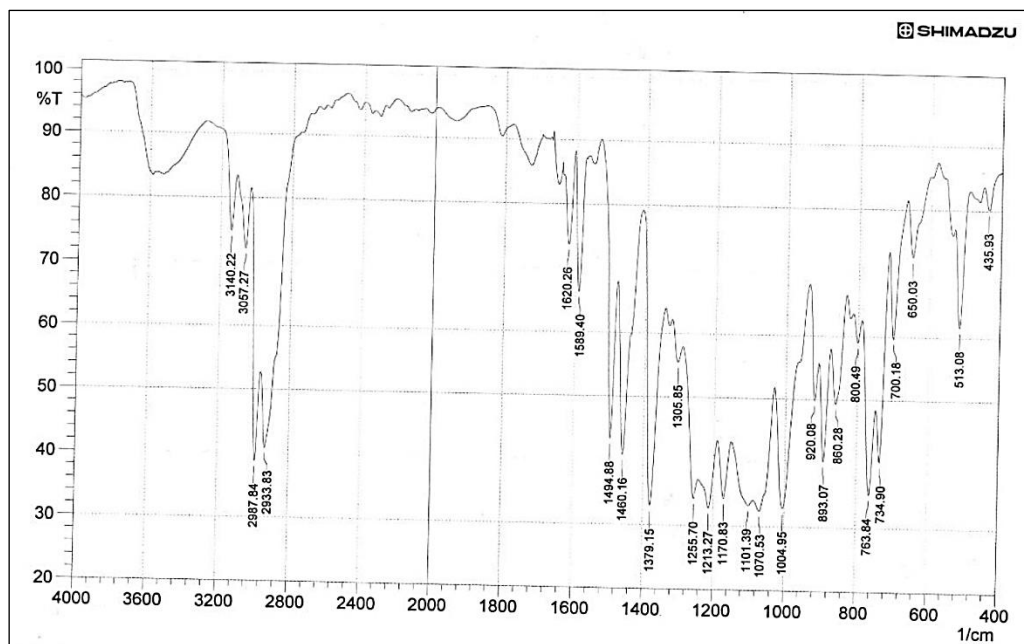


Figure (3-34). Fourier-transform infrared spectrum of derivative 72a

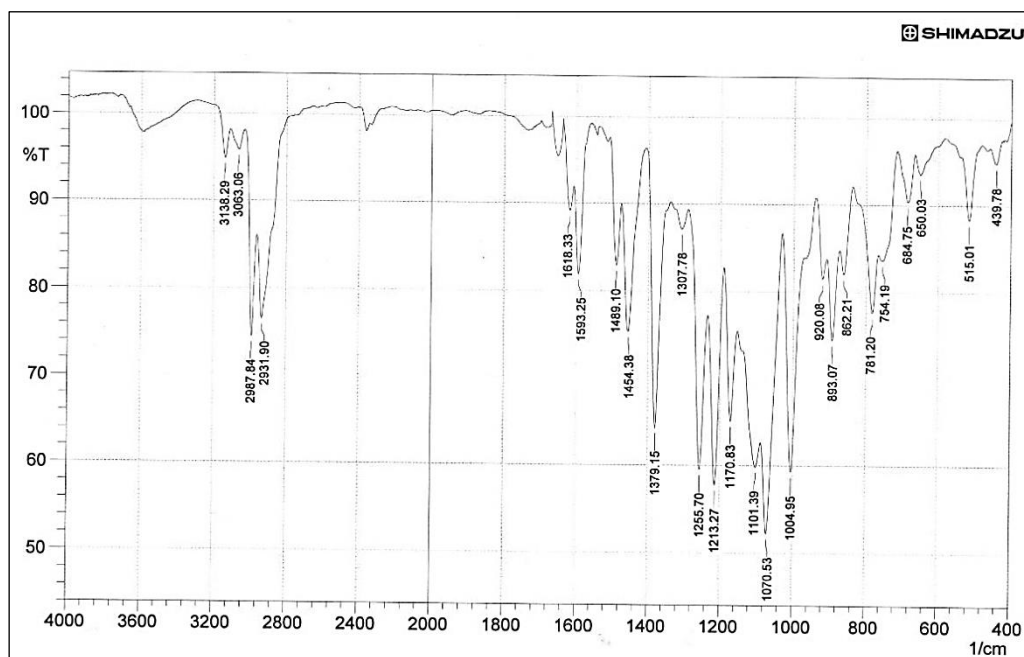


Figure (3-35). Fourier-transform infrared spectrum of derivative 72b

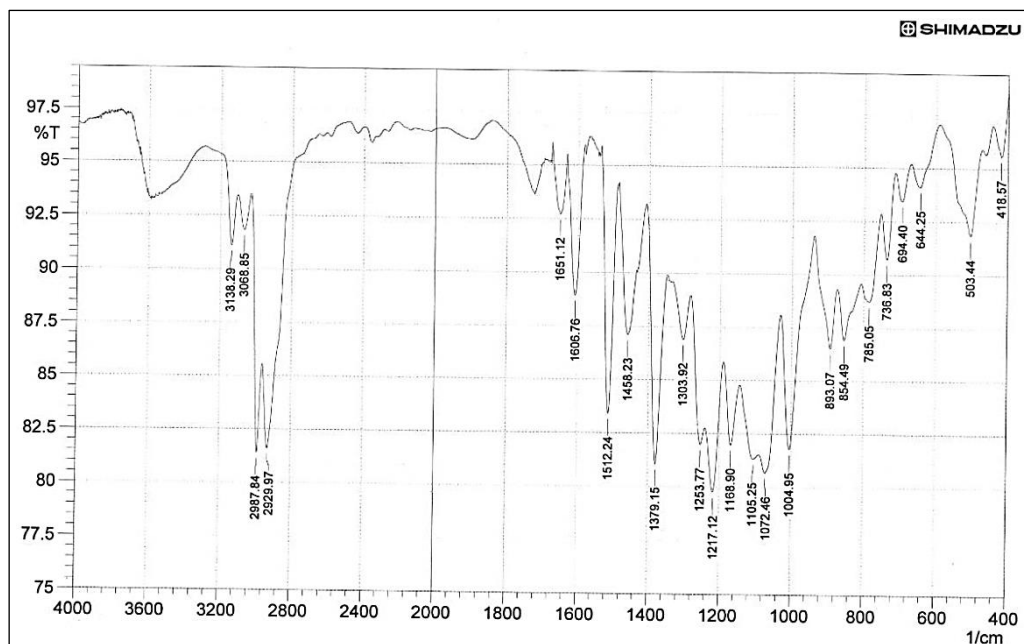
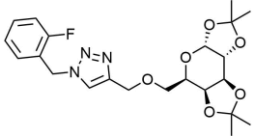
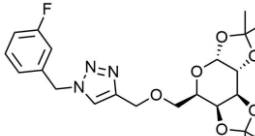
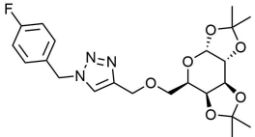


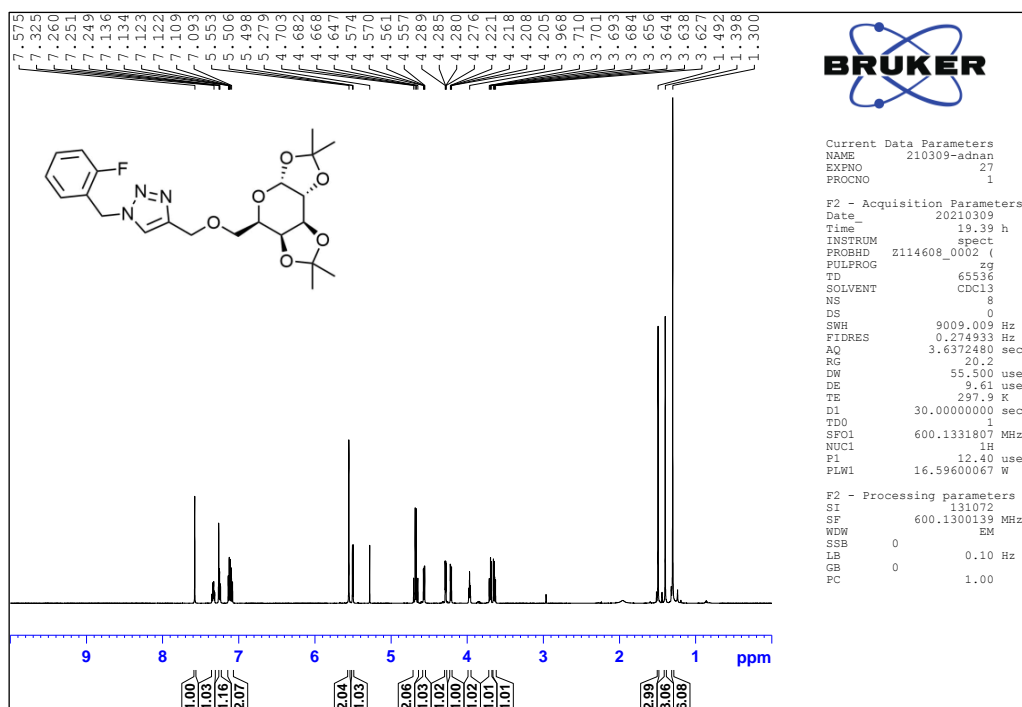
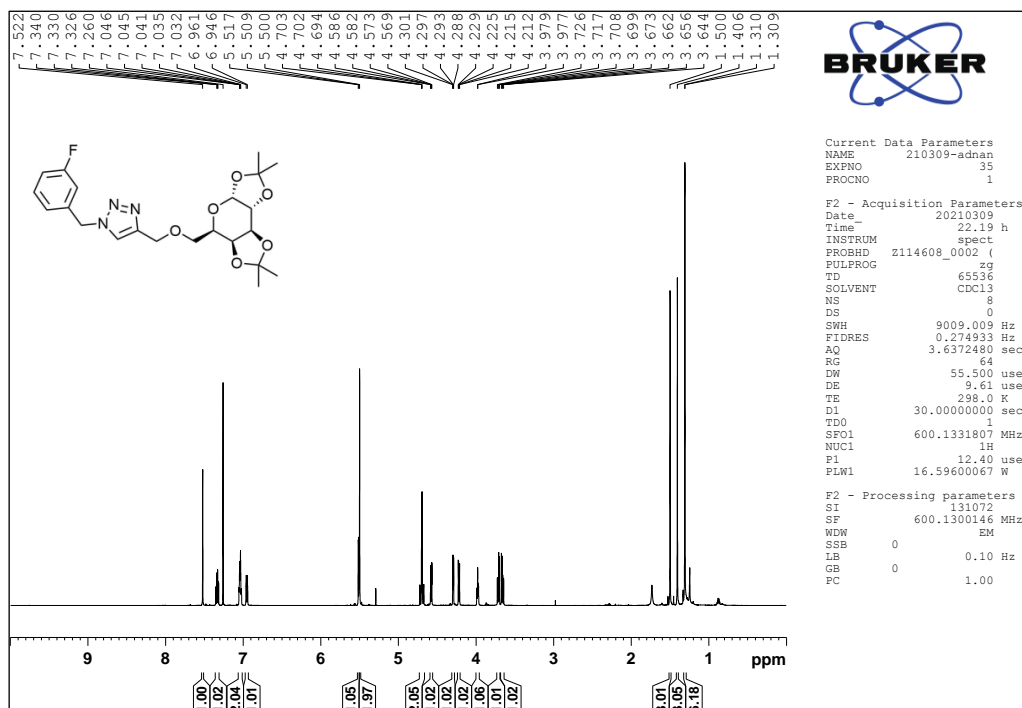
Figure (3-36). Fourier-transform infrared spectrum of derivative **72c**

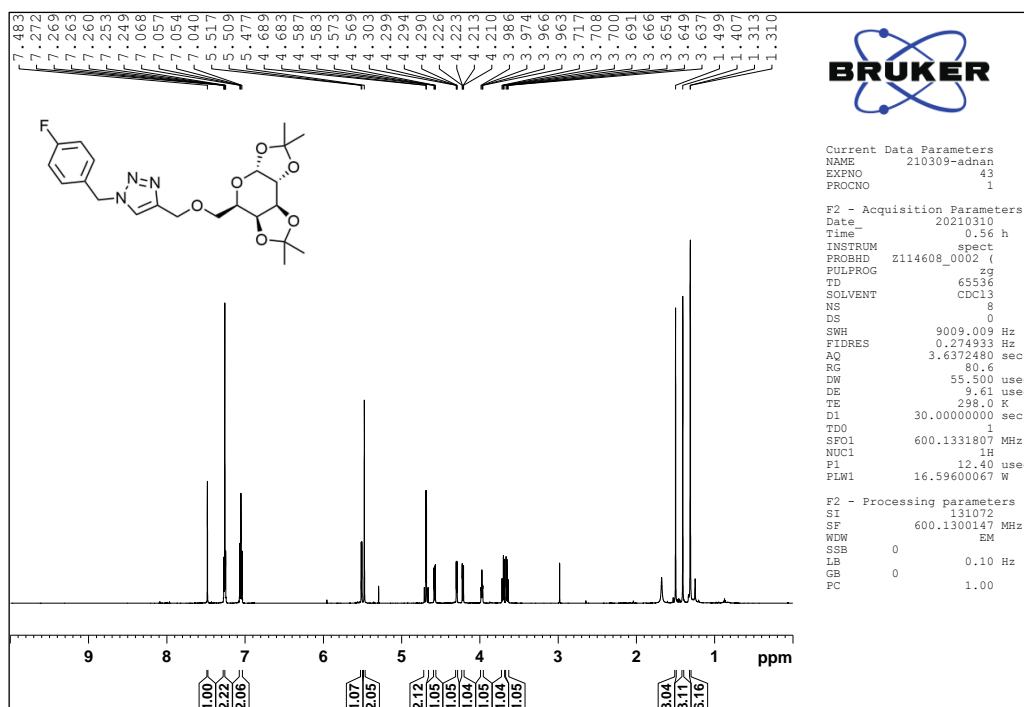
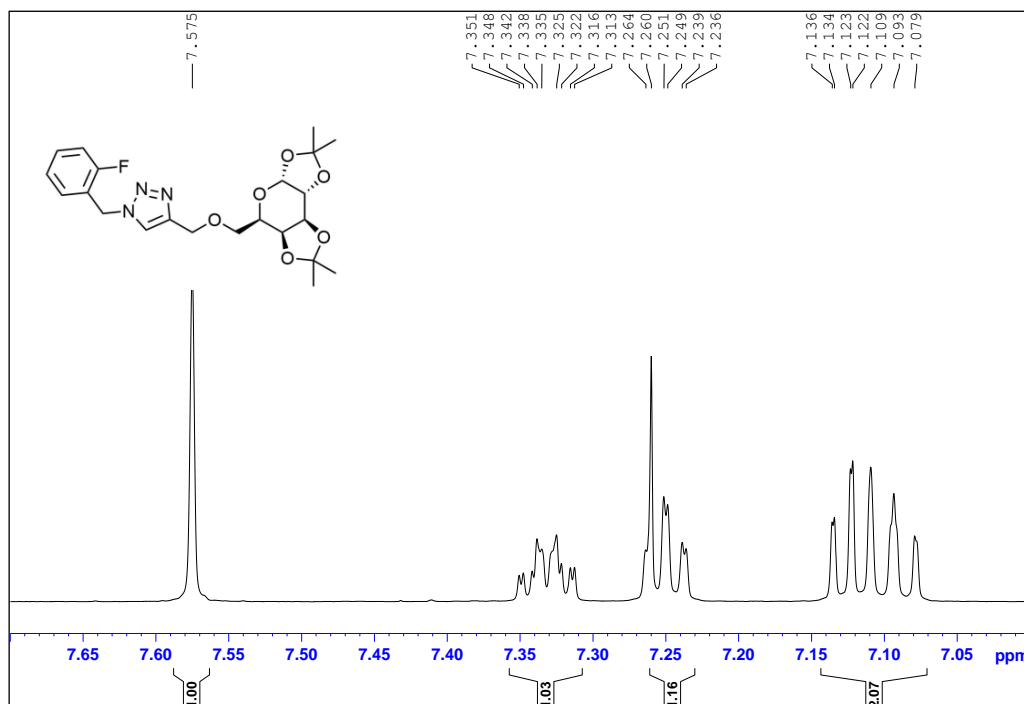
Additionally, ^1H NMR spectra of compounds **72a–c** (Figures 37–39) approve the construction of 1,4-disubstituted monotriazole derivatives through the appearance of a singlet at 7.58 ppm, 7.52 and 7.48 ppm for the derivatives **72a**, **72b** and **72c** respectively, which signifies the existence of the 1,4- disubstituted monotriazole isomer. Moreover, the presence of the Ar protons' signals from 7.36 ppm to 6.94 ppm (Figure 40–42) and the benzylic protons singlet between 5.55 ppm and 5.51 ppm is concrete evidence of the azide-alkyne cycloaddition. It is also important to mention that there is significant shift downfield of doublet of doublet of the $-\text{O}-\text{CH}_2-$ protons (protons 3 in the alkyne structure) from 4.24 ppm and 4.19 ppm in compound **71** to be two doublets between 4.71 ppm and 4.65 ppm. Other pyranose protons signals; 5.51 (d, $J = 5.0$ Hz, 1H, H1'), 4.58 (dd, $J = 7.9, 2.4$ Hz, 1H, H3'), 4.29 (dd, $J = 5.0, 2.4$ Hz, 1H, H2'), 4.22 (dd, $J = 7.9, 1.9$ Hz, 1H, H4'), 3.98 (ddd, $J = 7.0, 5.6, 1.8$ Hz, 1H, H5'), 3.71 (dd, $J = 10.3, 5.4$ Hz, 1H, H6'a), 3.66 (dd, $J = 10.3, 7.1$ Hz, H, H6'b), are also illustrated in the zoomed in spectra of triazoles **72a–c** (Figures 43–45). All

isopropylidene protons appear between 1.50 ppm and 1.30 ppm (Figures 37–39). The ^1H NMR data of triazoles **72a–c** are summarized in Table 2.

Table (3- 2). Comparison of ^1H NMR data of triazoles **72a–c**

Compound	Structure	Aromatic region (Figure 40–42)	Aliphatic region (Figures 43–45)
72a		7.58 (s, 1H, H5), 7.33 (dddd, $J = 13.6, 7.3, 5.4, 1.7$ Hz, 1H, Ar-H), 1.7 Hz, 1H, Ar-H), 7.12 (td, $J = 7.5, 1.0$ Hz, 1H, Ar-H), 7.09 (m, 1H, Ar-H)	5.55 (s, 2H, Ar-CH ₂ -triazole), 5.50 (d, $J = 5.0$ Hz, 1H, H1'), 4.69 (d, $J = 12.5$ Hz, 1H, triazole-CH ₂ -CHO), 4.66 (d, $J = 12.5$ Hz, 1H, triazole-CH ₂ -CHO), 4.57 (dd, $J = 8.0, 2.4$ Hz, 1H, H3'), 4.28 (dd, $J = 5.0, 2.4$ Hz, 1H, H2'), 4.21 (dd, $J = 7.9, 1.9$ Hz, 1H, H4'), 3.97 (ddd, $J = 7.1, 5.4, 1.8$ Hz, 1H, H5'), 3.70 (dd, $J = 10.3, 5.5$ Hz, 1H, H6'a), 3.64 (dd, $J = 10.2, 7.0$ Hz, H, H6'b), 1.49 (s, 3H, CH ₃), 1.40 (s, 3H, CH ₃), 1.30 (s, 6H, C(CH ₃) ₂)
72b		7.52 (s, 1H, H5), 7.34 (ddd, $J = 13.7, 7.9, 5.8$ Hz, 1H, Ar-H), 7.05–7.02 (m, 2H, Ar-H), 6.95 (dt, $J = 9.2, 1.8$ Hz, 1H, Ar-H)	5.51 (d, $J = 5.0$ Hz, 1H, H1'), 5.50 (s, 2H, Ar-CH ₂ -triazole), 4.71 (dd, $J = 12.5, 0.5$ Hz, 1H, triazole-CH ₂ -CHO), 4.68 (dd, $J = 12.6, 0.5$ Hz, 1H, triazole-CH ₂ -CHO), 4.58 (dd, $J = 7.9, 2.4$ Hz, 1H, H3'), 4.29 (dd, $J = 5.0, 2.4$ Hz, 1H, H2'), 4.22 (dd, $J = 7.9, 1.9$ Hz, 1H, H4'), 3.98 (ddd, $J = 7.0, 5.6, 1.8$ Hz, 1H, H5'), 3.71 (dd, $J = 10.3, 5.4$ Hz, 1H, H6'a), 3.66 (dd, $J = 10.3, 7.1$ Hz, H, H6'b), 1.50 (s, 3H, CH ₃), 1.40 (s, 3H, CH ₃), 1.31 (s, 6H, C(CH ₃) ₂)
72c		7.48 (s, 1H, H5), 7.25 (app t, $J = 7.5, 2$ Hz, Ar-H), 7.05 (app t, $J = 8.6$ Hz, 2H, Ar-H)	5.51 (d, $J = 5.1$ Hz, 1H, H1'), 5.48 (s, 2H, Ar-CH ₂ -triazole), 4.70 (d, $J = 12.5$ Hz, 1H, triazole-CH ₂ -CHO), 4.67 (d, $J = 12.6$ Hz, 1H, triazole-CH ₂ -CHO), 4.58 (dd, $J = 7.9, 2.4$ Hz, 1H, H3'), 4.29 (dd, $J = 5.0, 2.4$ Hz, 1H, H2'), 4.22 (dd, $J = 7.9, 1.9$ Hz, 1H, H4'), 3.97 (ddd, $J = 7.0, 5.4, 1.7$ Hz, 1H, H5'), 3.70 (dd, $J = 10.3, 5.5$ Hz, 1H, H6'a), 3.65 (dd, $J = 10.3, 7.0$ Hz, H, H6'b), 1.50 (s, 3H, CH ₃), 1.41 (s, 3H, CH ₃), 1.312 (s, 3H, CH ₃), 1.31 (s, 3H, CH ₃)

Figure (3-37). Proton NMR chart (CDCl₃, 600 MHz) of compound 72aFigure (3-38). Proton NMR chart (CDCl₃, 600 MHz) of compound 72b

Figure (3-39). Proton NMR chart (CDCl₃, 600 MHz) of compound **72c**Figure (3-40). Magnified aromatic region proton nuclear magnetic resonance spectrum (CDCl₃, 600 MHz) of triazole **72a**

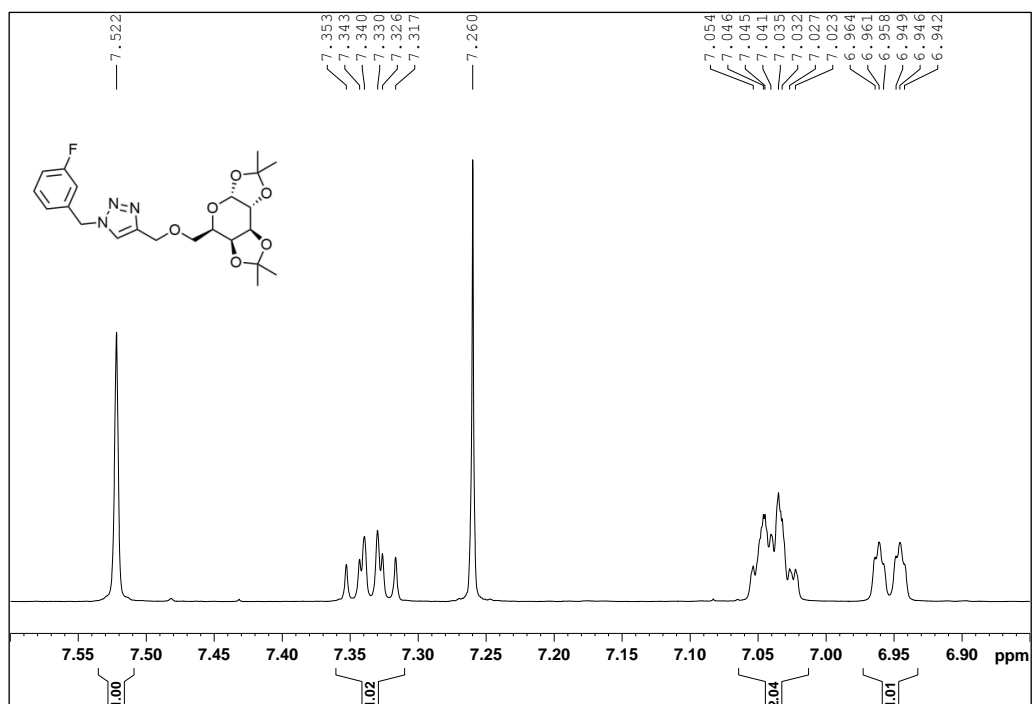


Figure (3-41). Magnified aromatic region proton nuclear magnetic resonance spectrum (CDCl_3 , 600 MHz) of triazole **72b**

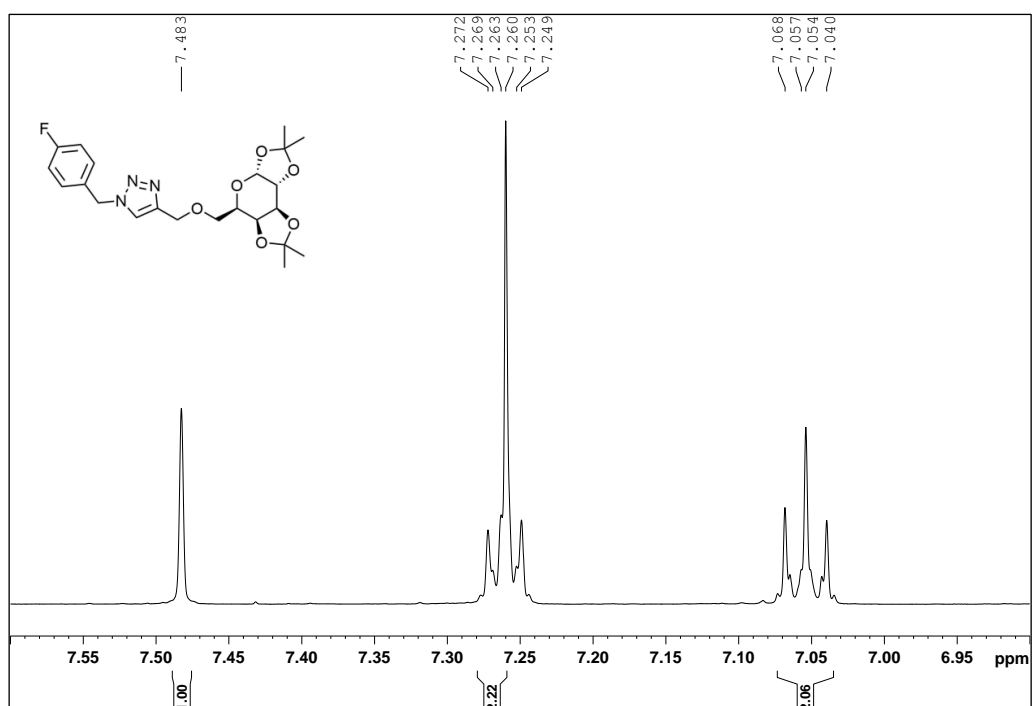


Figure (3-42). Magnified aromatic region proton nuclear magnetic resonance spectrum (CDCl_3 , 600 MHz) of triazole **72c**

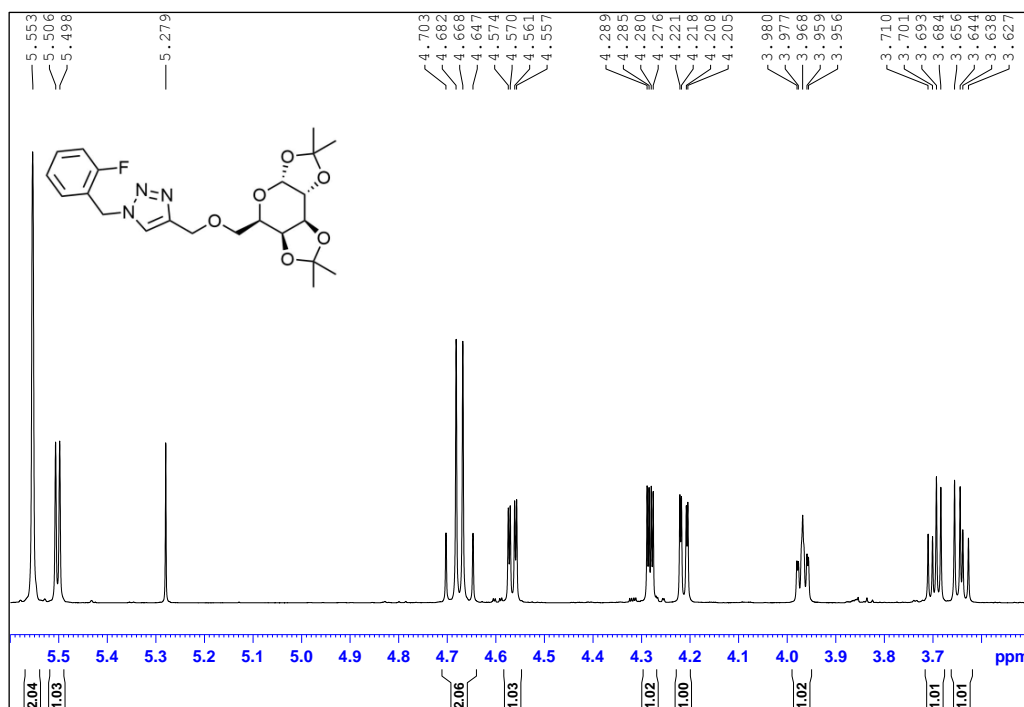


Figure (3-43). Magnified aliphatic region proton nuclear magnetic resonance spectrum (CDCl_3 , 600 MHz) of triazole **72a**

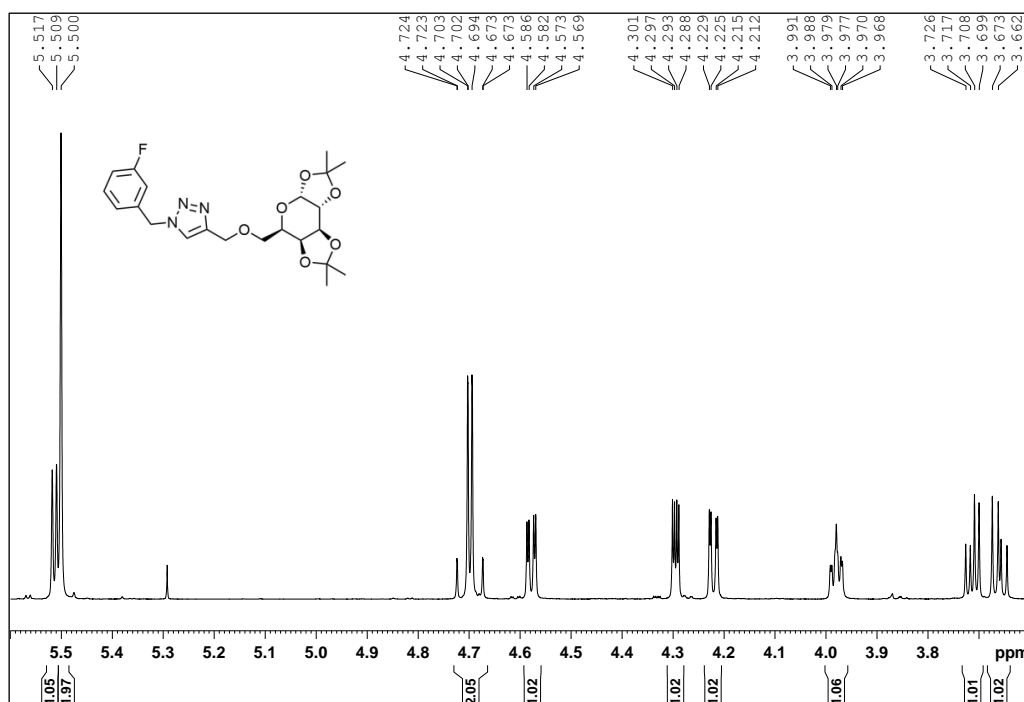


Figure (3-44). Magnified aliphatic region proton nuclear magnetic resonance spectrum (CDCl_3 , 600 MHz) of triazole **72b**

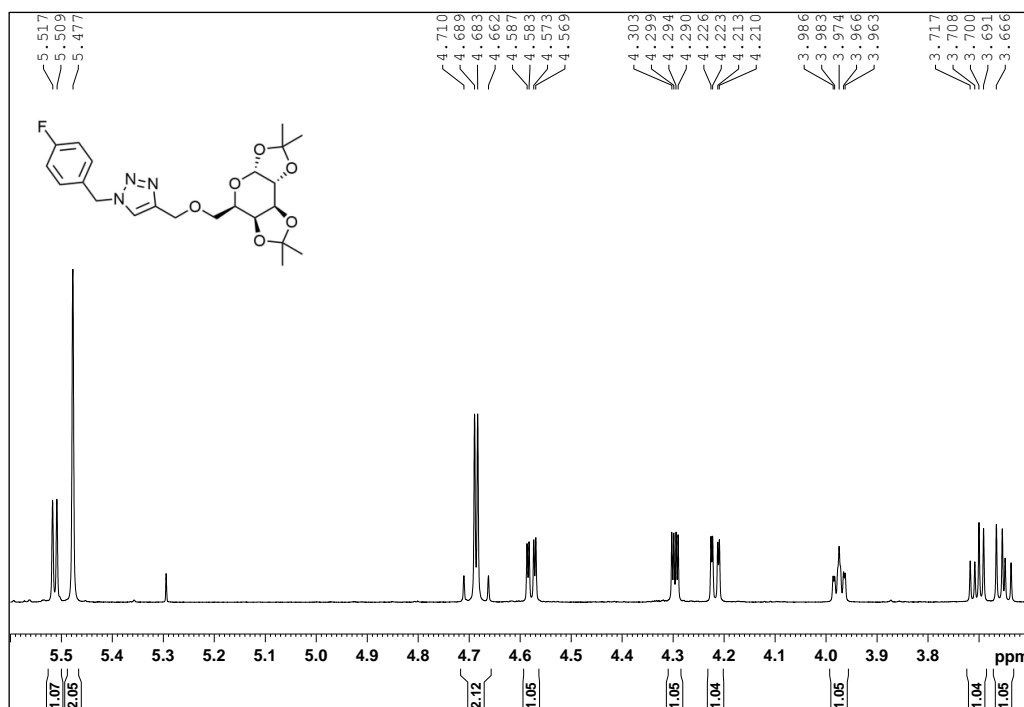
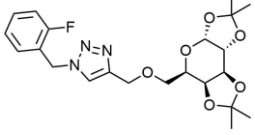
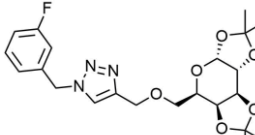
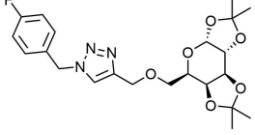
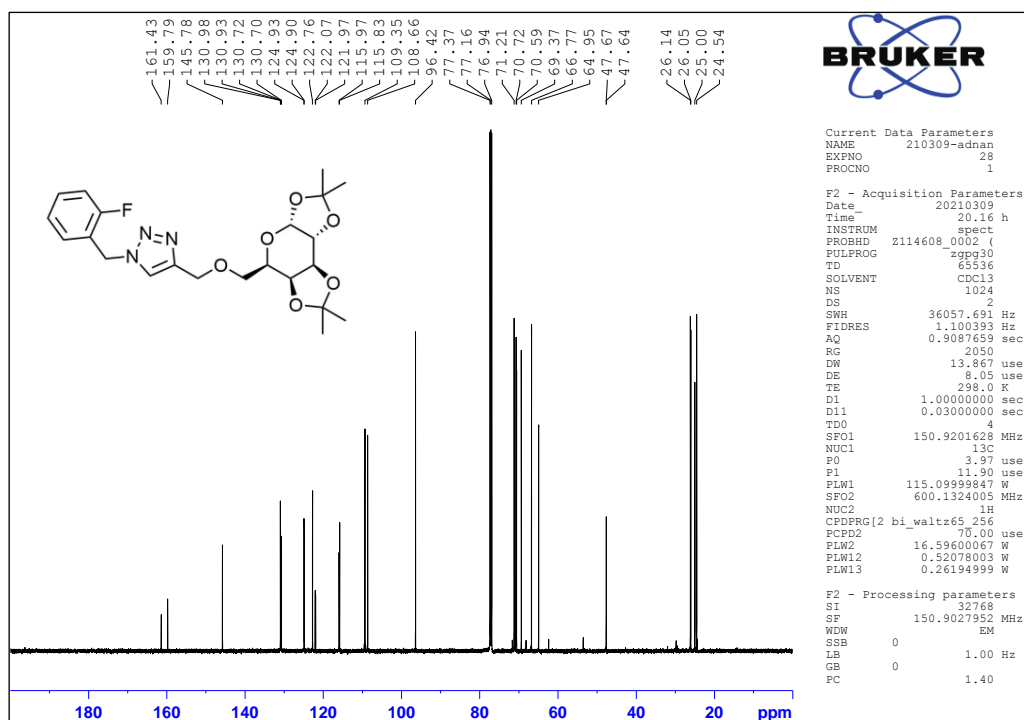
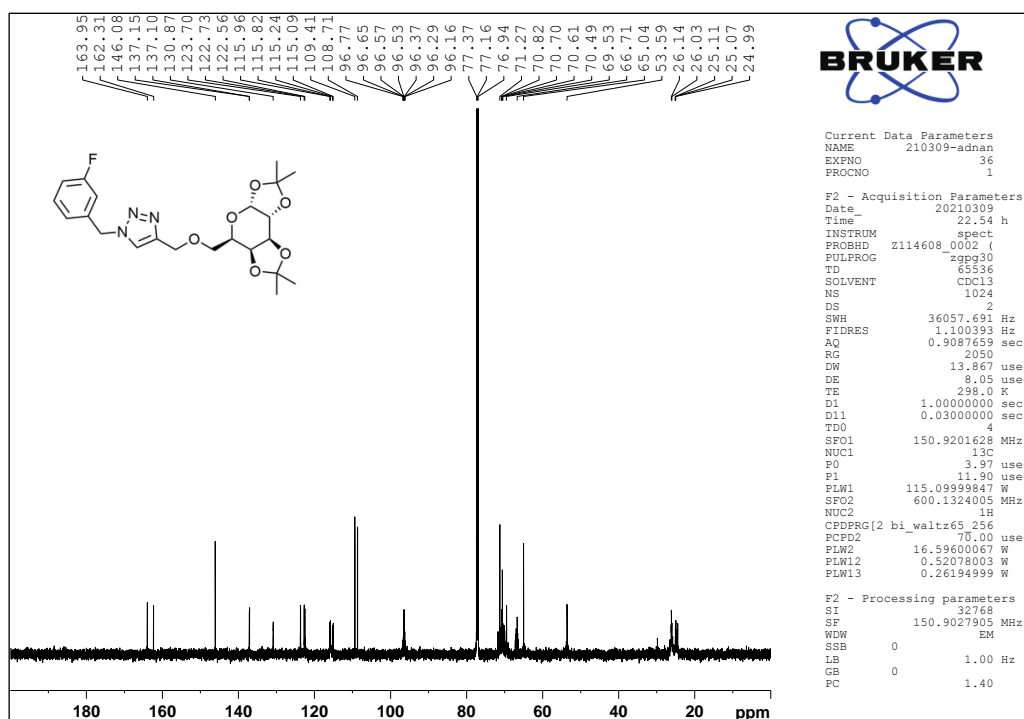


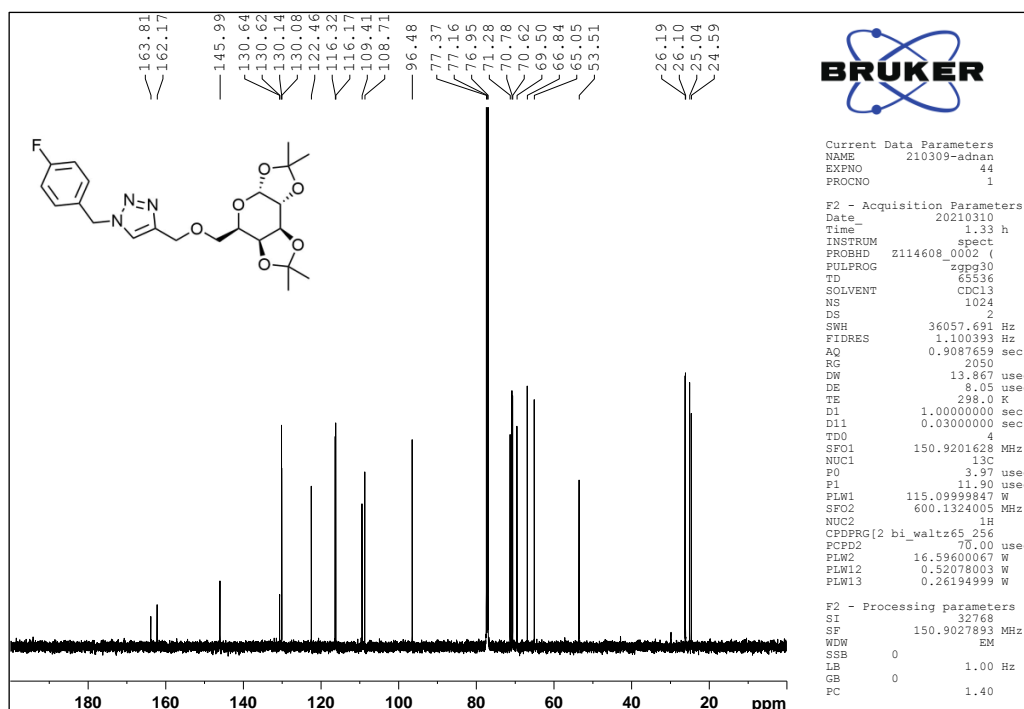
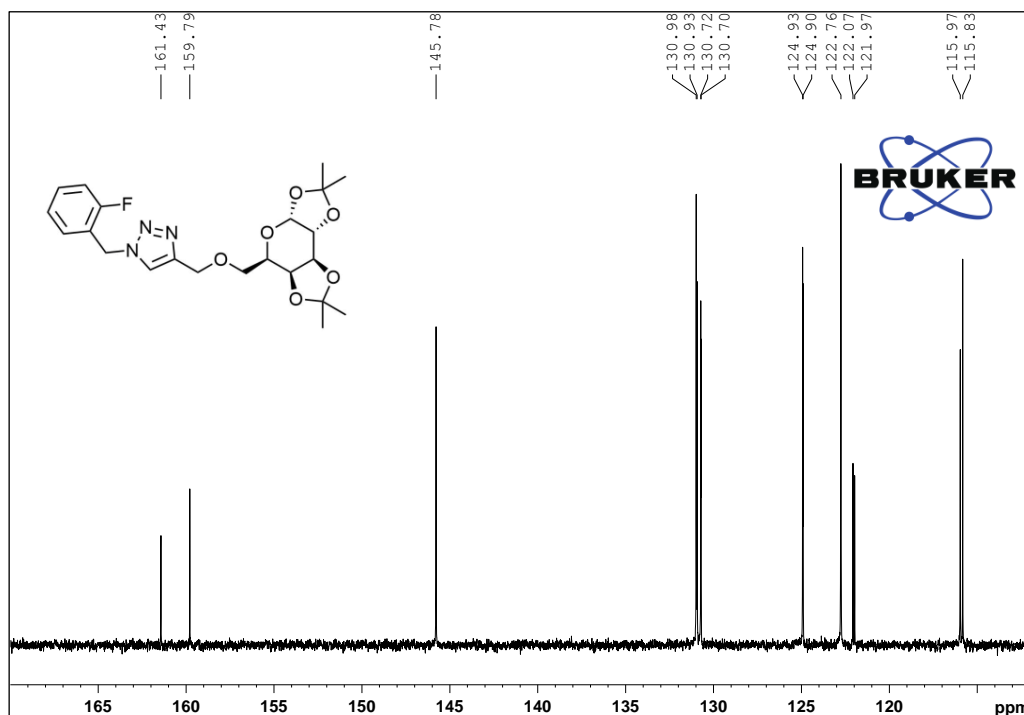
Figure (3-45). Magnified aliphatic region proton nuclear magnetic resonance spectrum (CDCl_3 , 600 MHz) of triazole **72c**

The $^{13}\text{C}\{^1\text{H}\}$ NMR spectra (Figures 46–48) of compounds **72a–c** exhibited the constitution of extreme pure of compounds as they have the same number of carbon signals regarding to every compound. Initially, the Ar area contains all benzyl ring peaks between 163 ppm and 116 ppm. Moreover, the peaks of the two carbon atoms of triazole ring appear at ~ 145 ppm and 122 ppm (Figures 49–51). The noteworthy click reaction does not influence the cyclic acetal protecting groups. This is because that the locations of the acetal carbon signals at 109.0 ppm, 108.0 ppm, 26.0–24.0 ppm did not alter after the click reaction. All other signals in $^{13}\text{C}\{^1\text{H}\}$ NMR spectra are assigned to either sugar pyran ring carbon signals or to the methylene carbon atoms. The comparison of carbon-13 NMR signals is illustrated in Table 3.

Table (1-3). Comparison of $^{13}\text{C}\{^1\text{H}\}$ NMR data of the synthesized triazoles **72a–c**

Compound	Structure	Aromatic region (Figure 49–51)	Aliphatic region (Figures 46–48)
72a		160.6 (d, $J = 247.8$ Hz, ArC), 145.8 (C4), 131.0 (d, $J = 7.8$ Hz, ArC), 130.7 (d, $J = 3.0$ Hz, ArC), 124.9 (d, $J = 4.0$ Hz, ArC), 122.8 (C5), 122.0 (d, $J = 14.3$ Hz, ArC), 115.9 (d, $J = 21.2$ Hz, ArC).	109.3 (C(CH ₃) ₂), 108.6 (C(CH ₃) ₂), 96.4 (C1'), 71.2 (C4'), 70.7 (C3'), 70.6 (C2'), 69.4 (C6'), 66.8 (C5'), 65.0 (triazole -CH ₂ - CHO), 47.7 (d, $J = 4.3$ Hz, Ar-CH ₂ -triazole), 26.1 (CH ₃), 26.0 (CH ₃), 25.0 (CH ₃), 24.0 (CH ₃)
72b		163.1 (d, $J = 247.9$ Hz, ArC), 146.1 (C4), 137.1 (d, $J = 7.1$ Hz, ArC), 130.9 (ArC), 123.7 (C5), 122.7 (d, $J = 26.1$ Hz, ArC), 115.9 (d, $J = 20.9$ Hz, ArC), 115.2 (d, $J = 22.1$ Hz, ArC).	109.4 (C(CH ₃) ₂), 108.7 (C(CH ₃) ₂), 96.5 (m, 1C, C1'), 71.3 (C4'), 70.8 (d, $J = 17.5$ Hz, C3'), 70.6 (m, 1C, C2'), 69.5 (C6'), 66.8 (m, 1C, C5'), 65.0 (triazole -CH ₂ - CHO), 53.6 (Ar-CH ₂ -triazole), 26.1 (CH ₃), 26.0 (CH ₃), 25.0 (m, CH ₃), 24.6 (m, CH ₃)
72c		163.0 (d, $J = 247.8$ Hz, ArC), 146.0 (C4), 130.6 (d, $J = 3.3$ Hz, ArC), 130.1 (d, $J = 8.7$ Hz, ArC), 122.4 (C5), 116.2 (d, $J = 21.9$ Hz, ArC).	109.4 (C(CH ₃) ₂), 108.7 (C(CH ₃) ₂), 96.5 (C1'), 71.3 (C4'), 70.8 (C3'), 70.6 (C2'), 69.5 (C6'), 66.8 (C5'), 65.0 (triazole -CH ₂ - CHO), 53.5 (Ar-CH ₂ -triazole), 26.18 (CH ₃), 26.1 (CH ₃), 25.0 (CH ₃), 24.6 (CH ₃).

Figure (3-46). Carbon-13 NMR chart (CDCl₃, 150 MHz) of triazole **72a**Figure (3-47). Carbon-13 NMR chart (CDCl₃, 150 MHz) of triazole **72b**

Figure (3-48). Carbon-13 NMR chart (CDCl₃, 150 MHz) of triazole **72c**Figure (3-49). Magnified aromatic region carbon-13 nuclear magnetic resonance spectrum (CDCl₃, 150 MHz) of triazole **72a**

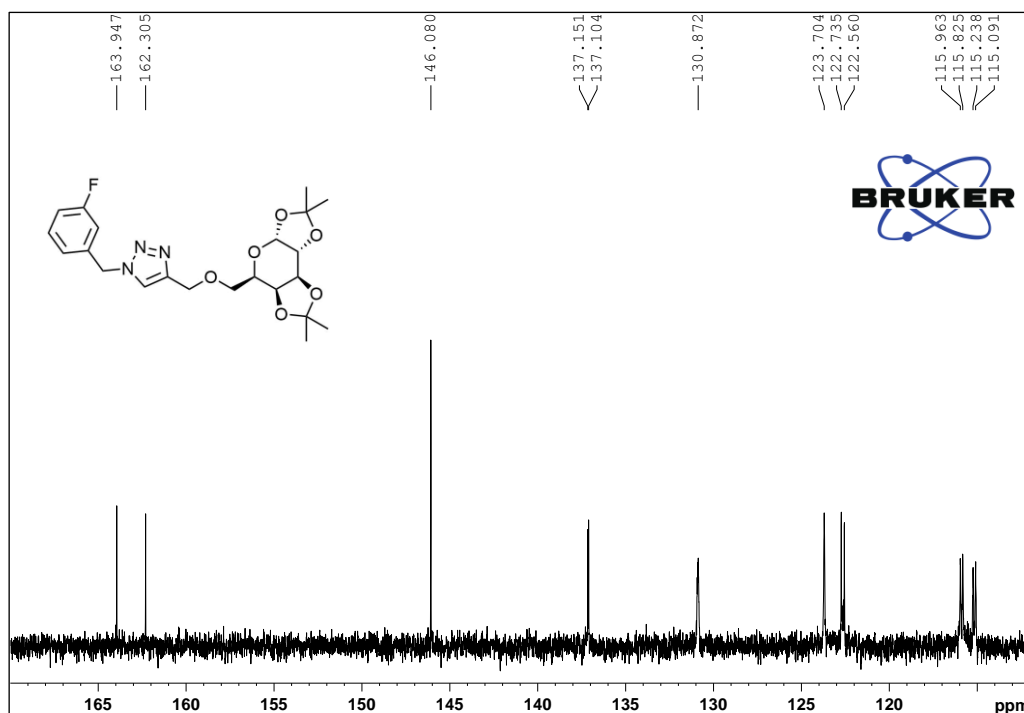


Figure (3—50). Magnified aromatic region carbon-13 nuclear magnetic resonance spectrum (CDCl₃, 150 MHz) of triazole **72b**

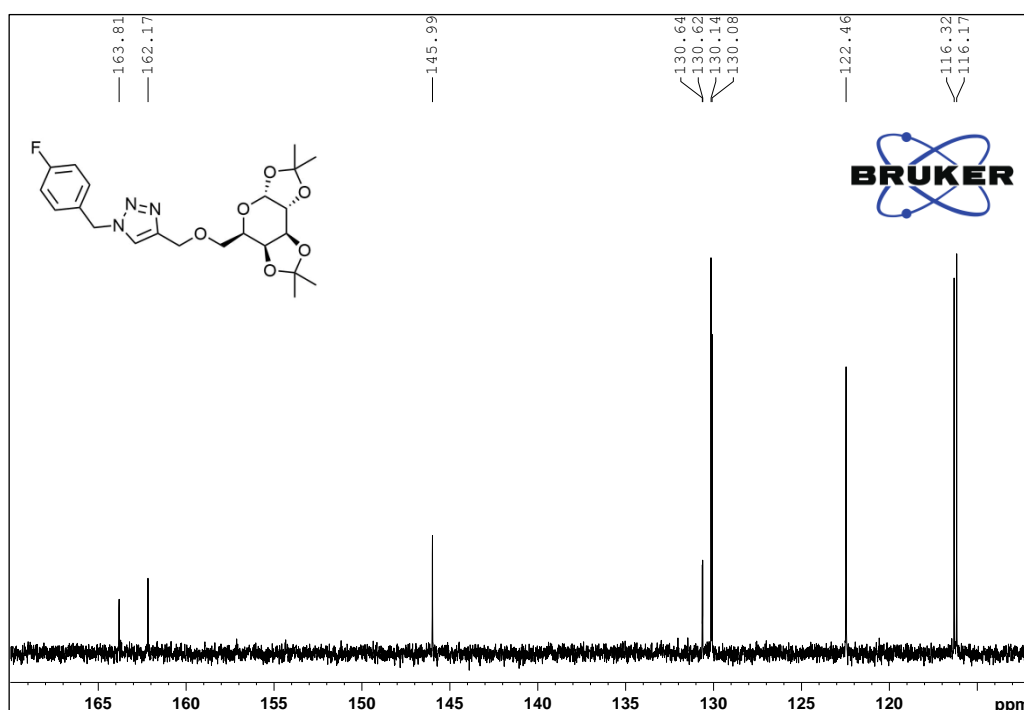


Figure (3-51). Magnified aromatic region carbon-13 nuclear magnetic resonance spectrum (CDCl₃, 150 MHz) of triazole **72c**

The ^{19}F NMR spectra (Figures 52–54) demonstrated one fluorine signal due to fluorine atom attached to the aromatic ring at -118.2 ppm, -111.6 ppm, -112.8 ppm for compounds triazole derivatives **72a**, **72b** and **72c** respectively. The splitting of the fluorine signal is caused by fluorine-hydrogen or fluorine-carbon splitting (Figures 55–57).¹⁰¹

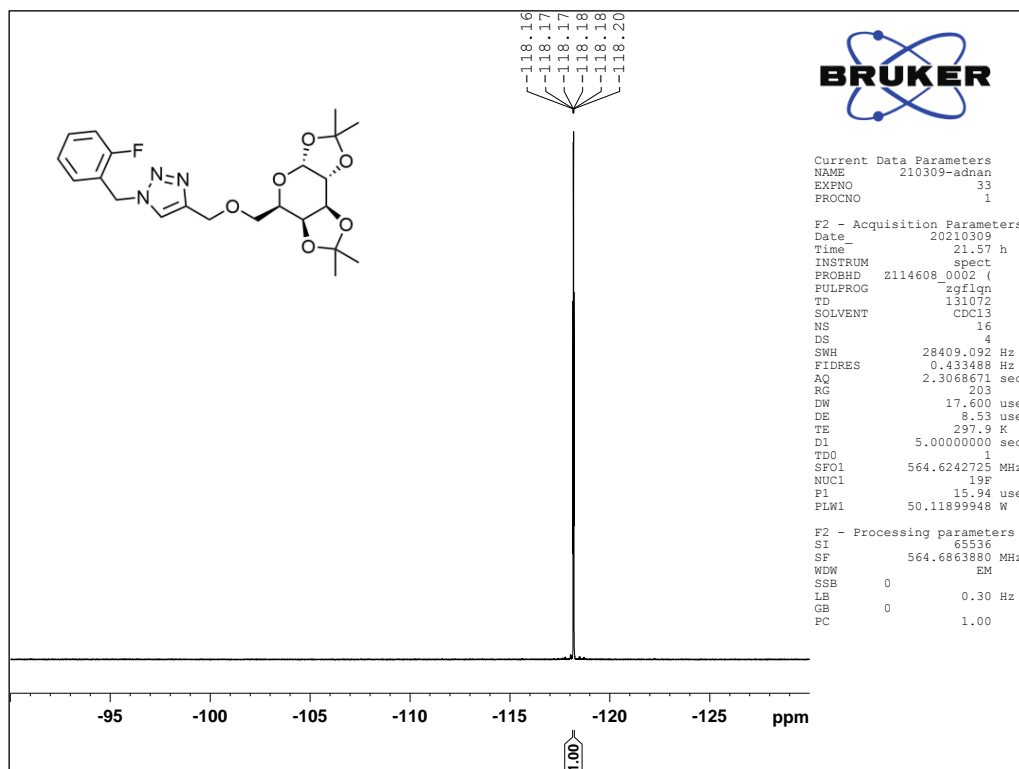
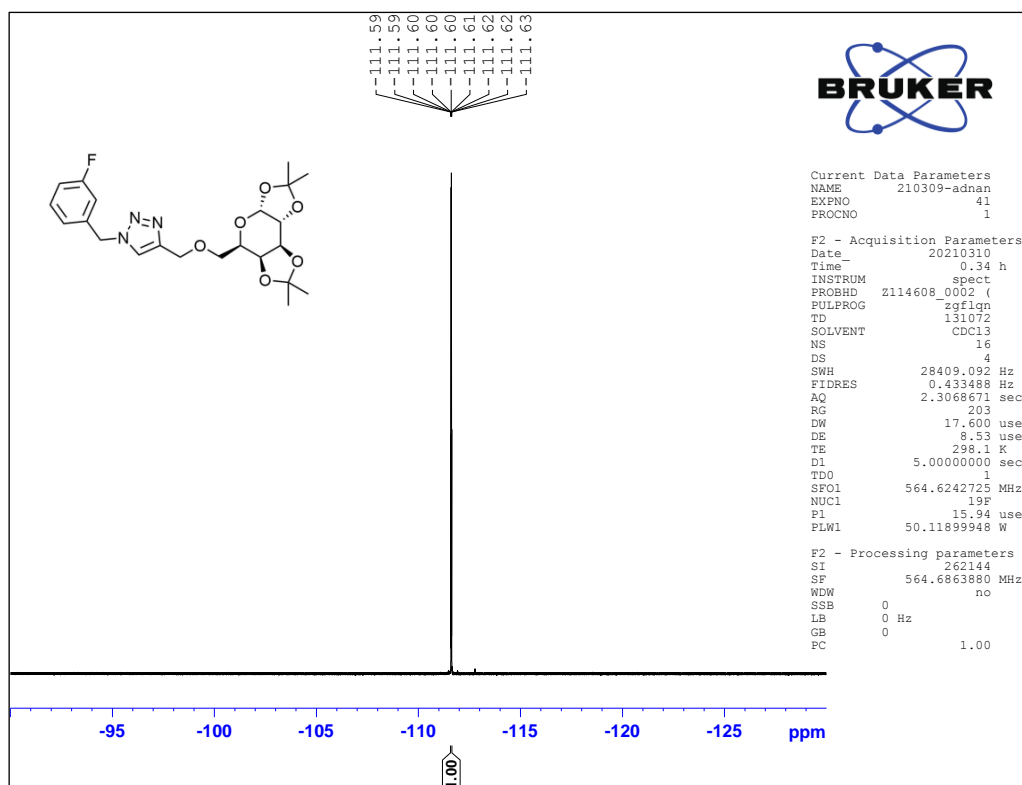
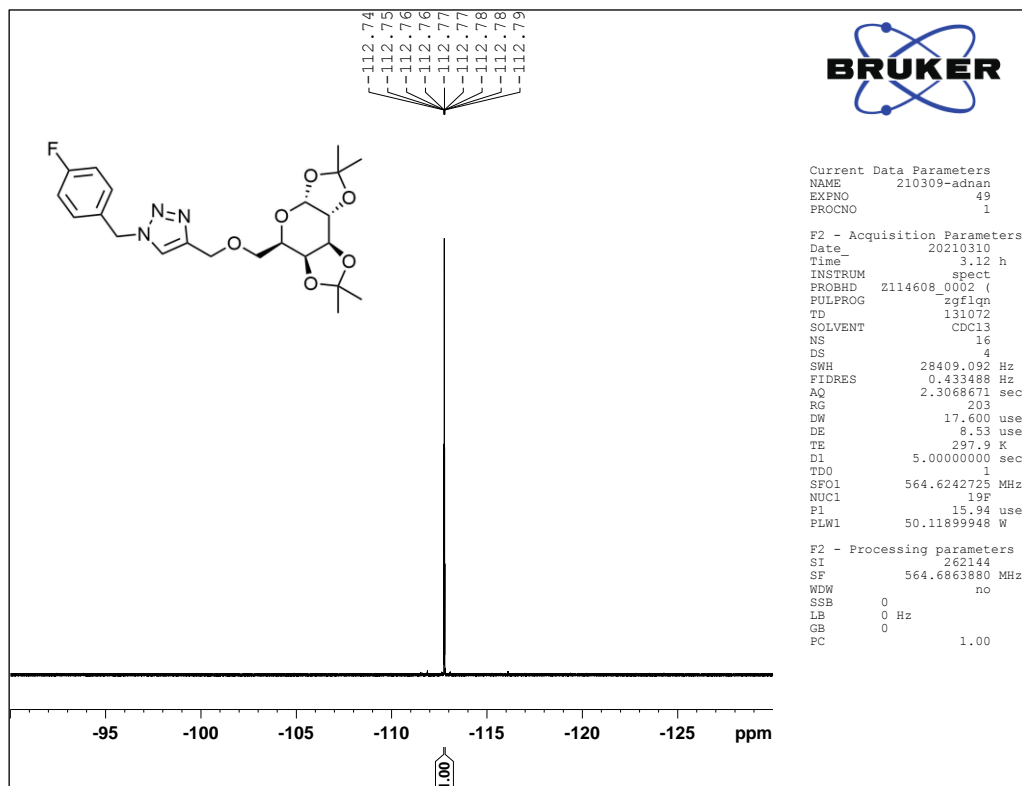


Figure (3-52). Fluorine-19 NMR chart (CDCl_3 , 564 MHz) of triazole **72a**

Figure (3-53). Fluorine-19 NMR chart (CDCl₃, 564 MHz) of triazole **72b**Figure (3-54). Fluorine-19 NMR chart (CDCl₃, 564 MHz) of triazole **72c**

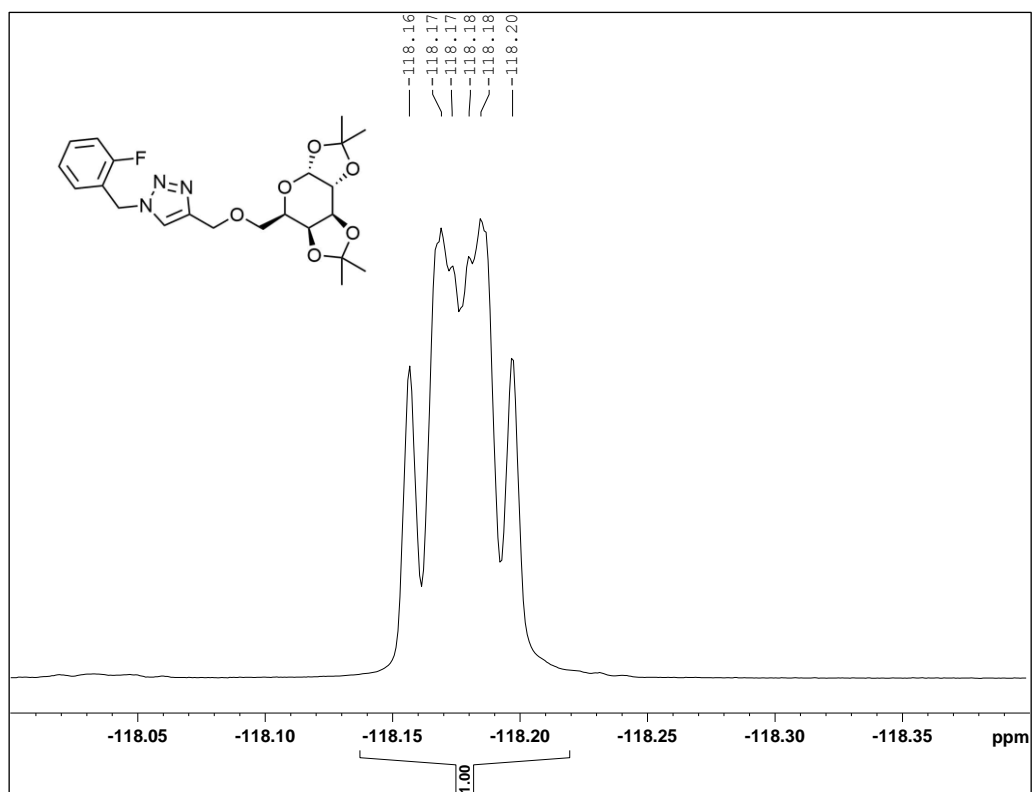


Figure (3-55). Magnified Fluorine-19-NMR chart (CDCl₃, 564 MHz) of compound

72a

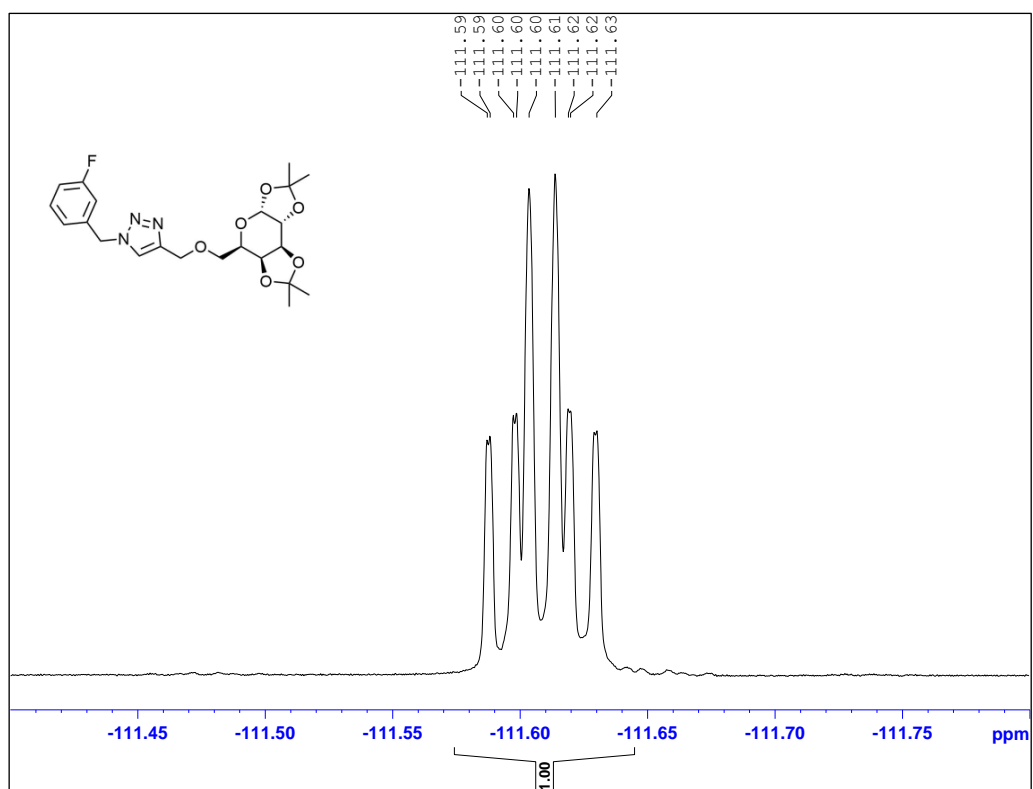
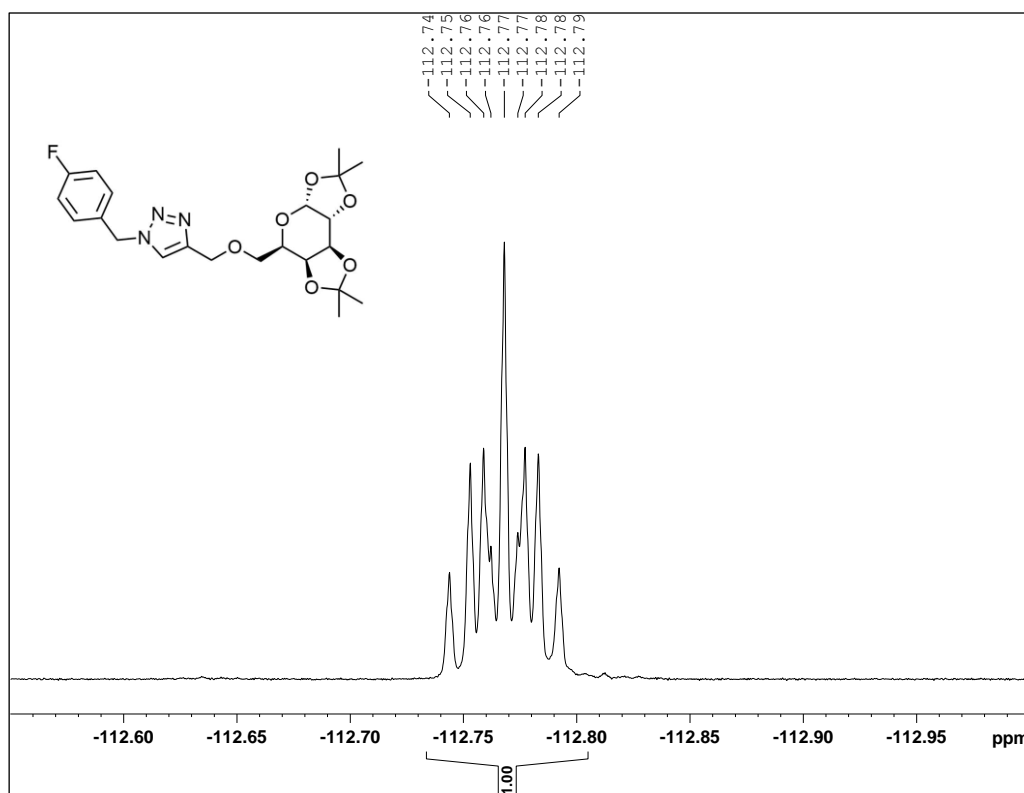


Figure (3-56). Magnified Fluorine-19-NMR chart (CDCl₃, 564 MHz) of compound**72b****Figure (3-57).** Magnified Fluorine-19-NMR chart (CDCl₃, 564 MHz) of compound**72c**

The precise identification of triazole derivatives **72a–c** is also accomplished by two-dimensional nuclear magnetic resonance method ¹H–¹H COSY, ¹H–¹³C HSQC and ¹H–¹³C HMBC. COSY spectra are efficient tools to characterize proton–proton correlation by displaying cross signals between the protons on adjacent carbon atoms. The extended ¹H–¹H COSY spectra (Figures 55–57) of compound **72a–c** show the cross signals between pyranose protons, and they are nearly comparable. Nonetheless, the magnified spectra (Figures 58–60) of the aromatic part of compounds **72a–c** display significant differences between the three compounds **72a–c** resulting from the location of fluorine on the aromatic ring that led to various splitting patterns.

Obviously, this is also shown in the one-dimensional NMR charts of the derivatives 72a–c.

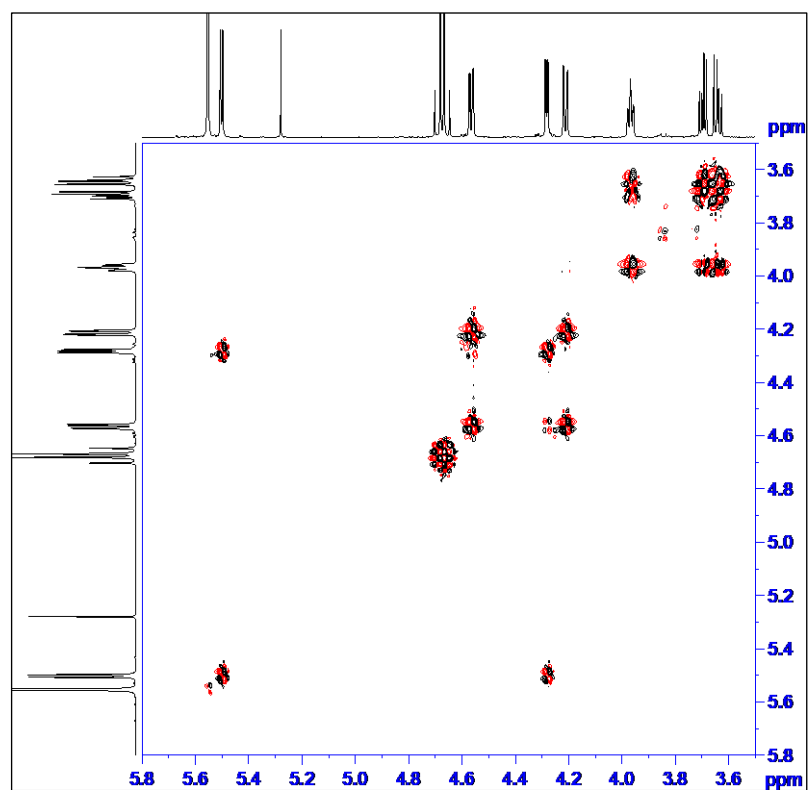


Figure (3-58). Zoomed in ¹H–¹H COSY (600 MHz, CDCl₃) of compound 72a

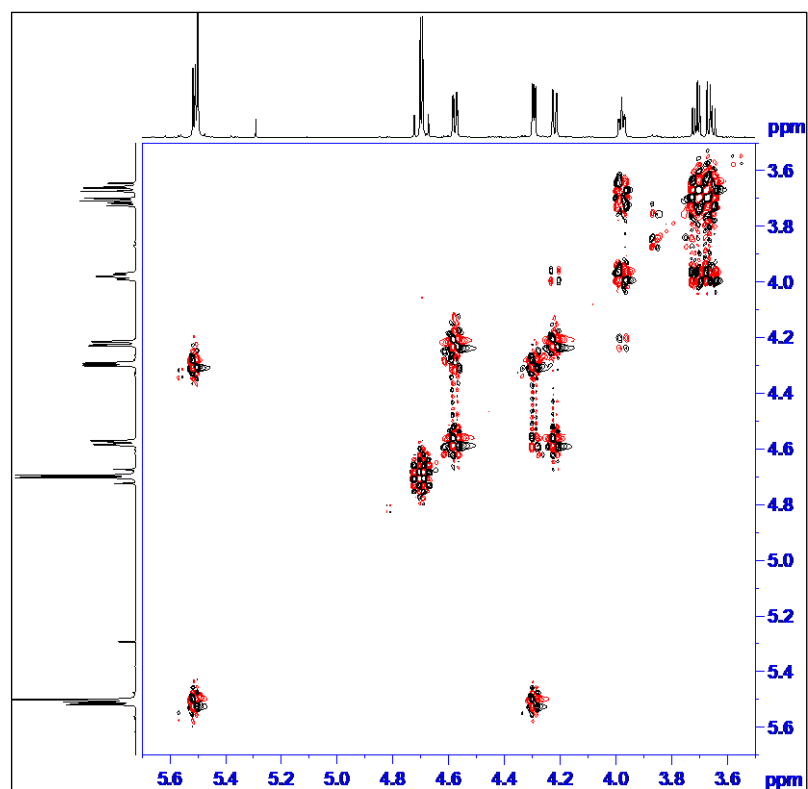


Figure (3-59). Zoomed in ^1H - ^1H COSY (600 MHz, CDCl_3) of compound **72b**

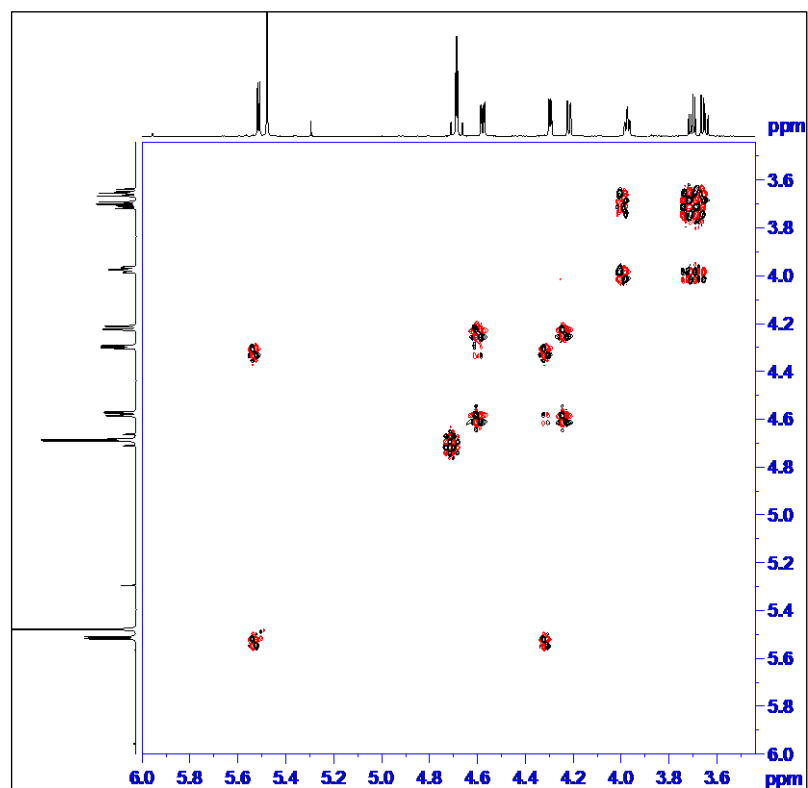


Figure (3-60). Zoomed in ^1H - ^1H COSY (600 MHz, CDCl_3) of compound **72c**

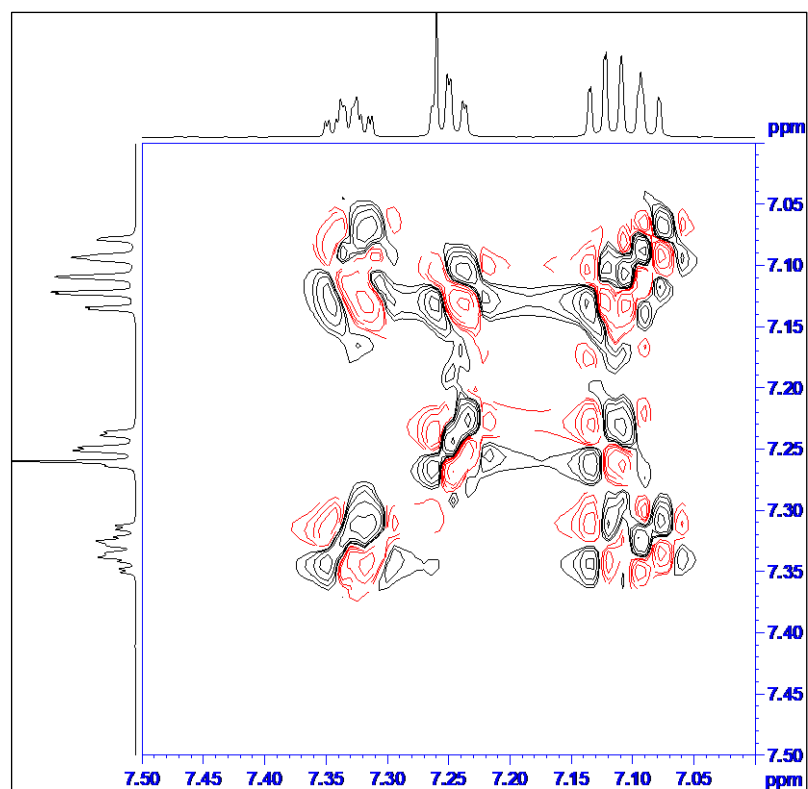


Figure (3-61). Magnified ^1H - ^1H COSY (CDCl_3 , 600 MHz) of triazole 72a

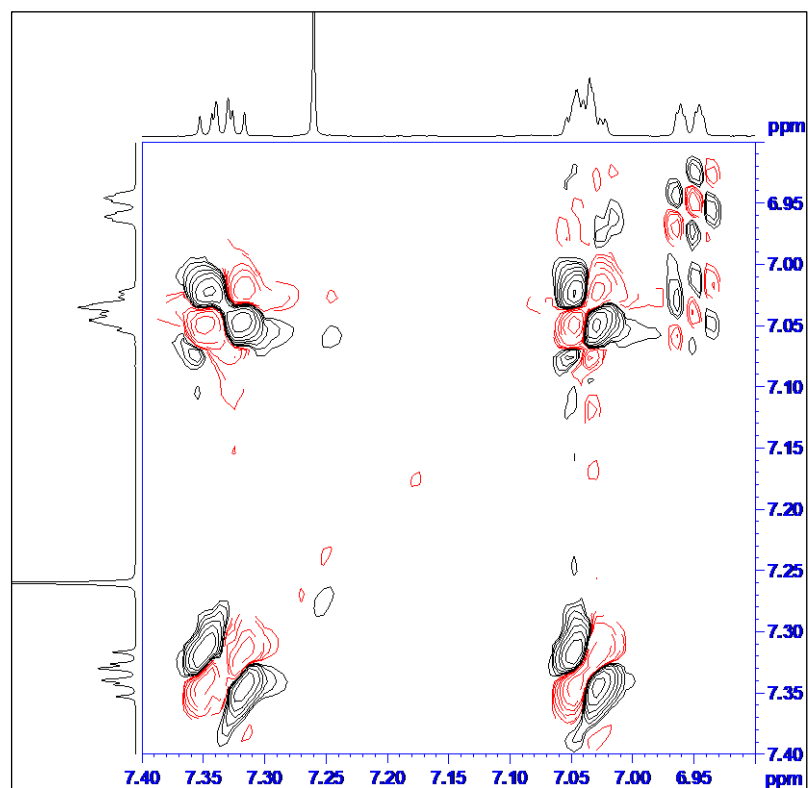


Figure (3-62). Magnified ^1H - ^1H COSY (CDCl_3 , 600 MHz) of triazole 72b

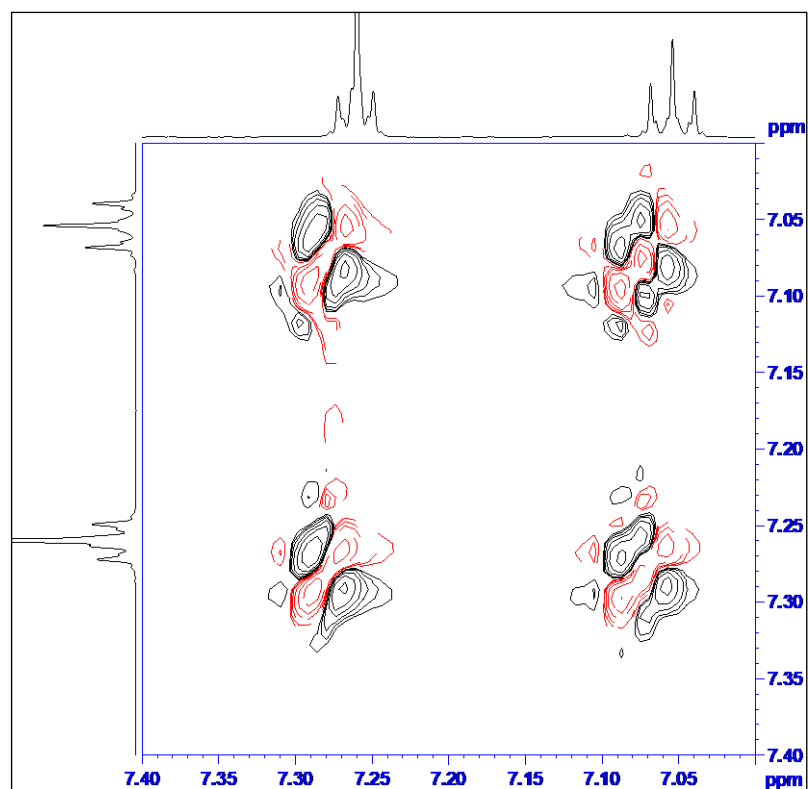


Figure (3-63). Magnified ^1H - ^1H COSY (CDCl_3 , 600 MHz) of triazole **72c**

Compounds **72a–c** were also accurately characterized utilizing Heteronuclear Single Quantum Coherence HSQC (Figures 61–65) and Heteronuclear Multiple Bond Correlation HMBC (Figures 66–68). Once again, sugar core region of the compounds **72a–c** displayed almost similar spectra. However, the Ar region displayed clear distinctions among the three derivatives due to the different location of the fluorine substitution of each derivative.

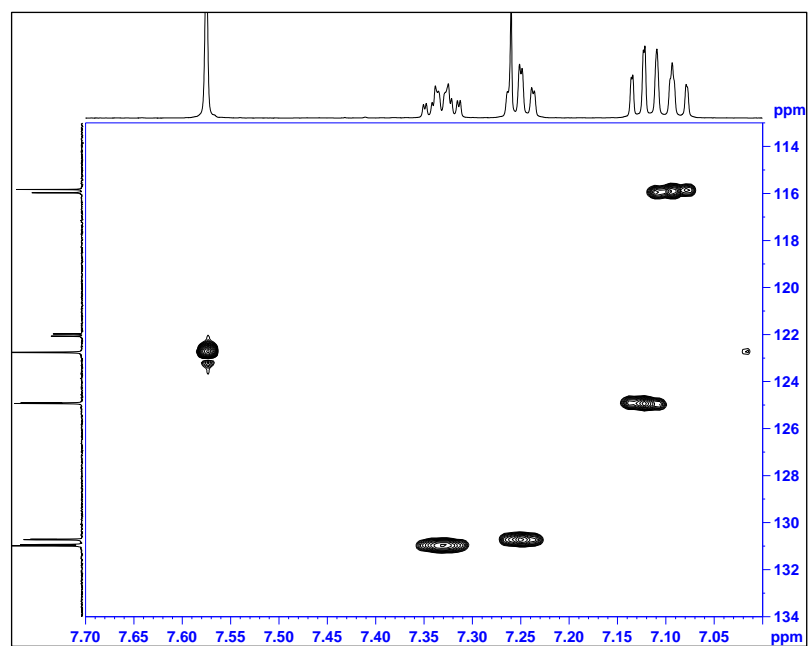


Figure (3-64). Magnified aromatic region ^1H - ^{13}C HSQC (CDCl_3 , 600 MHz) of triazole **72a**

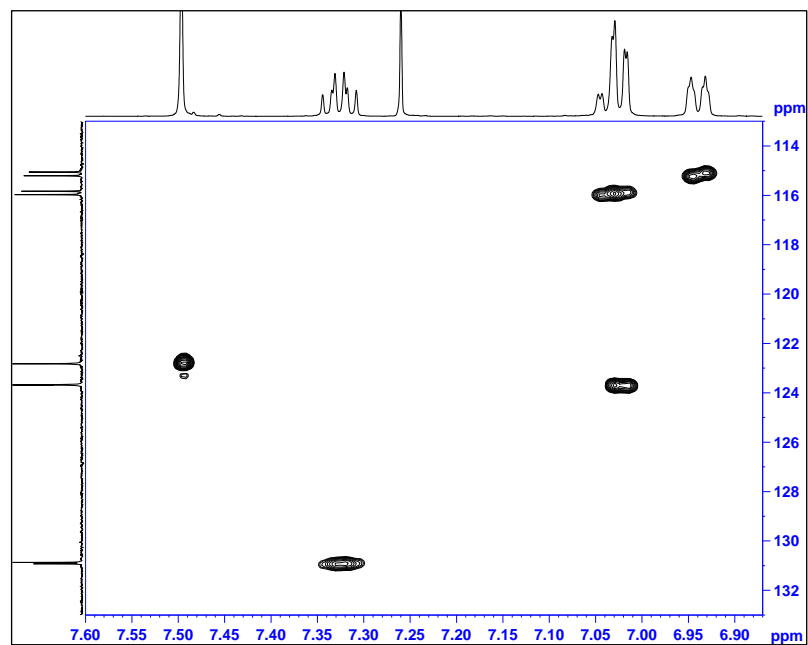


Figure (3-65). Magnified aromatic region ^1H - ^{13}C HSQC (CDCl_3 , 600 MHz) of triazole **72b**

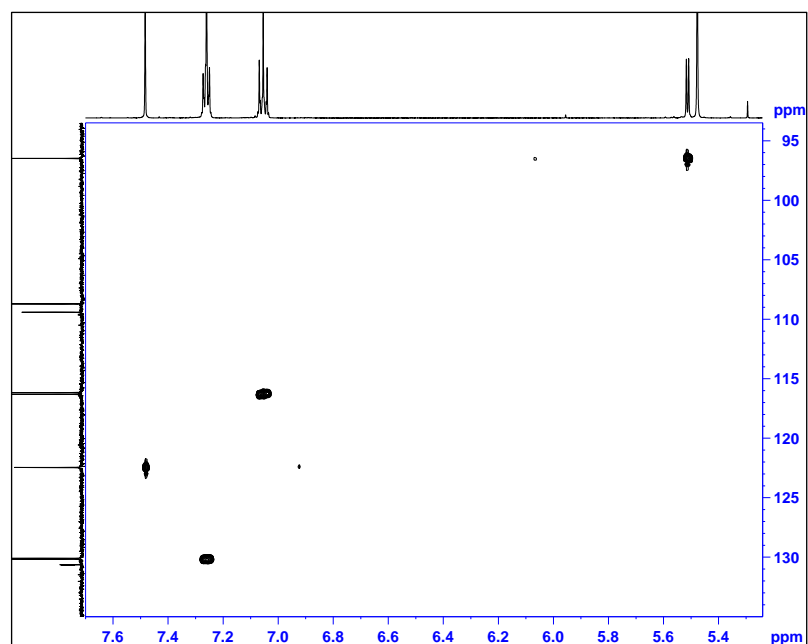


Figure (3-66). Magnified aromatic region ^1H - ^{13}C HSQC (CDCl_3 , 600 MHz) of triazole **72c**

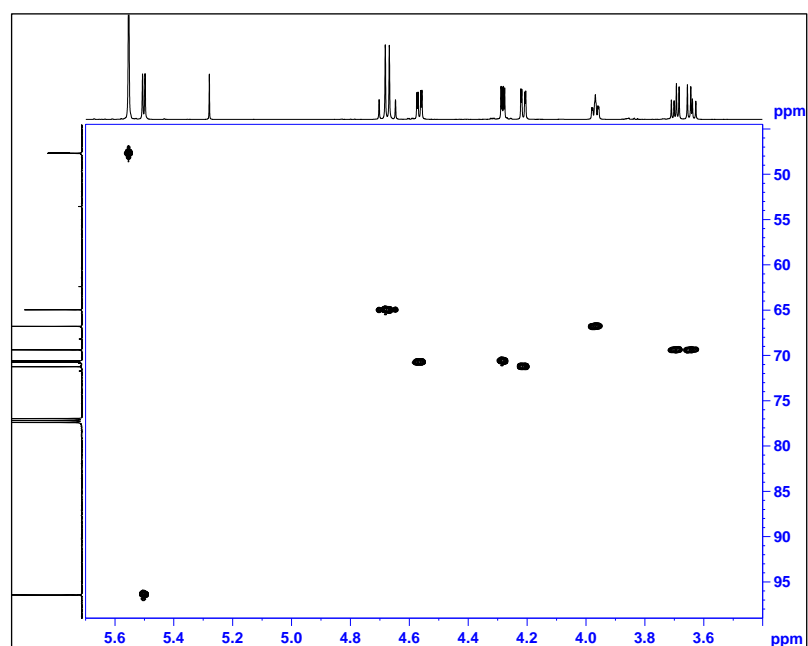


Figure (3-67). Magnified aliphatic region ^1H - ^{13}C HSQC (CDCl_3 , 600 MHz) of triazole **72a**

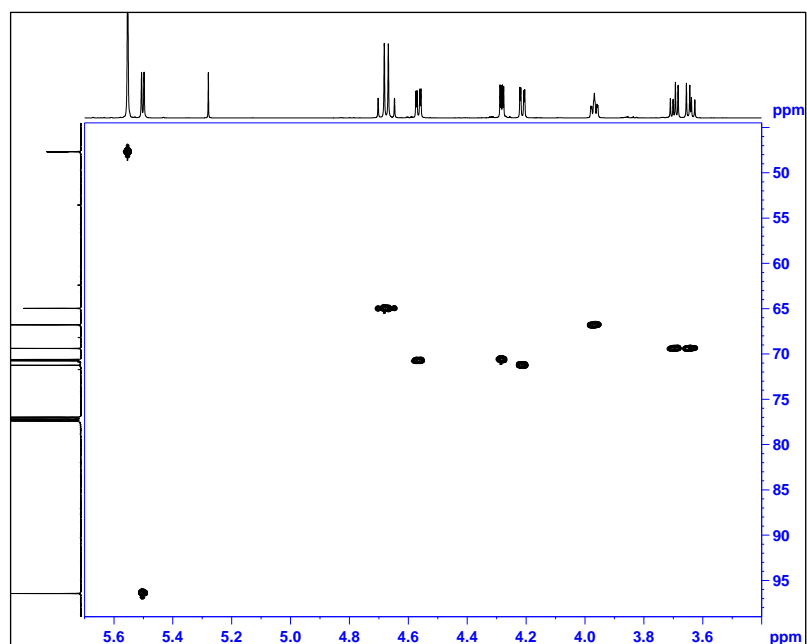


Figure (3-68). Magnified aliphatic region ^1H - ^{13}C HSQC (CDCl_3 , 600 MHz) of triazole **72b**

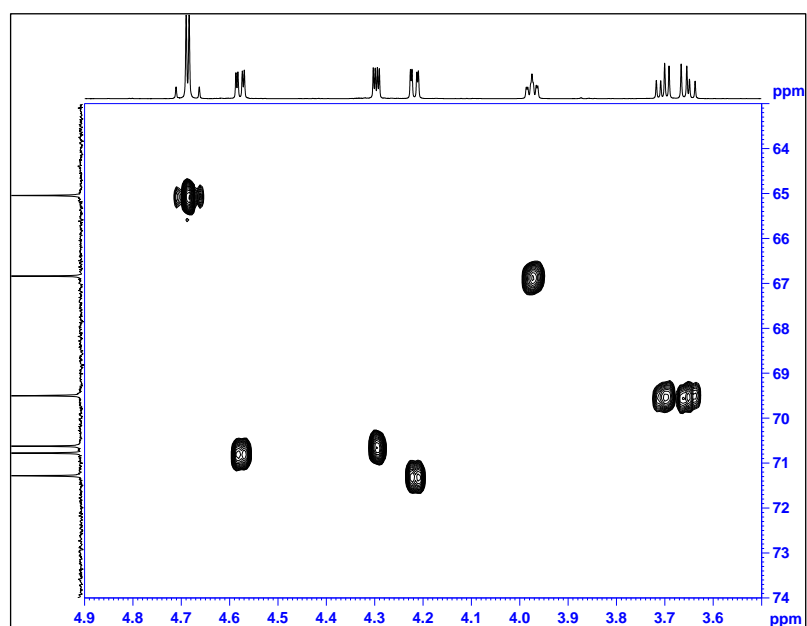


Figure (3-69). Magnified aliphatic region ^1H - ^{13}C HSQC (CDCl_3 , 600 MHz) of triazole **72c**

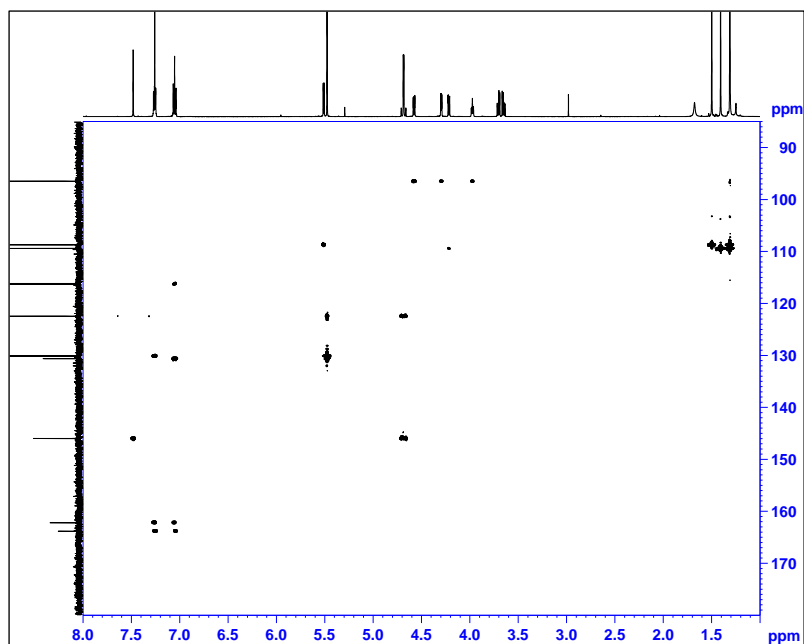


Figure (3-70). Magnified aliphatic region ^1H - ^{13}C HMBC (CDCl_3 , 600 MHz) of triazole **72a**

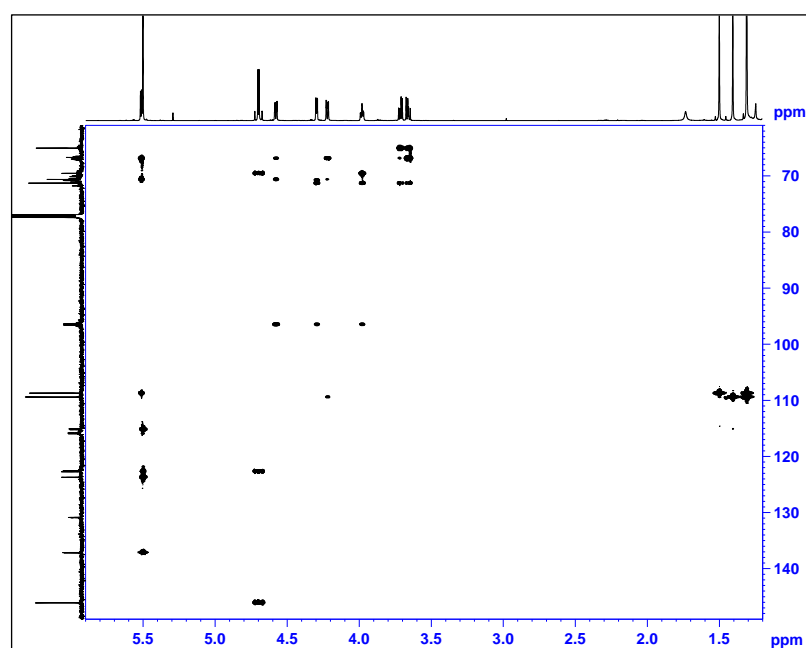


Figure (3-71). Magnified aliphatic region ^1H - ^{13}C HMBC (CDCl_3 , 600 MHz) of triazole **72b**

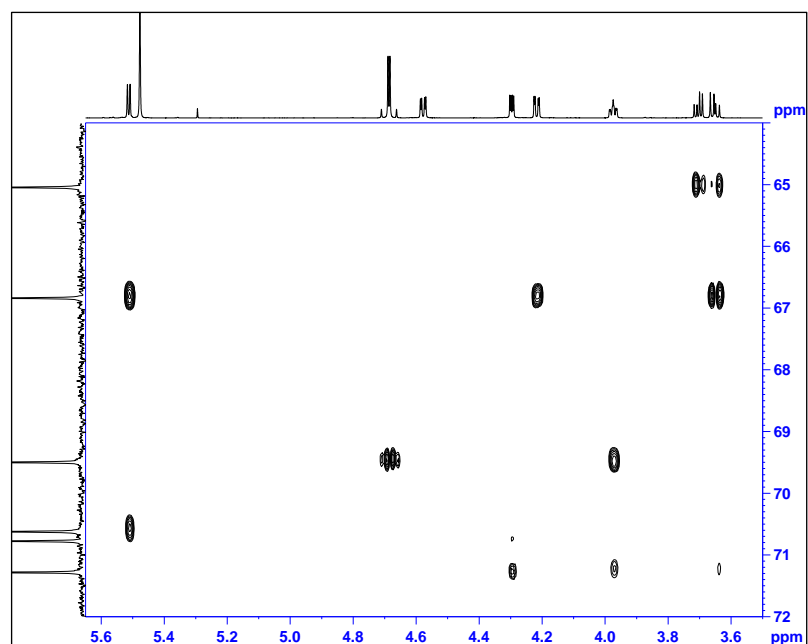


Figure (3-72). Magnified aliphatic region ^1H - ^{13}C HMBC (CDCl_3 , 600 MHz) of triazole **72c**

Ultimately, High Resolution Mass Spectra were employed to characterize the exact molecular weight of every compound. HRMS analyses (Figures 70–72) major signals at m/z 472.1852, 472.1852 and 472.1853 were assigned for the derivatives **72a**, **72b** and **72c** respectively which agrees with the formula $\text{C}_{22}\text{H}_{28}\text{FN}_3\text{O}_6\text{Na}^+$.

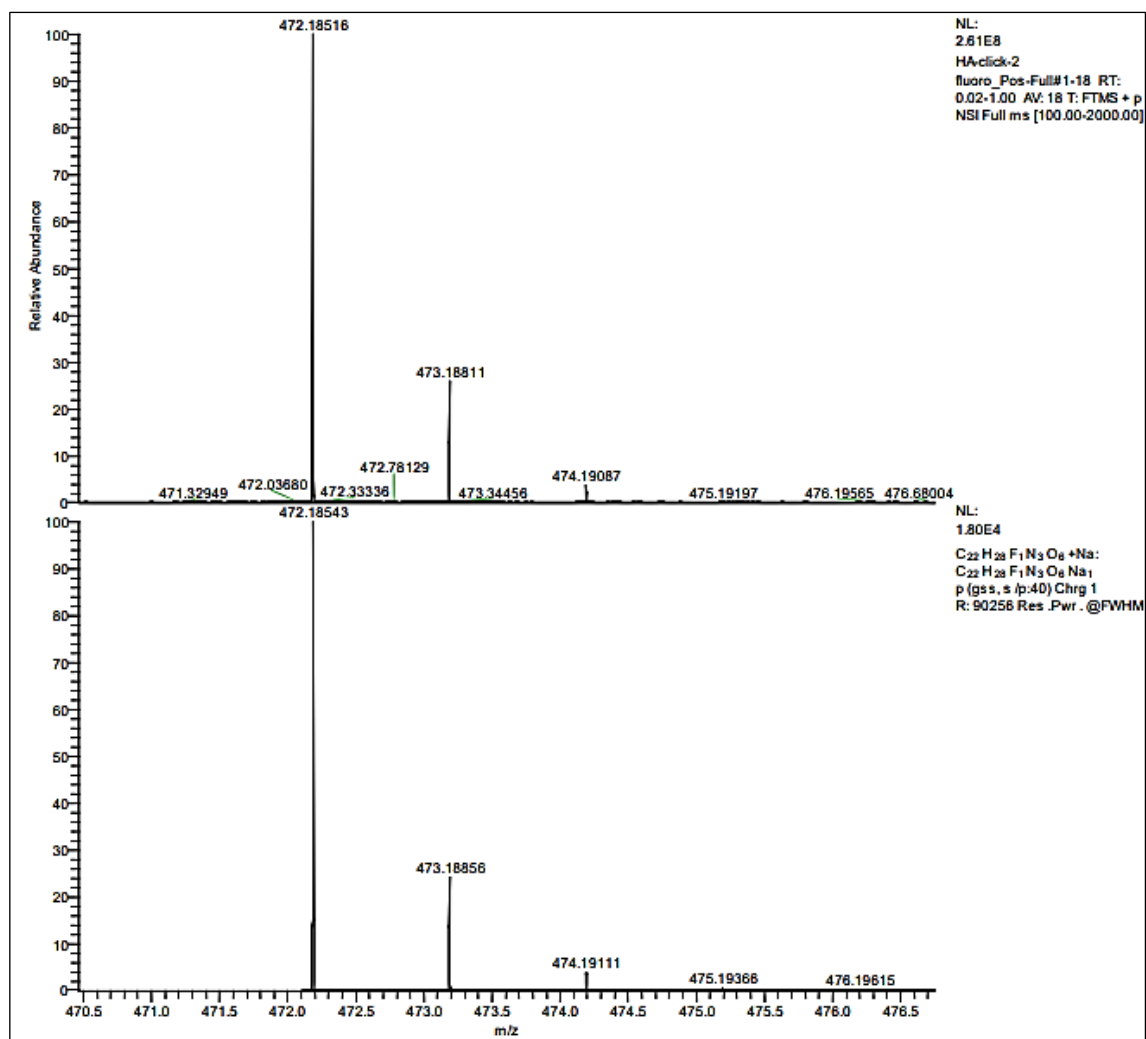


Figure (3-73). High-resolution mass spectrum of triazole **72a**

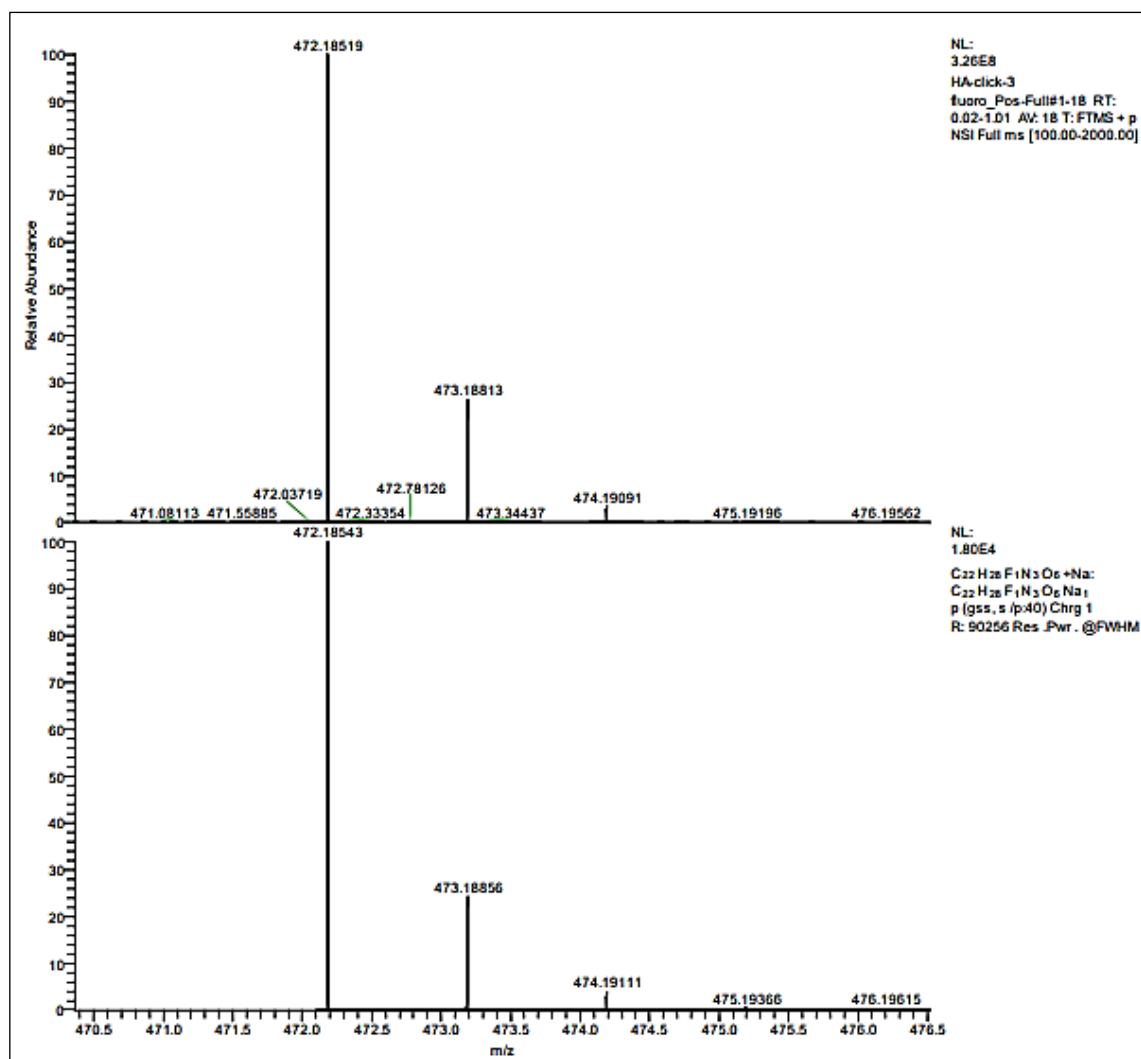


Figure (3-74). High-resolution mass spectrum of triazole **72b**

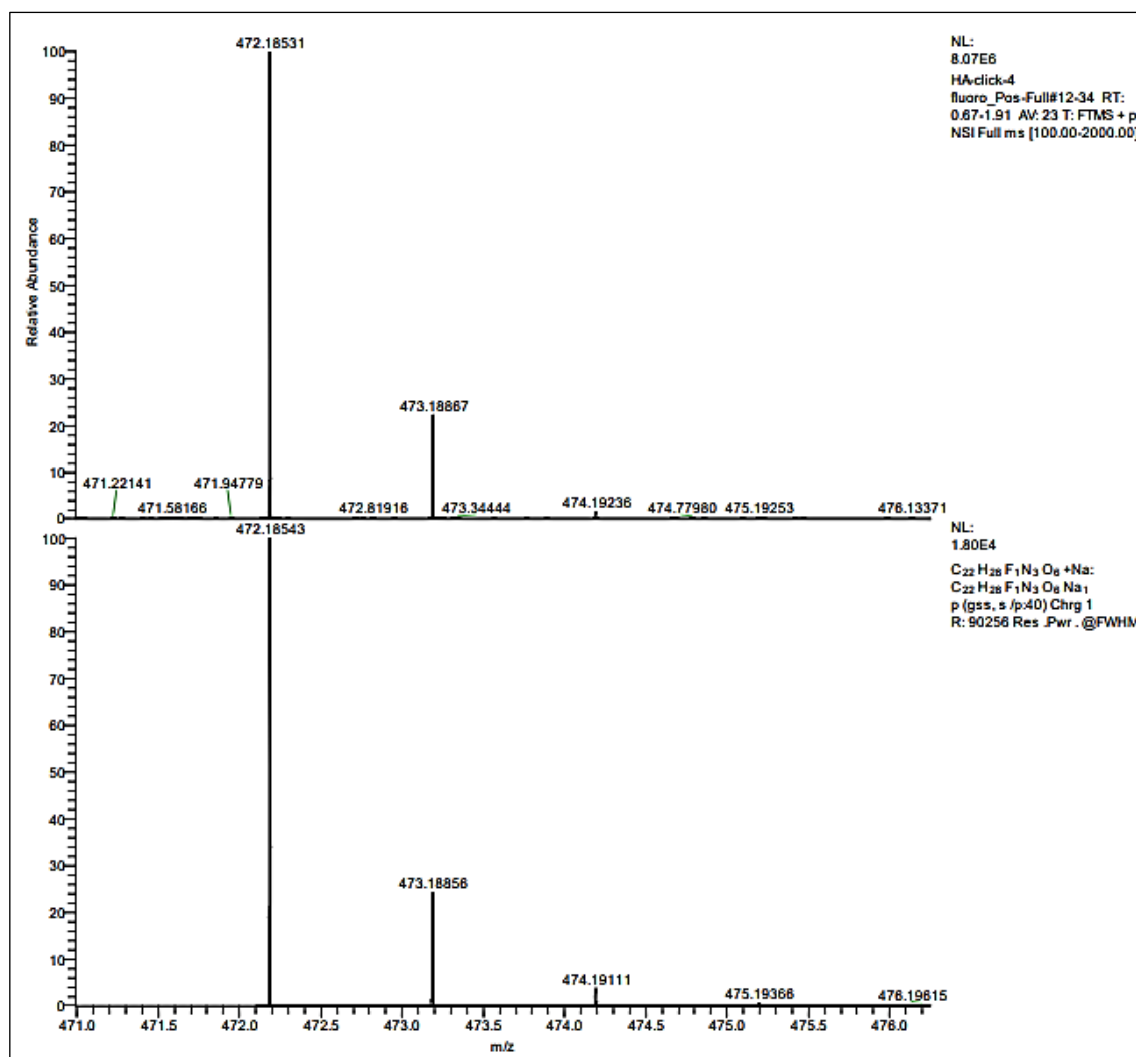
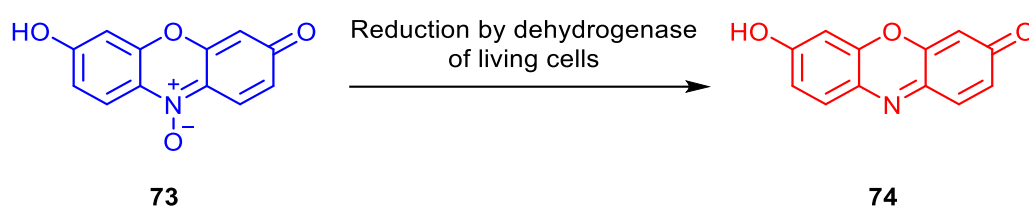


Figure (3-75). High-resolution mass spectrum of triazole 72c

3.5. Cytotoxicity of triazole derivatives 72a–72c

The *in vitro* cytotoxicity of compounds 72a–72c have been tested versus human mesenchymal stem cells MSCs utilizing alamarBlue as an indicator in two concentrations 1.0 mM and 0.5 mM. AlamarBlue is a calorimetric technique based on the reducing of non-toxic synthetic dye 7-hydroxy-10-oxido-phenoxazin-10-ium-3-one (73), by the biological cells, particularly by dehydrogenase enzymes, to the resofurin (74) (Scheme 30).^{102,103}



Scheme (3-30). The reducing of compound 73 to the compound 74 by dehydrogenase of biological cells

The concentration of the red dye resofurin (74) and the amount of the fluorescence produced increase as the amount of the living in the assay rises. Table 4 and Figure 73 illustrate that compounds 72a–72c possess fair cytotoxicity. Normally and at 1.0 mM concentration, compounds 72b and 72c have higher cytotoxic effect 70% and 75% respectively while the cytotoxicity of the derivative 72a is 90% at the same concentration. Derivative 72a has fluorine in ortho position and this can restrict the rotation about sigma bond, which in turn affect the hydrophobicity of the molecules and hence disturbs the diffusion of the molecule into cells through the lipid bilayer membrane.^{104–106} Nevertheless, reducing the concentration of compounds 72a–c to the half 0.5 mM maintains the cytotoxicity of derivatives 72a, 72b and 72c at 95%, 100% and 90% respectively.

Table (3-4). Cytotoxicity of triazoles 72a–72c versus human MSCs

Compound No.	Cells Viability%	
	1.0 mM	0.5 mM
Control	100%	
72a	90%	95%
72b	70%	100%
72c	75%	90%

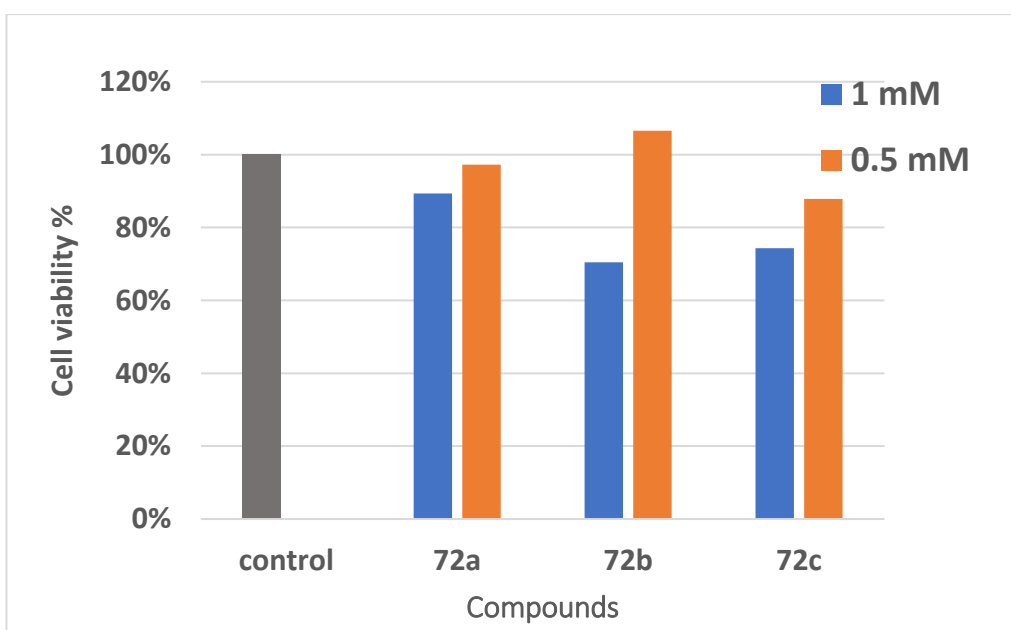


Figure (3-76). MSCs Cytotoxicity analyses using almarBlue method that planted 24h on top of triazoles **72a–72c**

3.6.Conclusion

1,2,3-Triazole are essential category of organic molecules that have extensive variety of applications. This thesis contained the preparation of new type of 1,2,3-triazole derivatives starting of commercially available monosaccharide (D-galactose). The prepared compounds have been entirely identified by TLC and spectroscopic techniques; FTIR, NMR and HRMS. Introduction of fluorine-substituted aromatic ring in the compounds increases the hydrophobicity as the fluorine is lipophilic element. This improved the features of derivatives for the medicinal applications. The cytotoxicity of the cyclic acetal-containing triazoles **72a–72c** versus human mesenchymal stem cells MSCs was acceptable at 0.5 mM. However, there was no or slight cytotoxicity at 1.0 mM.

3.7.Future work

It is highly advised to screen the synthesized compounds at higher concentrations; 2.0 mM, 3.0 mM and 4.0 mM. It is also suggested to examine the toxicity of the deprotected set of the 1,2,3-triazole derivatives **72a–72c** against human mesenchymal stem cells due to their amphiphilic properties. This will accelerate the diffusion of the compounds in the biological cells through the lipid bilayer membrane and accordingly provides better results. Also, it is suggested that the prepared derivatives examined versus different types of pathogenic microbes due to the same cause. Furthermore, the prepared derivatives might be employed as chelates in the production of various organometallic complexes that possess various functions in the pharmaceutical, catalysis or material science fields.

REFERENCES

References

- 1- M. Saito, *Coord. Chem. Rev.*, 2012, 256(5-8), 627-636.
- 2- N.M. Aljamali, *Asian J. Res. Chem.*, 2014, 7(11), 975-1006.
- 3- C.T. Walsh, M.A. Fischbach, *J. Am. Chem. Soc.*, 2010, 132(8), 2469-2493.
- 4- J.W.H. Li, J.C. Vederas, *Science.*, 2009, 325(5937), 161-165.
- 5- A.M. Abdella, A.M. Abdelmoniem, I.A. Abdelhamid, *Lect. Heterocycl. Chem.* 2020, 57(4), pp.1476-1523.
- 6- P. Arora, V. Arora, H.S. Lamba, D. Wadhwa, *Int. J. Pharm. Sci. Res.*, 2012, 3(9), 2947.
- 7- Z.X. Xu, L. Xu, J.H. Cheng, Z.X. He, Q. Wang, X. Hu, *Fuel Process. Technol.*, 2018, 182, 37-44.
- 8- K.H. Hellwich, R.M. Hartshorn, A. Yerin, T. Damhus, A.T. Hutton, *Pure Appl. Chem.*, 2020, 92(3), 527-539.
- 9- M. Choury, A. Basilio Lopes, G. Blond, M. Gulea, *Molecules.*, 2020, 25(14), 3147.
- 10- R. Kevorkyants, A.V. Emeline, D.W. Bahnemann, *J. Solid State Chem.*, 2020, 282, p.121082.
- 11- H.M.Y. Al-labban, A.A.J. Aljanaby, *Int. J. Pharm. Res.*, 2020, 1.
- 12- A. Leclair, Q. Wang, J. Zhu, *ACS Catal.*, 2022, 12, 1209-1215.
- 13- Y. Higashio, T. Shoji, *APPL CATAL A-GEN.*, 2004, 260(2), 251-259.
- 14- H.N. Matsuura, A.G. Fett-Neto, *Plant toxins.*, 2015, 2(7), 1-15.
- 15- A. Domagala, T. Jarosz, M. Lapkowski, *Eur. J. Med. Chem.*, 2015, 100, 176-187.
- 16- S. H. Sumrra, U. Habiba, W. Zafar, M. Imran, Z. H. Chohan, *J. Coord. Chem.*, 2020, 73(20-22), 2838-2877.
- 17- S. Kumar, S. L. Khokra, A. Yadav, *Future J. Pharm. Sci.*, 2021, 7(1), 1-22.

- 18-** J. A. Bladin, Ber. Dtsch. Chem. Ges., 1885, 18(1), 1544-1551.
- 19-** K. Vinod and K. Kamalneet, J. Nat. Prod., 2014, 2014, **4**, 115-130.
- 20-** G. Wang, Z. Peng, J. Wang, X. Li and J. Li, Eur. J. Med. Chem., 2017, 125, 423-429.
- 21-** Y. A. Al-Soud, M. N. Al-Dweri, N. A. Al-Masoudi, Il Farmaco, 2004, 59, 775-783.
- 22-** P. Zoumpoulakis, C. Camoutsis, G. Pairas, M. Soković, J. Glamočlija, C. Potamitis and A. Pitsas, Bioorg. Med. Chem., 2012, 20, 1569-1583.
- 23-** V. Padmavathi, G. Sudhakar Reddy, A. Padmaja, P. Kondaiah, S. Ali, Eur. J. Med. Chem., 2009, 44, 2106-2112.
- 24-** X.-M. Chu, C. Wang, W.-L. Wang, L.-L. Liang, W. Liu, K.-K. Gong, K.-L. Sun, Eur. J. Med. Chem, 2019, 166, 206-223.
- 25-** A. Kashyap, O. Silakari, Elsevier sci., 2018, 323-342.
- 26-** A. Singh, A. Argal, D. Kumer, S. K. Jain, World J. Pharm. Res., 2020, 9(7), 441-469.
- 27-** W. L. Truett, D. R. Johnson, I. M. Robinson, B. A. Montague, J. Am. Chem. Soc., 1960, 82, 2337-2340.
- 28-** O. Baltzer, H. v. Pechmann, Justus Liebigs Ann. Chem., 1891, 262, 314-324.
- 29-** T. J. Zhang, Y. Zhang, S. Tu, Y. H. Wu, Z. H. Zhang, F. H. Meng, Eur. J. Med. Chem., 2019, 183, 111717.
- 30-** E. Loukopoulos, G. E. Kostakis, Coord. Chem. Rev., 2019, 395, 193-229.
- 31-** K. A. Kumar, Int. J. ChemTech Res., 2013, 5, 3032.
- 32-** S. Ito, Y. Tokimaru, K. Nozaki, ChemComm., 2015, 51(1), 221-224.
- 33-** R. Huisgen, Angew. Chem., 1955, 67, 439-463.
- 34-** A. Michael, J. prakt. Chem., 1893, 48, 94-95.
- 35-** C. W. Tornøe, C. Christensen, M. Meldal, J. Org. Chem., 2002, 67, 3057-3064.

- 36-** V. V. Rostovtsev, L. G. Green, V. V. Fokin, K. B. Sharpless, *Angew. Chem. Int. Ed.*, 2002, 41, 2596-2599.
- 37-** H. C. Kolb, M. G. Finn and K. B. Sharpless, *Angew. Chem. Int. Ed.*, 2001, 40, 2004-2021.
- 38-** C. D. Hein, X.-M. Liu and D. Wang, *J. Pharm. Res.*, 2008, 25, 2216-2230.
- 39-** R. Huisgen, *Proc. Chem. Soc.*, 1961, 73, 357.
- 40-** H.U. Reissig M. Breugst, *Angew. Chem. Int. Ed.*, 2020, 59.
- 41-** M. Breugst, R. Huisgen, H.-U. Reissig, *Eur. J. Org. Chem.*, 2018, 2018, 2477-2485.
- 42-** J. M. Holub, K. Kirshenbaum, *Chem. Soc. Rev.*, 2010, 39(4), 1325-1337.
- 43-** B. Gui, X. Liu, Y. Cheng, Y. Zhang, P. Chen, M. He, C. Wang, *Angew. Chem.*, 2020, 134(2), e202113852.
- 44-** P. Wu, A. K. Feldman, A. K. Nugent, C. J. Hawker, A. Scheel, B. Voit, V. V. Fokin, *Angew. Chem.*, 2004, 116(30), 4018-4022.
- 45-** L. Zhu, C. J. Brassard, X. Zhang, P. M. Guha, R. J. Clark, *Chem. Rec.*, 2016, 16(3), 1501-1517.
- 46-** M. V. de Souza, C. F. da Costa, V. Facchinetti, C. R.B. Gomes, P. M. Pacheco, *Curr. Org. Synth.*, 2019, 16(2), 244-257.
- 47-** P. Sharma, S. Rohilla, N. Jain, *J. Org. Chem.*, 2015, 80(8), 4116-4122.
- 48-** E. Haldon, M. C. Nicasio, P. J. Pérez, *Org. Biomol. Chem.*, 2015, 13(37), 9528-9550.
- 49-** S. Neumann, M. Biewend, S. Rana, W. H. Binder, *Macromol. Rapid Commun.*, 41(1), 1900359.
- 50-** A.I. Mohammed, *Asian J. Chem.*, 2012, 24(12), 5585–5588.

- 51-** B.I. Vergara-Arenas, L. Lomas-Romero, D. Ángeles-Beltrán, G.E. Negrón-Silva, A. Gutiérrez-Carrillo, V.H. Lara, J.A. Morales-Serna, *Tetrahedron Lett.*, 2017, 58(28), 2690-2694.
- 52-** T. Gregorić, M. Sedić, P. Grbčić, A.T. Paravić, S.K. Pavelić, M. Cetina, S. Raić-Malić, *Eur. J. Med. Chem.*, 2017, 125, 1247-1267.
- 53-** M. Znati, M. Horchani, L. Latapie, H. Ben Jannet and J. Bouajila, *J. Mol. Struct.*, 2021, 1246, 131216, DOI: 10.1016/j.molstruc.2021.131216.
- 54-** T. Kiranmye, M. Vadivelu, S. Sampath, K. Muthu, K. Karthikeyan, *Sustainable Chem. Pharm.*, 2021, 19, 100358.
- 55-** J.A. Mokariya, A.G. Kalola, P. Prasad and M.P. Patel, *Mol Divers.* 2021. DOI: 10.1007/s11030-021-10212-8.
- 56-** J. Castillo, N. Bravo, L. Tamayo, P. Mestizo, J. Hurtado, M. Macías, and J. Portilla, *ACS Omega*, 2020, 5 (46), 30148–30159.
- 57-** T. Kiranmye, M. Vadivelu, S. Sampath, K. Muthu, K. Karthikeyan, *Sustain. Chem. Pharm.*, 2021, 19. DOI: 100358,10.1016/j.scp.2020.100358.
- 58-** E. Bonandi, M. S. Christodoulou, G. Fumagalli, D. Perdicchia, G. Rastelli, D. Passarella, *Drug Discov. Today.*, 2017, 22(10), 1572-1581.
- 59-** R. Varala, H.B. Bollikolla, C. M. Kurmarayuni, *Curr. Org. Synth.*, 2021, 8(2), 101-124.
- 60-** I. Torres-Moya, J.R. Carrillo, Á. Díaz-Ortiz, P. Prieto, *Chemosensors.*, 2021, 9(9), 267.
- 61-** R. Varala, H. B. Bollikolla and C. M. Kurmarayuni, *Curr. Org. Synth.*, 2021, 18. [DOI:10.2174/1570179417666200914142229](https://doi.org/10.2174/1570179417666200914142229)
- 62-** S. Kantheti, R. Narayan and K.V. Raju, *RSC Adv.*, 2015, 5, 3687–3708.

- 63-** N. Touj, I. Özdemir, S. Yaşar and N. Hamdi, *Inorganica Chim. Acta*, 2017, 467, 21–32.
- 64-** M. Rogawski and W. Löscher, *Nat. Rev. Neurosci.*, 2004, 5, 553–564.
- 65-** S. Zhou, Y. Xin, J. Wang, C. Wu, and T. Sun, *Org. Process. Res. Dev.*, 2021, 25 (7), 1648–1657.
- 66-** M. Bonnefond, R. Florent, S. Lenoir, B. Lambert, E. Abeilard, F. Giffard, M. Louis, N. Elie, M.
- 67-** S. Sahoo, K.N. Sindhu and K. Sreeveena, *Res. J. Pharm. Technol.*, 2019, 12(10). DOI: 10.5958/0974-360X.2019.00882.5.
- 68-** I. E. Valverde, A. Bauman, C. A. Kluba, S. Vomstein, M. A. Walter and T. L. Mindt, *Angew. Chem. Int. Ed.*, 2013, 52, 8957–8960.
- 69-** R. Jwad, D. Weissberger, and L. Hunter, *Chem. Rev.*, 2020, 120 (17), 9743–9789.
- 70-** A. Gabba, S. Robakiewicz , B. Taciak, K. Ulewicz, G. Broggin, G. Rastelli, M. Krol, P.V. Murphy and D. Passarella, *Eur. J. Org. Chem.*, 2017, 2017, 60–69.
- 71-** D.C. Schröder, O. Kracker, T. Fröhr, J. Góra, M Jewginski, A. Nieß, I. Antes, R. Latajka, A. Marion, N. Sewald, *Front. Chem.*, 2019, 7. DOI: 10.3389/fchem.2019.00155.
- 72-** Z. Fallah, M. Tajbakhsh, M. Alikhani, B. Larijani, M.A. Faramarzi, H. Hamedifar, M. Mohammadi-Khanaposhtani, M. Mahdavi, *J. Mol. Struct.*, 2022, 132469. DOI: 10.1016/j.molstruc.2022.132469.
- 73-** A. I. Mohammed, N. H. Mansour and L. S. Mahdi, *Arab. J. Chem.*, 2017, 10, S3508–S3514.
- 74-** A. I. Mohammed, R. S. Jwad and N. A. Al-Radha, *Int. J. Chem. Sc.*, 2013, 11, 1–11.

- 75-** T. El Malah, H. F. Nour, A. A. E. Satti, B. A. Hemdan, W. A. El-Sayed, *Molecules*, 2020, 25(4), 790. DOI:10.3390/molecules25040790.
- 76-** S. Nerella, S. Kankala and B. Gavaji, *Nat. Prod. Res.*, 2021, 35(1), 9–16.
- 77-** V.N. Holanda, E.M.de Araújo Lima, W.V. da Silva, R.T. Maia, R. de Lima Medeiros, A. Ghosh, V. L. de Menezes Lima and R.C. de Figueiredo, *J. Biomol. Struct.*, 2021, DOI:10.1080/07391102.2020.1871073.
- 78-** R. Corona-Sánchez, A. Sánchez-Eleuterio, C. Negrón-Lomas, Y. Ruiz Almazan, L. Lomas-Romero, G.E. Negrón-Silva and Á.C. Rodríguez-Sánchez, *R. Soc. Open Sci.*, 2020, 7, 200290. DOI:10.1098/rsos.200290.
- 79-** M.M. Karbasi, Z. Mirjafary, H. Saeidian and J. Mokhtari, *J. Mol. Struct.*, 2021, 1227, 129535. DOI: 10.1016/j.molstruc.2020.129535
- 80-** A. Nahle, R. Salim, F. El Hajjaji, M. R. Aouad, M. Messali, E. Ech-chihbi, B. Hammoutid and M. Taleb, *RSC Adv.*, 2021, 11, 4147–4162.
- 81-** D. Zhang, J. Lu, C. Shi, K. Zhang, J. Li and L. Gao, *Corros. Sci.*, 2021, 178, 109063. DOI: 10.1016/j.corsci.2020.109063.
- 82-** D. V. Francis, D. H. Miles, A. I. Mohammed, R. W. Read and X. Wang, *J. Fluor. Chem.*, 2011, 132, 898–906.
- 83-** H.C. Braga, A.D. Wouters, F.B. Zerillo, D.S. Lüdtke, *Carbohydr. Res.*, 2010, 345(16), 2328–2333.
- 84-** R.S. Jwad, *Al-Nahrain Journal of Science*, 2011, 14(1), 1–10.
- 85-** M. J. Mohammed, A. A. H. Kadhum, A. I. Mohammed and S. H. Abbood Al-Rekabi, *J. Chem. Soc. Pak.*, 2020, 42, 103–108.
- 86-** F. Neese, *Comput. Mol. Sci.*, 2012, 2(1), 73–78.
- 87-** F. Neese, *Comput. Mol. Sci.*, 2017, 8, e1327. DOI: 10.1002/wcms.1327

- 88-** E. V. Tret'yakova, E. V. Salimova and L. V. Parfenova, *Nat. Prod. Res.*, 2020, DOI: 10.1080/14786419.2020.1762187.
- 89-** J. Jampilek, *Molecules*, 2019, 24(21), 3839–3842. DOI: 10.3390/molecules24213839.
- 90-** R. Huisgen, *J. Org. Chem.*, 1968, 33, 6, 2291–2297.
- 91-** S. Oae and Y. Kadoma, *Phosphorus, Sulfur, Silicon Relat. Elem.*, 1997, 123, 293–300.
- 92-** T. A. Hamlin, M. Swart and F. M. Bickelhaupt, *ChemPhysChem*, 2018, 19, 1315–1330.
- 93-** S. D. Yoh, M. Lee, K. Son, D. Cheong, I. Han, and K. Shim, *Bull. Korean Chem. Soc.*, 1999, 20(4), 466–468.
- 94-** N. Muller and D. T. Carr, *J. Phys. Chem.*, 1963, **67**, 112–115.
- 95-** T. Wanga and A. V. Demchenko, *Org. Biomol. Chem.*, 2019; 17, 4934–4950.
- 96-** 38-B. Klaus, *Curr. Org. Chem.*, 2019, 23(27). 3040–3063.
- 97-** P. Klukowski and M. Schubert, *Bioinformatics*, 2019, 35(2), 293–300.
- 98-** P. E. Marszalek, Y. Pang, H. Li, J. El Yazal, A. F. Oberhauser and M.J. Fernandez, *Proceedings of the National Academy of Sciences PNAS*, 1999, 96(14), 7894–7898.
- 99-** M. Inagaki, R. Iwakuma, S. Kawakami, H. Otsuka and Rakotondraibe, *J. Nat. Prod.*, 2021, **84**(7), 1863–1869.
- 100-** B. Coxon, *Adv. Carbohydr. Chem. Biochem.*, 2009, **62**, 17–82.
- 101-** J.W. Emsley, L. Phillips and V. Wray, *Prog. Nucl. Mag. Res. Sp.*, 1976, **10**, 83–752.
- 102-** S. N. Rampersad, *Sensors*, 2012, **12**, 12347–12360.
- 103-** J. Mikus and D. Steverding, *Parasitol. Int.*, 2000, **48**(3), 265–269.

- 104-** R.S. Jwad, A.H.C. Pang, L. Hunter, and R.W. Read, *Aust. J. Chem.*, 2019, **72**, 213–225
- 105-** W. J. Dunn and Svante Wold, *Bioorg. Chem.*, 1980, **9**, 1980, 505–523.
- 106-** N.J. Yang and M.J. Hinner, in *Methods in Molecular Biology*, eds A. Gautier and M. Hinner, Humana Press, New York, 2015, vol. **1**, ch. 2, pp. 29–53.

الخلاصة

تضمنت هذه الرسالة تخليق مشتقات 1،2،3-ترايازول جديدة مستندة على الكلاكتوز المحتوي على جزء فلوروبنزيل ودراسة خصائصها السمية. في البداية ، تم تحضير 2-فلور- ، 3-فلور و 4-فلوروبنزيل أزيد (68a-c) من خلال تفاعل بروميدات البنزيل المقابلة (67a-c) مع أزيد الصوديوم في مذيب ثنائي مثيل سلفوكسايد DMSO عند 50 درجة مئوية لمدة 24 ساعة للحصول على الأزيدات المذكورة في منتج جيد جداً إلى ممتاز 81-92%. و في خطوة موازية ، تم استخدام كلوريد الزنك وحمض الكبريتيك لتحفيز تفاعل D-جلاكتوز (69) مع وصول الأستون في درجة الحرارة المحيطة لمدة 6 ساعات للحصول على 1,2:3,4-di-O- isopropylidene- α -D-galactose (70) بمنتج جيد جداً 81% تم تفاعل هذا المشتق مع بروميد البروبارجيل في ثنائي مثيل فورمامايد DMF عند صفر درجة مئوية إلى درجة حرارة الغرفة. لإنتاج 6-O-prop-2-ynyl-1,2:3,4-di-O-isopropylidene- α -D-galactose (71) يمنتج 88% علاوة على ذلك تم تحديد شكل المشتق 71 الفراغي باستخدام الدراسة الحسابية وتقنية الرنين النووي المغناطيسي ثنائي الأبعاد 2D NMR. أخيراً تم تصنيع مشتقات 1،2،3-ترايازول (72a-c) من خلال تفاعل تحفيز ألكين-أزيد النحاسي (CuAAC) للألكاين 71 مع الأزيدات الأروماتية (68a-c) بوجود أسكورات الصوديوم وكبريتات النحاس في مذيب ثنائي مثيل سلفوكسايد DMSO عند 50 درجة مئوية لمدة 36 ساعة للحصول على مشتقات 1،2،3-ترايازول المستهدفة (72a-c) بمنتج 83-90% تم تشخيص المركبات المحفزة بتقنيات كروماتوغرافيا الطبقة الرقيقة TLC و مطيافية الأشعة تحت الحمراء FT-IR و مطيافية الرنين النووي المغناطيسي NMR و COZY و HSQC و HMBC و HRMS. تم فحص المركبات (72a-c) تجاه الخلايا الجذعية للحمية البشرية ووجد أن هذه المشتقات لها سمية خلوية معتدلة.

الإهداء

لأكبر مُحبٍ وداعِمٍ، أُمِّي
لصاحب الرُّوح الطَّيِّبة وحاملِ الإبتِسَامَةِ، أبِي
لمُلهِمِي، أَخُوْتِي ورُسُلِي
لمَصْدَرِ قُوْتِي ودَعَمِي وحُبِّي، زَوْجِي عَلِي
لقُرَّةِ عَيْنِي ابْنَتِي مِيَا
لكُلِّ أصدقائي

بِسْمِ اللَّهِ الرَّحْمَنِ الرَّحِيمِ

{يَرْفَعِ اللَّهُ الَّذِينَ آمَنُوا مِنْكُمْ وَالَّذِينَ أُوتُوا الْعِلْمَ دَرَجَاتٍ وَاللَّهُ
بِمَا تَعْمَلُونَ خَبِيرٌ}

صَدَقَ اللَّهُ الْعَلِيِّ الْعَظِيمِ

سُورَةُ الْمُجَادَلَةِ الْآيَةِ (١١)



جامعة كربلاء

كلية العلوم

قسم الكيمياء

تحضير ودراسة الفعالية الحيوية والتراكيب لمشتقات ١،
٢، ٣، ترايازول المستند على D- كالكثوز

رسالة مقدمة إلى

مجلس كلية العلوم- جامعة كربلاء

كجزء من استكمال متطلبات نيل درجة الماجستير

في علوم الكيمياء

من قبل

هاله حسام عبد الكاظم

إشراف

أ.د. باقر عبد الزهرة جود

أ.د. عدنان إبراهيم محمد